Environmentally driven orchestration of metabolisms by *Prochlorococcus* spp.

A Dissertation Presented for the

Doctor of Philosophy

Degree

The University of Tennessee, Knoxville

Martin James Szul

May 2016

ACKNOWLEDGEMENTS

I would like to acknowledge a number of people who have provided much assistance and support - without their help I would not have been able conduct the research discussed within. First and foremost, my mentor, Erik Zinser and committee members – Jeff Becker, Alison Buchan, Shawn Campagna, and George O'Toole who have guided me through my graduate research, showed me how to ask questions. Additional recognition is due to my collaborators who have stayed with me through the days (and nights) of experiments described within – Shawn Campagna and his graduate students: Jessica Gooding, Jesse Middleton, Stephen Dearth, who have helped in the collection and analyzation of the metabolomics data as well as Zackary Johnson and his graduate students: Yajuan Lin, Maria De Oca Echarte, and Sara Blineby, who have performed primary production measurements. I also would like to thank the Captains and crews of the *R.V.* Cape Hatteras, *R.V.* Atlantic Explorer, and the *R.V.* Kilo Moana who safely took me to and returned me from the blue waters of the Atlantic and Pacific Oceans. Lastly, I would be amiss without thanking the Zinserlab members – Jeff Morris, Jeremy Chandler, Lanying Ma, and Megan Silbaugh - who provided moral support and addition sets of trusted hands as needed.

It almost goes without saying that my family and wife, Brenna, have played an instrumental role over the past 7 years providing the love and support I needed to keep moving as my research stumbled along. Without your support and guidance I would not be where I am today. With sincere and heartfelt thoughts, I thank you.

ABSTRACT

In the oligotrophic waters of the world's open oceans physical factors such as pH, salinity, and temperature are generally stable. The nutrient limited conditions as well as the low environmental variability endemic to these ecosystems select for specialists that gain fitness advantages through minimalism, efficiency, and thrift. These physical characteristics are thought to reduce nutrient demand while allowing for constant metabolic activity and growth, but the mechanisms that promote these fitness advantages are currently unknown. To better understand how these physiologies improve selective fitness for the dominant phytoplankton, we observed metabolic parameters under environmental conditions typical to these waters. In an environment characterized by low physical variation, the cellular processes of our model organisms – the genomically streamlined phytoplankton *Prochlorococcus* spp. – follow the trends of their ultimate energy source: the predictable daily oscillations of solar energy. Through observations on metabolic biomarkers associated with carbon, energy, and nitrogen metabolism over diel photic cycles, we sought to gain insights into the coordination of these intersecting metabolisms as a function of the time of day. We found that although cellular carbon and energy stores vary over the photic period, incorporation of ammonium into glutamate can occur throughout the diel cycle. Efficiency and thrift in nitrogen metabolisms are thought to be under strong selective pressure as inorganic nitrogen is the growth limiting nutrient for *Prochlorococcus* in the North Pacific Subtropical Gyre. To develop a deeper understanding of metabolic processes utilized by nitrogen limited phytoplankton, we performed laboratory and field experiments, investigating metabolisms of nitrogen limited and nutrient replete pure cultures as well as the effect of a nitrogen pulse on metabolisms of natural populations in the North Pacific. Low rates of carbon fixation and flow of fixed carbon through large metabolic pools were observed in our nitrogen limited experiments and may suggest reduced growth under limiting conditions is not caused by lack of metabolic precursors, but through the polymerization of biological macromolecules such as proteins and nucleic acids. These data provide primary observations of the metabolic balance of carbon, energy and nitrogen metabolisms in the most abundant photosynthetic organism on Earth.

TABLE OF CONTENTS

CHAPTER 1: Life in the Oligotrophic Open Oceans 1
Blue Water Deserts 2
Ecology and Evolution 2
Minimalism in the Genome of *Prochlorococcus* spp. 3
The Temporally Synchronized Cell Cycle of *Prochlorococcus* spp. 4
TCA 'Cycle': Bridging Carbon and Nitrogen metabolisms in *Prochlorococcus* 5
Ammonium assimilation 7
Regulation of nitrogen assimilatory metabolisms 7
Summary of dissertation 9
CHAPTER 2: Metabolic Analysis of *Prochlorocoocus* sp. MED 4 Over a Diel Light Cycle 12
Abstract 13
Introduction 13
Results and Discussion 16
Diel Metabolite analysis 16
Cell cycle analysis 21
Conclusions 28
Materials and Methods 33
Culturing and Sample collection 33
Diel Metabolomics Methods 33
Cell Energetic cycle methods 35
CHAPTER 3: Carbon Fate and Flux in *Prochlorococcus* Under Nitrogen Limitation 39
Abstract 40
Introduction 40
Results and Discussion 42
Conclusions 61
Materials and Methods 67
CHAPTER 4: Metabolomic Assessment of Inorganic Carbon Assimilation by Phytoplankton in the N. Pacific Ocean 72
Abstract 73
Introduction 73
Results 74
Discussion 78
Conclusion 83
Materials and Methods 85
CHAPTER 5: Life at the Limits: Observations on the Physiological Mechanisms Championed by *Prochloroccoccus* spp. 87
Abstract 88
Balancing Carbon and Nitrogen Metabolisms in *Prochlorococcus* 88
Nitrogen Metabolism and Energetic Potential over a Diel 89
Metabolic Effects of Nitrogen Limitation on *Prochlorococcus* 90
Application of a Metabolic Flywheel 92

Future Directions 95
REFERENCES 98
APPENDIX 104
VITA 115

LIST OF TABLES

Table 1. Targeted m/z ratios: ^{13}C and ^{15}N glutamate 23
Table 2. Photophysiology of nitrogen limited and replete cultures of VOL 29 48
Table 3. Experimental Station Details 77
Table S4. Diel glutamate isotopologue ion counts 105
Table S5. Nitrogen Limited and Nitrogen Replete metabolite pool data 107
Table S6. Nitrogen Limited and Nitrogen Replete metabolite ^{13}C labeling 110

LIST OF FIGURES

Figure 1: Branched TCA cycle in *Prochlorococcus* spp. 6
Figure 2: Carbon and Nitrogen labeling of Glutamate over the diel 19
Figure 3: Predicted labeling of glutamate by PepC. 22
Figure 4: Polysaccharide and Reductant pools over a diel cycle 26
Figure 5: Adenylate Energy Charge and Adenylate Phosphate pools over a diel 29
Figure 6: Culture growth analysis 43
Figure 7: VOL29 growth in described current and trial grow out experiments 44
Figure 8: Photosynthesis and cellular carbon and energy stores 46
Figure 9. Metabolite Pool Analysis 50
Figure 10: Metabolite Labeling by Isotopic Carbon 52
Figure 11: Glutamate and Aspartate isotopic labeling in natural populations 60
Figure 12: Model of the Interaction between Photophysiology and Metabolisms in *Prochlorococcus* sp. VOL29 65
Figure 13: Experimental design and heat map of untargeted MS features from POWOW2 Exp1.1 75
Figure 14: Intracellular Glutamate Pools and inorganic carbon incorporation 79
Figure 15: Intracellular Glutamine Pools and inorganic carbon incorporation 80
Figure 16: Nitrogen assimilation mechanism model in *Prochlorococcus* and whole community microcosms 84

CHAPTER 1: LIFE IN THE OLIGOTROPHIC OPEN OCEANS

Blue Water Deserts

Life persists. Under the most extreme environmental conditions evolution has selected for elegant solutions that not only allow for survival, but for the proliferation of the unifying biological characteristic – *life*. This concept can be highlighted through the perseverance of plankton in the vast and desolate deserts of the world's tropical and subtropical oligotrophic open oceans. In these environments nutrient deficiency limits biological activity, but the collective metabolisms by the community that thrives in these harsh ecosystems are thought to drive global biological and physical processes. Estimates of the primary productivity in the euphotic zones of these waters have attributed half of the total observed daily on a global scale [1, 2]. This primary production provides a base for food webs and helps to support ocean-wide fisheries. Additionally, the inorganic carbon sequestration by these metabolisms impact global climate and may help buffer anthropogenic release of inorganic carbon.

Far from the reaches of land-based allochthonous nutrient inputs, life in the highly stratified and nutrient poor surface layer of the open ocean relies on biological recycling and fixing of nutrients or deep water mixing events that can carry nutrients from the subsurface. Because these mechanisms enrich waters at very low rates, the lack of nutrients in the surface waters limits biological abundance and the low biological load allows for light to penetrate down to approximately 200 meters. In addition to the low nutritional quality of these waters, the open ocean biomes have a high degree of environmental predictability attributed to the daily oscillation of solar energy. Reduction of response type regulation with tight temporal (diel) regulation may reduce costs associated with prokaryotic metabolisms by segregating antagonistic metabolic pathways as a function of the time of day (photic period).

Ecology and Evolution

Prochlorococcus spp. are both physiological and evolutionary curiosities. These cyanobacteria are the dominant phytoplankton in the world's vast tropical and subtropical open oceans in terms of both abundance and primary production [3-6]. The relatively stable conditions of the oligotrophic oceans relieve its inhabitants from the necessity to alter metabolisms during sudden changes in the environment (*e.g.* temperature, pH). In these

relatively static ecosystems, *Prochlorococcus* enjoys fitness advantages paralleled by its heterotrophic planktonic counterpart – *Pelagibacter* spp. Both of these organisms appear to have generated their ecological success from fitness advantages gained through "genomic streamlining" [7]. Organisms under this mechanism of selection reduce some of the nutritional and energy costs associated with the maintenance, replication, and utilization of genetic information through the gradual loss of genes nonessential to life in their environments. It is this process that is believed to have shaped the genomic and physiological characteristics of *Prochlorococcus* spp. selecting for not only the smallest free-living photosynthetic organism in both physical and genomic size, but one that relies on both leaked public goods (e.g. Black Queen Hypothesis [8]) and nutrient thrift [9, 10] for competitive advantage.

The fitness advantages enjoyed by the genomic minimalists of the oligotrophic open oceans dissipate as nutrient pools increase and/or vary unpredictably. In coastal, upwelling, or otherwise eutrophic regions; organisms capable of exploiting fluctuating nutrient pools and tolerating acute stresses are at a selective advantage over the metabolically limited oligotrophic specialists. The copiotrophs that thrive in these environments are thought to rely on the maintenance of large amounts of genetic information for their metabolically diverse and physiological plastic phenotypes to promote their fitness but the cost to maintain this genetic diversity may reduce fitness when nutrients are scarce. Contrarily, oligotrophic specialists – uncomplicated by secondary and ancillary metabolic processes – champion the simple and elegant choreography of metabolisms centered on preserving their ecological fitness through physiological efficiency. We believe that through a greater characterization of the fundamental mechanisms employed by the most abundant photosynthetic organism on Earth, it will be possible to generate a basic understanding for effects of photic energy availability and nutrient limitation on photosynthesis and metabolism.

Minimalism in the Genome of *Prochlorococcus* spp.

Prochlorococcus spp. are a prototrophic photoautotrophs; that is, these organisms are capable of producing all the biological molecules needed for life using only inorganic nutrients and sunlight. This extraordinary feat is even more remarkable considering that these organisms

appear to have reduced their genetic capacity to encode only for the essential genes in this nutrient poor and stable environment. This evolutionary process, known as genomic streamlining, allows for the loss of genes that are specific to seldom needed metabolic capacities. The gene loss events occurring in this process are suspected to have caused *Prochlorococcus* to maintain the smallest genome of any known free-living photoautotroph [11, 12]. Analysis of the small genome in the diverse strains of *Prochlorococcus* has revealed a 'core' and 'flexible' genome [13]. The genes encoded in the core genome are shared across ecotypes of *Prochlorococcus* and appear to encode all the necessary genes for a functional cell whereas the flexible genome appears to consist of genes that may be specific to the niche which the organism has evolved fitness [11].

The Temporally Synchronized Cell Cycle of *Prochlorococcus* spp.

In the oligotrophic oceans these minimal, free-living cyanobacteria use sunlight to drive carbon fixation through the Calvin cycle. This process reduces all the carbon and energy to carry them through the night while performing all the necessary metabolic functions of the cell. Like their ultimate energy source that follows a daily oscillation of availability, tight temporal coordination of cellular processes over diel light cycles have been observed in both laboratory [14-17] and field studies [18]. These observations suggest that during the morning a majority of the daily inorganic carbon is fixed and assimilated as biomass as cells grow in size. During the afternoon DNA replication proceeds as cells prepare to divide in the late evening and early night period [16, 18, 19]. Gene loss of certain components for the biological clock and conservation of others suggests that temporal regulation of metabolisms in *Prochlorococcus* is a necessary function, but complicated mechanisms are not necessary [17]. In an organism where genomic information is discarded if the products of that gene do not provide fitness advantages, the tight diel growth cycle observed in *Prochlorococcus* suggests the choreographed metabolisms driving these pathways provide an unparalleled photoautotrophic efficiency for life under constant nutrient limitation.

TCA 'Cycle': Bridging Carbon and Nitrogen metabolisms in *Prochlorococcus*

In many organisms the tricarboxylic acid (TCA) cycle provides two major metabolic functions, the first of these functions is to generate energetic potential through the catabolic oxidation of acetyl-CoA to CO_2. The second function is to generate essential metabolic precursors for anabolic metabolisms including those employed in nitrogen assimilation. During photic periods, cyanobacteria utilize solar energy to provide the reductant and ATP demanded for metabolisms and at night they are capable of oxidizing stored carbon and energy through the pentose phosphate pathway (PPP). This oxidative pathway generates ATP and NADPH while releasing CO_2. Differential expression of a few key genes can reverse the catabolic nature of this pathway and drive the reductive PPP, commonly referred to as the Calvin cycle. This pathway uses ATP and NADPH generated by photosynthetic electron transport to fix CO_2.

Because the oxidative PPP can meet the energetic demand for carbon and energy when photic energy is not available, the catabolic function of the TCA cycle in cyanobacteria is redundant and may cause futile cycling if active during periods when carbon fixing is occurring. Although the oxidative function of the TCA cycle can be replaced by the PPP, the second function of the TCA cycle – production of metabolic precursors – must still be fulfilled. For this reason cyanobacteria were thought to have the lost the gene encoding for 2-oxoglutarate dehydrogenase (OGDH; Fig. 1) disrupting canonical TCA cycle generating two bifurcated branches preventing cyclic flow of carbon but allowing for the production of the necessary metabolites [20, 21]. However, evidence now suggests that all cyanobacteria except *Prochlorococcus* and marine *Synechococcus* spp. have two enzymes that rejoin the two branches that bypass this gap in the cycle [22]. The reasons why *Prochlorococcus* and *Synechococcus* lack the OGDH bypass are not known, but it may suggest that completion of cycle may provide disadvantages in the open ocean.

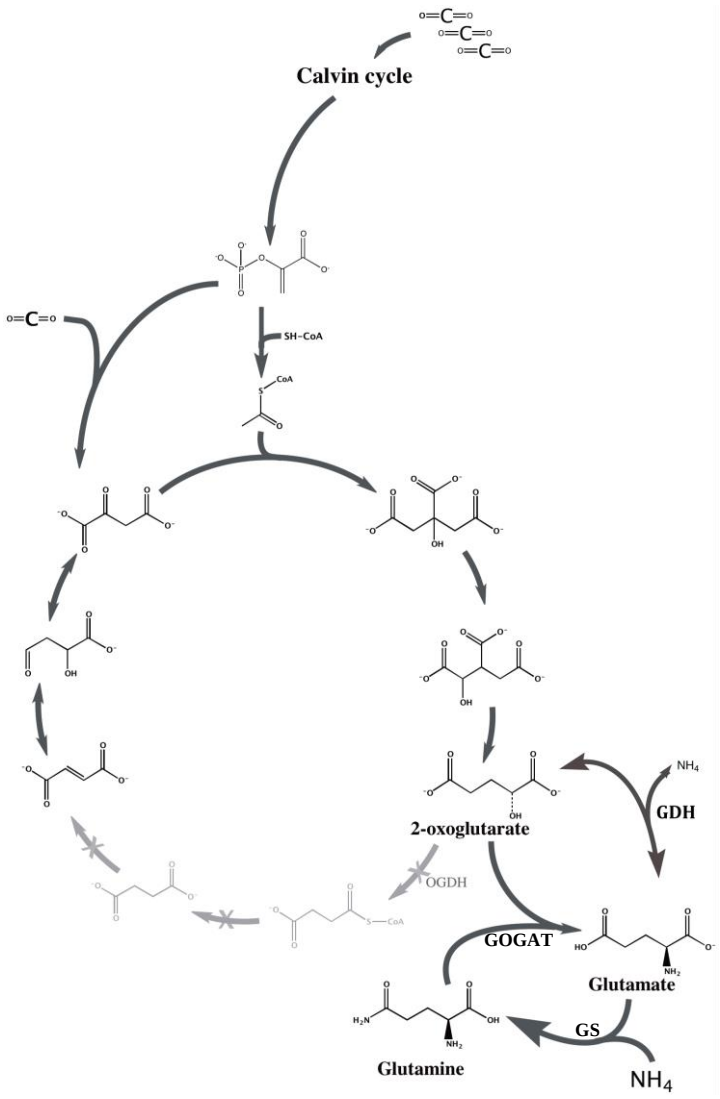


Figure 1: Branched TCA cycle in *Prochlorococcus* spp.

The incomplete TCA cycle in *Prochlorococcus*. Reactions catalyzed by enzymes with no homologous genes in *Prochlorococcus* genomes are displayed as light grey arrows with crosses. The glutamate dehydrogenase (GDH) genes have been observed in some, but not all *Prochlorococcus* genomes. In addition to ammonium (NH_4^+), metabolites and enzymes discussed in this chapter are highlighted; 2-oxoglutarate, glutamate, glutamine, glutamine-oxoglutarate amidotransferase (GOGAT), and glutamine synthetase (GS).

Ammonium assimilation

Prochlorococcus use ammonium as their preferred nitrogen source [21], but ecotypic variation allows for some strains to utilize additional forms of reduced inorganic nitrogen [23, 24]. Following transport of labile nitrogen into the cell it must converted to its most reduced state, ammonium, before assimilation can begin. Like all bacteria, *Prochlorococcus* utilize 2-oxoglutarate (2-OG) generated from their (bifurcated) TCA cycle as the carbon skeleton for the assimilation of nitrogen, but unlike most cyanobacteria *Prochlorococcus* spp. lack a complete TCA cycle. Therefore, 2-OG acts as an endpoint in the TCA cycle branch, and further metabolic processes are limited to those associated with nitrogen assimilation and anabolic pathways that utilize glutamate (Fig. 1).

Nitrogen can be assimilated onto the carbon backbone of 2-OG through the action of either one of two enzymatic reactions: low affinity glutamate dehydrogenase (GDH) or high affinity glutamine synthase – 2-oxoglutarate amidotransferase (GS-GOGAT). Ammonium assimilation in cyanobacteria is generally thought to be performed through the GS-GOGAT cycle [21] and because most strains of *Prochlorococcus* – including those investigated in the studies described within – do not encode for the GDH enzyme [25] we do not consider it to be of significance in our system. The high affinity GS-GOGAT nitrogen assimilatory cycle is performed by two enzymatic steps; glutamine synthetase (GS) performs the ATP-dependent condensation of ammonium and glutamate producing glutamine with the newly assimilated nitrogen as the amido group and ferredoxin dependent GOGAT catalyzes the reaction between glutamine and 2-oxoglutarate where glutamine donates its amido nitrogen to the 2-OG generating two glutamate molecules. This cycle produces glutamate and glutamine that can in turn serve as nitrogen donors in transamination reactions that generates all nitrogenous biological molecules.

Regulation of nitrogen assimilatory metabolisms

Under N limiting conditions, lack of substrate for the GS-GOGAT cycle is thought to cause pooling of 2-OG. These pools are believed to serve as the intracellular signal for nitrogen limiting conditions, interacting with three cyanobacterial nitrogen regulators – NtcA, PipX, and

P_{II} – and modulating their activity [21, 26-28]. Briefly, when low nitrogen availability slows GS-GOGAT it causes pooling of 2-OG, NtcA can bind the abundant 2-OG and PipX resulting in the activation of the NtcA. This complex is then involved in upregulation of both itself and nitrogen assimilatory mechanisms (e.g. nitrogen acquisition, carbon fixation, and GS). In addition to binding to NtcA, 2-OG can bind P_{II}. The P_{II}-2-OG complex sequesters the P_{II} signal transduction protein from its capability to signal nitrogen availability. When nitrogen is abundant, high activity of GS-GOGAT draws down pools of 2OG reducing the association of 2OG and P_{II}. The free P_{II} can then promote the synthesis of nitrogen rich arginine by binding and promoting the key biosynthetic enzyme *N*-acetyl-glutamate-kinase [26, 29]. PipX-P_{II} binding is inhibited by 2-OG suggesting P_{II} might compete for PipX under nitrogen stress when 2-OG is high [26, 30].

The lack of a complete TCA cycle suggests *Prochlorococcus* may employ novel regulation at the intersection of carbon and nitrogen metabolic processes, as all carbon that flows down the oxidative branch of the TCA cycle must go through the nitrogen assimilation process, making it a particularly interesting candidate to study the regulation of nitrogen and carbon. Unfortunately, the lack of a genetic system in *Prochlorococcus* makes traditional methods of regulational studies difficult. Previous investigations regarding the mechanisms around this regulatory system relied on transferring actively growing nitrogen replete cultures to starved conditions and observing the response. While these studies provide evidence that *Prochlorococcus* transcribes the three known regulatory proteins that act on the intersection of carbon and nitrogen – P_{II}, PipX, and NtcA – these regulators have not been observed to perform as described in other systems, including those of the closely related marine *Synechococcus*. For example, contrary to what has been observed in other cyanobacteria Palinska et al. have shown in *Prochlorococcus* that P_{II} does not undergo phosphorylation in response to the species of nitrogen available [31] and Lindell et al. provide data showing like other cyanobacterial systems transcription of *ntcA* is upregulated under nitrogen stress but the transcriptional abundance ammonia transporter gene *amt1* is not correlated with *ntcA* and appears to be constitutively expressed [32]. Additional studies show contrasting results where nitrogen stress has been

observed to induce GS transcription upregulation [33] but both abundance and activity of GS does not appear to respond in kind [34]. Transcription of genes involved in carbon acquisition and fixation suggest strain MED4 decreases carbon fixation during N-stress [33]. The authors of these reports have reconciled the differences in regulation by acknowledging *Prochlorococcus* may not utilize other species of nitrogen that are implicated in the phosphorylation of P_{II} in other cyanobacterial systems and in the constantly low nitrogen environment of the oligotrophic oceans constitutive acquisition of free ammonium may provide competitive advantages. Although these regulatory systems do not behave as exactly as observed in other cyanobacterial systems, these carbon and nitrogen regulatory mechanisms are retained in the genomes of *Prochlorococcus* and thus are suspected to have important roles.

Summary of dissertation

The research performed for my dissertation was designed to strengthen and develop the physiological roadmap for the metabolism of *Prochlorococcus* under conditions found in the natural environment. Using previous research as my foundation, I describe a series of three experiments designed to answer key questions regarding mechanisms employed by *Prochlorococcus* to thrive in a nutrient-poor environment:

- **In *Prochlorococcus*, can nitrogen assimilation occur outside the period of apparent upregulation during the early evening? How are cellular carbon and energy stores managed over diel cycles (*i.e.* photosynthate and/or glycogen catabolism) and does the temporal management of these stores affect the diel pattern of nitrogen assimilation?**

- **Under nitrogen limiting and replete conditions, what is the fate and flux of fixed energy and carbon? Can metabolite pools or the rate of carbon passing through these pools serve as biomarkers for nutrient status of *Prochlorococcus*? In natural oligotrophic communities do large phytoplankton and *Prochlorococcus* utilize similar metabolic pathways to assimilate nutrients as they become available?**

Chapter 2: To investigate the mechanisms utilized by *Prochlorococcus* that efficiently manage metabolic pathways as a function of their ever changing, but predictable energy source, we performed a set of experiments where cultures entrained in a solar cycle were sampled at various points during a simulated day. We discovered that *Prochlorococcus* can assimilate ammonia during the day as well as night. Our data may be understood to suggest that the loose control of carbon flow through metabolic pathways allows for opportunistic ammonium assimilation while specific temporal periods appear to be under tighter control. We hypothesize the atypical metabolism observed at this time may be tied to the availability of carbon and energy stores.

Chapter 3: To improve our understanding of the fate and flux of carbon and energy under nutrient stress, metabolic and physiological characteristics were observed in cultures grown under nitrogen limiting and nutrient replete conditions. Our observations of the balance of carbon and energy metabolisms under nitrogen limitation show carbon utilization and other physiological properties were strikingly different under nitrogen limited and – replete conditions. Cultures grown in nitrogen limited chemostats were observed to maintain large metabolic pools with low rates of labeled carbon moving through these pools. This may suggest metabolism and growth is not constrained at the stage of small metabolite production but rather the production of macromolecules from metabolites. While pools and the flow of recently fixed carbon through these pools were quantified, it has become clear that future investigations will be required to ascertain if such differences were due to passive effects, or if there is regulatory control at play for the anabolic pathways analyzed.

Chapter 4: To discern the effects of nutrient limitation on the metabolisms of plankton in oligotrophic environments, we compared intracellular metabolic profiles of cells grown in nitrogen-augmented microcosms to those of unamended controls in both *Prochlorococcus*-enriched and whole seawater samples. Our data provide evidence that large phytoplankton may respond to nitrogen enrichment by upregulating metabolic pathways allowing for recently fixed isotopically labeled carbon to be observed in nitrogen assimilatory metabolites. While nitrogen

influx induced the same metabolic response for pool sizes in *Prochlorococcus*-enriched microcosms, the lack of inorganic carbon incorporation into these metabolites suggest alternative mechanisms may be employed.

CHAPTER 2:

METABOLIC ANALYSIS OF *PROCHLOROCOOCUS* SP. MED 4 OVER A DIEL LIGHT CYCLE

Abstract

The daily oscillation of sunlight is suspected to be the most prominent variable recognized by plankton in the oligotrophic open oceans. The combined effect of this daily ebb and flow of energy and genomic streamlining in *Prochlorococcus* spp. is suspected to select for physiological characteristics to best utilize the daily flow of this energy source. Previous research has shown both natural and laboratory populations of *Prochlorococcus* undergo cell cycles predictably over diel periods but attempts to decipher the regulation through studies of the abundance of transcripts and proteins over the diel led to unclear results. To investigate the mechanisms utilized by *Prochlorococcus* that efficiently manage metabolic pathways as a function of their ever changing; but predictable energy source, we performed a set of experiments where metabolic biomolecules associated with carbon, nitrogen and energy metabolism were observed in cultures entrained in a solar cycle were sampled throughout a simulated day. We discovered that *Prochlorococcus* can assimilate ammonia during the day as well as night. Our data may be understood to suggest that the loose control of carbon flow through metabolic pathways allows for opportunistic ammonium assimilation while specific temporal periods appear to be under tighter control. We hypothesize the atypical metabolism observed at this time may be tied to the availability of carbon and energy stores.

Introduction

Throughout the remote and expansive waters of the oligotrophic open oceans each day is much like the day preceding it and those that follow. In the sunlit depths, the relatively warm temperature and low nutrient concentrations remain at nearly constant levels resulting in extremely stable ecosystems where the daily solar cycle provides one of the few dynamic environmental variables. These conditions select for remarkable facets of life including the evolution and subsequent dominance of a group of ultra-small and efficient photosynthetic phytoplankton, the *Prochlorococcus* genus [6]. As organisms that rely on the 'feast and famine' of photic energy as their ultimate energy source, the population must balance their collection, production, and utilization of energetic currency (ATP, glycogen, reducing potential) with

metabolic demands to optimize continuous growth in order to outpace competition and predation. For these microbes, much like the environment in which they thrive, metabolic pathways are thought to be utilized in a predictable pattern over the course of the day [15], but day-to-day variation is minimal. An estimated octillion (10^{27}) [5] of the world's smallest and most abundant photosynthetic organisms are physiologically synchronized as a function of the daily ebb and flow of solar energy to prevent futile cycling of antagonistic metabolic processes.

The coordination of this metabolic dance is even more remarkable considering their miniscule genome - the smallest known for any free-living photosynthetic organism. Studies suggest the genome of *Prochlorococcus* spp. was incrementally reduced through an evolutionary mechanism known as genome streamlining. This process drives organisms to retain only the physiological characteristics that are regularly used while redundant or ancillary genes can become inactive and eventually lost [8, 35]. In this manner genome streamlining guided the evolution of a simple and efficient photosynthetic machine. For example, *Prochlorococcus* does not have a traditionally functioning biological clock but appears to employ a timing mechanism that must be reset after each diurnal cycle. It has been observed that the gene responsible for the automatic reset of the biological clock, *kaiA*, appears to have been lost through stepwise deletion that has been attributed to genome streamlining [17, 36]. These findings have been described as simplified "hourglass" mechanism utilized in *Prochlorococcus* compared to the precise "Rolex" timepiece employed by more complex cyanobacterial systems [37]. From these findings one might infer the necessity of biological timing in cyanobacteria as the essential mechanism was not completely lost in *Prochlorococcus* spp. but reduced in a way that still allows rudimentary function. As such, like the elegant and streamlined "hourglass" timepiece employed by these microbes, the physiology of *Prochlorococcus* spp. will provide crucial insights for our collective understanding of the indispensable and efficient mechanisms involved in photosynthesis.

Prochlorococcus is a prototroph whose genome encodes all the genes required for the utilization of solar energy and carbon dioxide to build a cell; however, the way in which this blueprint is utilized is unknown. Given that their source of energy, sunlight, is abundant at times

and nonexistent at others, a deeper knowledge how energy utilization and biomass production is orchestrated during the transitions from day to night is imperative to establish a baseline for future investigations of global metabolic function in the *Prochlorococcus* cell. While the research community has made recent gains in understanding the regulation of gene expression in *Prochlorococcus*, there is a critical lack of information in how gene regulation at the level of mRNA and protein translate into control of metabolic flow. As the levels for both the mRNA [15] and protein [14] are known for this organism under similar diel growth conditions, we believe that by integrating these data sets with our metabolite and energy status data we will better understand the interplay between the informational, regulatory, and metabolic systems.

The low daily physical variability and predictable gradient of available solar energy the of the oligotrophic ocean help select for organisms that can "anticipate and prepare" for the conditions in the future. Transcript abundances for approximately 80% of *Prochlorococcus* genes vary as a function of the time of day [15]. The timing of the peaks and the upregulation of genes can provide insights into the preparation these cells go through to be ready for the next phase of growth. For example, the upregulation for the photosynthetic carbon fixation enzyme, RuBisCO, appears to begin in the middle of the night and reaches the maximal expression by late morning. This pattern suggests cells are prepared to collect and utilize solar energy hours before the sun rises [15]. Understanding how this minimal microbe is capable of dominating these ocean deserts will rely on observing how they regulate and coordinate metabolic processes over the daily cycle of light. Generation of a deeper understanding of the regulation of metabolic processes evolved to "anticipate and prepare" for the one constant variable realized by these genomic streamlined phytoplankton may provide insights into the keys for their ecological success.

Depending on current cellular demands, the collection of photic energy in cyanobacteria can be modulated through the linear and/or cyclic electron flow through their photosystems. The reduction of inorganic carbon is an energy intensive process requiring both ATP and reducing power to drive metabolites through the Calvin cycle. By segregating the photosynthetic demands

for carbon fixation and other anabolic metabolisms *Prochlorococcus* might be able to optimize their energetic collection and allocation to suit their current energetic demands. Linear electron flow through PSII and PSI provides a ratio of reductant to ATP that closely matches the demand for carbon fixation whereas cyclic electron flow around PSI will generate ATP at the expense of NADPH reduction. By modulating a combination of linear and cyclic electron flow, photosynthetic organisms can generate adenylate phosphate pools and reduction potentials to match their energetic demands. Previous observations have reported a significant fraction of total daily carbon fixed in *Prochlorococcus* occurs before midday [15, 38]. These observations suggest that during the morning a majority of the daily inorganic carbon is fixed and assimilated as metabolic biomass. During the afternoon small intermediate metabolites synthesized during the morning can be used for anabolic metabolisms such as protein and DNA synthesis. The synchronized cell cycles in *Prochlorococcus* have been established showing evidence for populations moving from G_1 growth phase in the morning to S phase in the afternoon as they prepare to divide after dusk [16, 18, 19]. The high demand of reducing potential in the morning may suggest demand for linear electron flow early in the day and cyclic electron flow around PSI during the afternoon as the demand for reduction potential decreases.

Here within we describe a set of two experiments designed to shed light on the temporal coordination of metabolisms in *Prochlorococcus.* In this series of experiments isotopically labeled carbon and nitrogen were followed through glutamate - the most abundant metabolite - as well as cellular carbon and energetic potential were observed over diel light cycles. Integration of these data with previous observations will help provide a fundamental, mechanistic understanding of how a series of biosynthetic machines are coordinated within a cell utilizing only very basic ingredients, primarily light, carbon dioxide, and water.

Results and Discussion

Diel Metabolite analysis

To improve upon our understanding of the role of temporal regulation and the balance of nitrogen and carbon metabolisms in *Prochlorococcus* we used LC-MS/MS to track both carbon

and nitrogen through the structure of glutamate for six time points over the course of one diel photic period. In our observations and in investigations of a wide diversity of other microbes including heterotrophic plankton [39], phytoplankton[40], and *E. coli* [41], glutamate has been observed as the abundant metabolite. The observations that this metabolite can be found in very high concentrations for many living system and possibly suggests a conserved metabolic importance in global metabolisms. At the intersection of nitrogen and carbon metabolisms levels of the pools of this metabolite and the rate of flow through these pools may play a key role in the balance of nitrogen and carbon metabolisms. By tracking isotopically labeled nitrogen and carbon through this metabolite over a diel cycle we stand to gain a deeper understanding of the regulation the important processes involved in nitrogen assimilation.

To better understand inorganic carbon and nitrogen incorporation into the structure of metabolites within *Prochlorococcus* we employed two analytical methods to model isotopically labeled carbon into metabolites; Mass Distribution Vector (MDV), which allows for an observation of the spread of isotopic labeling within the carbon backbone metabolite and Fractional Composition (FC) analysis, which accounts for the fraction of labeled to total atoms in each metabolite over the labeling time series[42].

Nitrogen:

Glutamate contains only one nitrogen atom per molecule, therefore the nitrogen isotopic labeling is either unlabeled (M+0) or fully labeled (M+1) allowing for the FC of the metabolite to reduce down to the ratio of unlabeled to labeled ion counts. Our FC analysis suggests that incorporation rates of nitrogen into glutamate are generally stable over the course of the diel. For most of our diel labeling experiments, we observed a linear incorporation of N throughout the time series. By the end of the 90 minute experiments, approximately one quarter of the glutamate ions contained the isotopically labeled nitrogen with slightly greater final labeling observed during the morning time point (3100; ~33%). The sole exception to this observation is just after sunset when we observed nitrogen incorporation to initiate at very high levels, but the FC decreased from 30 to 60 minutes and again from 60 to 90 minutes. During the first 30

minutes the FC suggests nitrogen incorporation rates were three times that for any other time point tested. At this time point approximately 25% of the glutamate ions observed contained an isotopically labeled nitrogen, but after this initial burst of nitrogen assimilation the FC drops significantly. The apparent high capacity for nitrogen assimilation but subsequent decrease in new nitrogen assimilation may provide evidence that a currently unknown regulatory mechanism balances acquisition and assimilation of nitrogen (Fig. 2) under the replete conditions tested. Interestingly, during the dusk period when this unique FC pattern is observed both the transcripts and proteins of the GS-GOGAT pathway are elevated [14, 15]. This could explain the high initial rate of ammonium assimilation, but the rapid drop in assimilation after 30 minutes indicates that factors other than protein abundance (e.g. substrate concentration, post-translational modification) may be at play shortly after the day to night transition in *Prochlorococcus*.

Carbon:

The five carbon structure of glutamate allows use of both FC and Mass Distribution Vector (MDV), analysis to observe the labeling trends. As stated above FC analysis provides an estimates the ratio of total labeled atoms to unlabeled atoms in the molecule. FC of glutamate (Fig. 2; hashed lines) showed labeling occurring at the greatest rates during the morning (3100) and both noon time points (1200/3600). During these times *Prochlorococcus* actively fixes a majority of the carbon it will fix over the course of the day and our data provides evidence that this recently fixed carbon can serve as substrate for nitrogen assimilatory pathways even though the genes that facilitate this are not at peak expression. During the afternoon as photosynthetic rates drop we observed a diminished rate of recently fixed carbon incorporating into the glutamate backbone. Not surprisingly, we observed the lowest rates of label incorporation from bicarbonate into glutamate at night, when absence of light energy restricts photosynthetic carbon fixation. What may be surprising is that although the rates are lowest at night, the observed rates are not equal. The midnight (2400) time point appears to be incorporating label at very low rates while the rates for just after sunset are not observed to increase over the labeling experiment (Fig. 2).

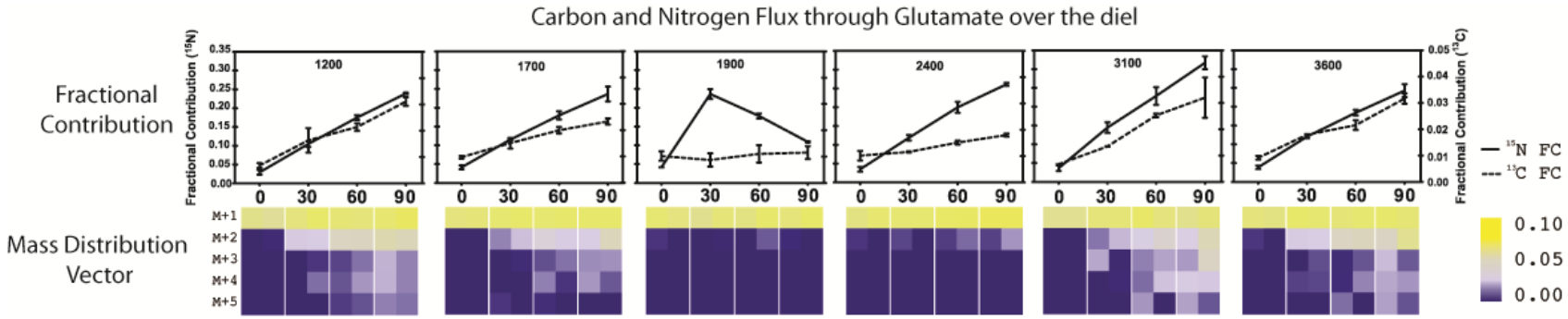


Figure 2: Carbon and Nitrogen labeling of Glutamate over the diel

Isotopic labeling of glutamate observed over six labeling experiments over a diel cycle in MED4. Experiments cover a 24 hour photic period begin and end at noon (1200 and 3600; respectively) with sunset and sunrise occurring at 1800 and 3000 respectively. Fractional Contribution (FC) of both isotopic nitrogen (solid line; left axis) and carbon (dashed line; right axis) in parallel experiments. Mass Distribution Vector (MDV) shows distribution of 13-C labeled isotopologues.

Carbon labeling patterns observed as the Mass Distribution Vectors (MDV). This analysis method describes the distribution of isotopic label between mass isotopomers of the metabolite but is sensitive the natural abundance of ^{13}C. Our analysis shows that although the morning (3100) and noon (1200 and 3600) glutamate ^{13}C FC is not significantly different, we observed a significant difference in the distribution of the label. During the morning time point (3100) we observed a larger proportion of multiply-labeled isotopomers (sum of M + 3, M +4, M+5) than we observed during the two noon time points (ANCOVA; 1200 reference, 3100 P=0.010, 3600 P=0.159), but less M+2 isotopomer. This may suggest that during the morning metabolic cycling within the Calvin cycle results in multiply labeled photosynthate (PGALD) that has an abundance of isotopic carbon prior to undergoing the metabolic pathway for glutamate synthesis. On the other hand, the increased abundance of low level ^{13}C labeling observed in the glutamate skeleton during the afternoon suggests a reduction in the cycling of previously labeled metabolites through the Calvin cycle. As discussed previously in the carbon FC of glutamate at 2400 is very low but we observe a trend indicating carbon is slowing being incorporated into the carbon skeleton of this metabolite. Our MDV analyses provides additional evidence of this occurring through an increase in the M+1 and M+2 isotopologues during the 2400 time point. Natural abundance of ^{13}C diminishes the appearance of this trend in our colorimetric heatmap but linear regression analysis shows an approximate 4 fold increase in the rate of carbon incorporation at midnight over the dusk time point where the combined MDV of M+1 and M+2 increases at a rate of $9.1*10^{-5}$ MDV*min^{-1} (R^2=.11) at dusk and $3.8*10^{-4}$*min^{-1} (R^2=.92) at midnight.

The LC- MS/MS used to observe metabolite abundance and labeling in these experiments relies on liquid chromatography to separate metabolites by physical characteristics prior to use of two mass spectrometry measurements to accurately identify metabolites. After chromatographic separation, the first quadrupole of the mass spectrophotometer measures the mass of the initial ion (metabolite parent mass). The ionized metabolite flies to the collision chamber where collision induced disassociation of the molecule generates fragments that are measured in the third quadrupole (product mass). The collected data provides information that allows for the

identification of metabolites with similar physical properties and parent mass to charge ratios while making observations on both the quantity of labeled atoms in each metabolite and allows for localization of the isotopic atom under specific circumstances.

One case where our LC-MS/MS data can provide localization of isotopic carbon in the structure of a metabolite is for glutamate. In the collision chamber, glutamate fragments so that the carbon at the amino terminus falls off (C1; Fig. 3). The product fragment containing four carbons (C2-C5) is measured in the third quadrupole allowing the researcher to determine whether the isotopic carbon in the parent molecule was originally at either the C1 or one of the C2-C5 positions (Table 1). Additionally, the stereospecificity of enzymes immediately preceding the *de novo* synthesis of glutamate (*i.e.* citrate synthase, aconitase, and isocitrate dehydrogenase) allows for the prediction that the anaplerotic carbon fixing enzyme immediately preceding glutamate synthesis, phosphoenolpyruvate carboxylase (PepC), will contribute the C5 carbon to glutamate in *de novo* synthesis. The traceable and enzyme specific introduction of carbon allows one to infer the activity of PepC in the generation of the carbon backbone of glutamate as all isotopic carbon associated with this enzyme would be measured in the C2-C5 fragment. During evening periods when solar energy is not available to fuel the Calvin cycle, we would expect all isotopic carbon fixed through the mechanisms of PepC. If this is the case we should observe an increase in the FC of Glutamate 1-1 and not 1-0. Interestingly our data show carbon incorporation into glutamate at our midnight time point generates a labeling pattern showing the carbon backbone became labeled for both fragments (Fig. 3, Table S4). The observed labeling of glutamate provides evidence that the carbon incorporated at midnight is fixed through the activities of both PepC and some other mechanism that results in labeling at the C1 position and suggests activity of the Calvin cycle, carbamoyl phosphatase or a previously unrecognized mechanism may be involved in this labeling pattern.

Cell cycle analysis

As the ultimate energy source for phytoplankton the daily ebb and flow of solar energy reflects strongly on temporal metabolic mechanisms segregated in a way to fuel constant growth.

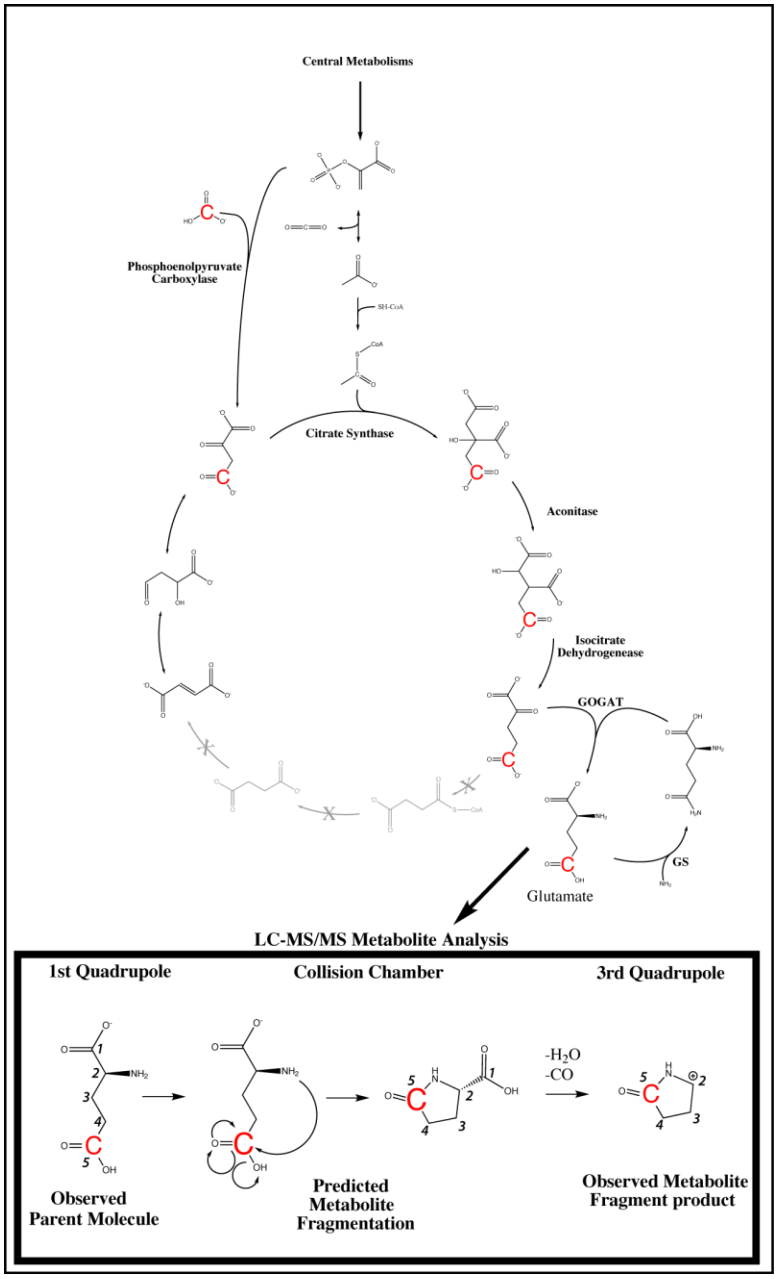
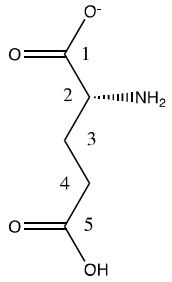
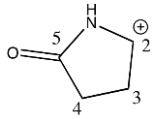


Figure 3: Predicted labeling of glutamate by PepC.

Isotopically labeled inorganic carbon (red C) fixed through the action of phosphoenolpyruvate carboxylase (PepC) contributes the C5 carbon in glutamate. The predictable fragmentation of glutamate in the mass spectrophotometer generates a fragment containing carbon atoms 2-5 of the parent glutamate molecule.

Table 1. Targeted m/z ratios: ^{13}C and ^{15}N glutamate

Glutamate Structure	Predicted fragment	Tracer isotope	Metabolite identification	Parent M/z	Product M/z	Labeled atoms observed in Parent	^{13}C atoms at location 1	^{13}C atoms at locations 2-5	^{15}N atoms observed in fragment
		^{13}C	Glutamate	148	84	0	0	0	n/a
			Glutamate 1-0	149	84	1	1	0	n/a
			Glutamate 1-1	149	85	1	0	1	n/a
			Glutamate 2-1	150	85	2	1	1	n/a
			Glutamate 2-2	150	86	2	0	2	n/a
			Glutamate 3-2	151	86	3	1	2	n/a
			Glutamate 3-3	151	87	3	0	3	n/a
			Glutamate 4-3	152	87	4	1	3	n/a
			Glutamate 4-4	152	88	4	0	4	n/a
			Glutamate 5-4	153	88	5	1	4	n/a
		^{15}N	Glutamate	148	84	0	n/a	n/a	0
			Glutamate 1-1	149	85	1	n/a	n/a	1

To provide for the steadfast energetic demands of continuous metabolisms during the predictable 'feast and famine' of available energy, cells must efficiently utilize solar energy available during photic periods while storing some to drive metabolic activities during aphotic periods. These processes generate a strong temporal demand for the regulation of energy collection, expenditure, and storage. In photosynthetic cells 'energetic currency' is generated through the light-driven reactions of photosynthesis that produce both reductants and ATP. Energetic status over the course of a diel photic period was observed through the measurements of the carbon and energy stores, the energetic potential, and reductant pools.

To gain a greater understanding of how *Prochlorococcus* modulate their energy stores over photic light cycles we performed an additional experiment to observe the cellular carbon and energy stores by tracking polysaccharide (glycogen) pools, the adenylate energy charge, and the ratio of the total pools of oxidized and reduced NADP[H] to NAD[H] over the course of one photic period beginning and ending at midnight.

Carbon and Energy Stores

Obligate phototrophs depend on solar energy during photic periods (daylight) to perform all the metabolic activities they perform over the course of a 24 hour cycle. Therefore they must allocate available energy to fix and store carbon and chemical energy for biological activities at night. For *Prochlorococcus*, like most cyanobacteria, these reserves are believed to be stored in the chemical structure of glycogen [43]. Glycogen is a large polymer of glucose monomers linked by linear α 1-4 glycosidic bonds or branched α 1-6 glycosidic bonds. The abundance of reducing ends, acting as points for enzymatic cleavage of glucose monomers, allows for quick utilization of carbon and energy stores when demand is high.

We report a significant increase in the pool of glycogen occurring throughout the photic period where we observed minimal pools of glycogen at dawn and a gradual increase in the pools as the photic period progressed. At dusk we observed peak glycogen pools that were observed decline throughout the night (Fig. 4). As discussed below, these data provide evidence for the

temporal regulation of glycogen synthesis and post transcriptional control of *glgA* in *Prochlorococcus*.

In the related phytoplankton *Synechococcus* species str. WH8103 both the transcriptional abundance of glycogen synthase (*glgA*) and stores of the polysaccharide were observed to increase throughout the afternoon [44]. Interestingly, peak abundance for the glycogen synthase gene at dawn in *Prochlorococcus* sp. MED4 [15] provides evidence that glycogen synthase (*glgA*) is upregulated much earlier than was observed in the previously mentioned *Synechococcus* strain. The divergent transcriptional regulation between these highly related cyanobacteria may reflect possible differences in the temporal utilization of metabolic pathways, but recent observation of peak protein abundance for these transcripts in *Prochlorococcus* suggest that although expression of the genes was observed at sunrise the proteins were observed at peak abundance closer to noon [14]. Our data correspond well with previous data that show pools of glycogen increase after noon while remaining low during the morning. This apparent lag between peak transcript and protein abundance may suggest post-transcriptional regulation on the glycogen synthase genes in *Prochlorococcus*. These observations suggest that although differences between temporal regulation on transcription are observed in *Prochlorococcus* and *Synechococcus*, overall regulation on glycogen synthesis may be maintained.

Reduction potential

The ratio of the total anabolic (NADP[H]) and catabolic (NAD[H]) reductant pools were measured over the course of the cell cycle. Our data show the ratio of these reductant pools vary as a function of the time of day (Fig. 4). Because NAD[H] is generally thought to be used in respiration and catabolic metabolisms while NADP[H] functions as an anabolic reductant, the ratio of these two reductants may provide insights into the overall metabolic state cells are growing under. During photic periods linear electron flow through photosystems II and I reduces $NADP^+$ to NADPH. This reductant pool is used in carbon fixation and other anabolic metabolisms. In addition to these processes, at night the catabolism of glycogen and the resulting glucose monomers are oxidized through the pentose phosphate pathway generating

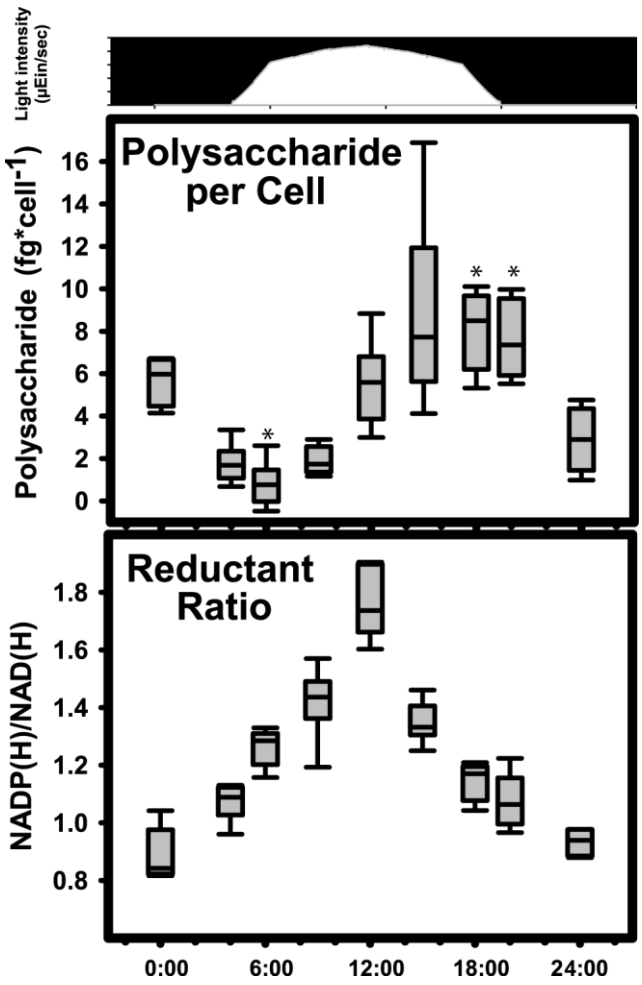


Figure 4: Polysaccharide and Reductant pools over a diel cycle

Pools of polysaccharide and the anabolic to catabolic reductant ratio in MED4 cultures. Experiments begin and end at midnight (0:00 to 24:00). For reference, experimental light levels simulating natural diel patterns are displayed as the white period above the figures. Asterisk indicates significant difference in pairwise multiple comparison (Dunn's method; $p < 0.005$)

reductant (NADPH). As such NADP[H] is thought to have important metabolic roles throughout the photoperiod. Without an intact TCA cycle the role of NAD[H] pools are poorly understood but they are expected to be involved in cellular respiration where the largest demand for this reductant would be expected to be during evening hours. We report the ratio of NADP[H] to NAD[H] over a diel cycle to increase during the early daylight hours until noon when it decreases throughout the afternoon (Fig. 4).

Adenylate Energy Charge

In biological systems, chemical energy is stored in the chemical bonds of phosphorylated nucleotides and the maintenance and control of these stores through metabolic mechanisms is central to all living cells. For *Prochlorococcus* the ultimate energy source, sunlight, is used to generate an electrochemical gradient that can be used to convert ADP to ATP through the use of the ATPase in the thylakoid membranes in a process called photophosphorylation. The ATP generated through photophosphorylation is utilized for immediate cellular demands including synthesis of biological molecules and cellular maintenance. During times when photophosphorylation cannot support cellular energy demands such as those experienced when light is not available, cells must regenerate ATP through respiration or substrate level phosphorylation. Therefore during the day light hours, when photic energy is abundant, *Prochlorococcus* must balance energy utilization of current cellular demands with the storage of energy in chemical bonds that can be used during the night.

The adenylate energy charge (AEC), first described by Atkinson in 1967 [45], measures the energetic potential of a population through the ratios of ATP, ADP, and AMP (AEC=([ATP] +0.5[ADP])/([ATP]+[ADP]+[AMP])). The resulting parameter, a scalar between 1 and 0, was defined by the authors as one half the average abundance of phosphate groups per nucleotide and provides a scaling index to compare the energetic status of organisms across diverse lineages that may have highly variable absolute pools of adenylate phosphates. As the universal cellular energy currency ATP concentration as well as its ratio to ADP and AMP (AEC) are not only involved in cellular regulation of energy utilization and storage but also in the regulation of

nutrient acquisition and biosynthetic pathways. The myriad of metabolic processes that rely on the ratio and pool sizes of the adenylate phosphate pool require delicate balance to maintain a stable and ready pool of energy for the cell while regulating appropriate metabolic activities. Across diverse life forms the AEC has been observed to fall within a narrow range for actively growing cells (0.7-0.9), but results describing this ratio in phytoplankton have been reported vary (0.3 – 0.8) [40, 46].

The AEC in *Prochlorococcus* MED 4 appears to be at homeostasis around 0.6 over the course of the diel (Fig. 5), but the homeostasis of the AEC over the diel is contrasted by the observation that the size adenylate phosphate pools fluctuate as a function of the time of day (Fig. 5). Our data show pools of these adenylate phosphate moieties to increase over the course of the day and decrease over night while the ATP:ADP was lowest at sunrise (0600; 0.87 ± 0.5) and greatest just after sunset (2000; 2.02 ± 0.6). The temporal variation in the adenylate pool but not the AEC may imply that the homeostatic AEC is essential for maintaining intracellular signaling, while energetic supply and demand may reflect on the temporally variable pool size of the adenylate phosphates as well as the ATP:ADP ratio.

These observed peaks for adenylate phosphate moieties occur a few hours prior to peak transcription and translation of adenylate kinase (AK; ATP + AMP ⇔ 2 ADP). This important regulatory enzyme has been implicated in the maintenance of the adenylate energy pool as the directionality of the reaction it catalyzes is dependent on the pools of its substrates and products. During the night when upregulation of this enzyme was observed, ATP pools diminish and cannot be replenished by photophosphoylation. Use of AK to balance the growing ADP pools with ATP and AMP may assist in the upkeep of ATP concentrations and maintenance of the AEC overnight.

Conclusions

The daily oscillations of solar energy into the surface layer of the open oceans is one of the few variables experienced by natural *Prochlorococcus* populations. Genomic streamlining

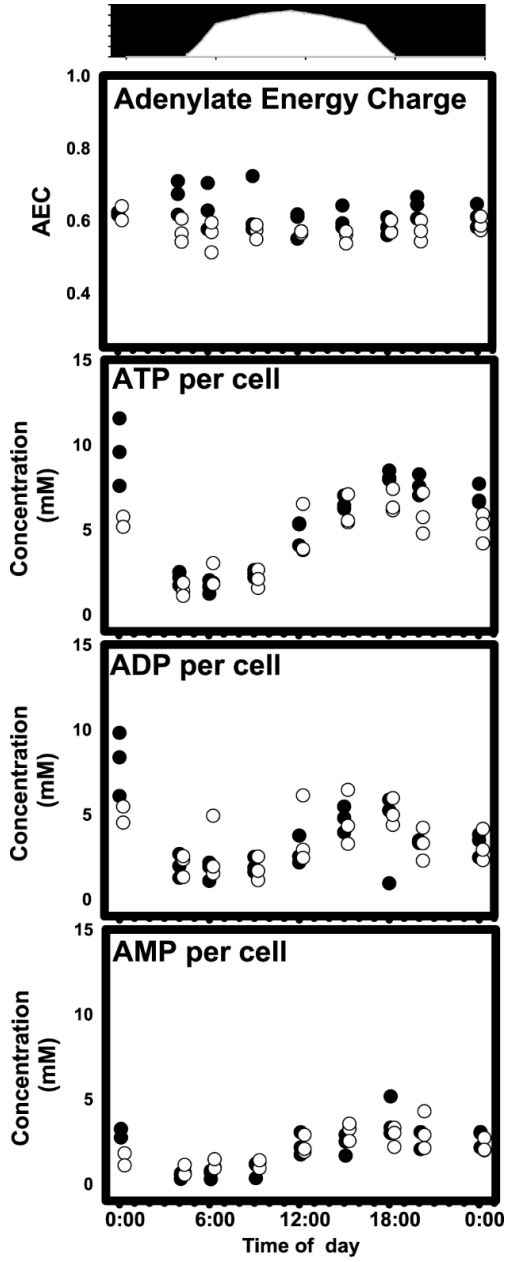


Figure 5: Adenylate Energy Charge and Adenylate Phosphate pools over a diel

The ratio of the Adenylate Energy Charge (AEC) and pools of adenylate triphosphate (ATP), adenylate diphosphate (ADP), and adenylate monophosphate (AMP) described above. Technical triplicates of biological replicates vat 1 (white circles) and vat 2 (black circles). Experiments begin and end at midnight (0:00 to 0:00). For reference, experimental light levels simulating natural diel patterns are displayed as the white period above the figures.

has given rise to the dominance of these simple and efficient "hourglass" wielding phytoplankton. During the daily feast and famine of solar energy, cyanobacteria must ensure consistent metabolic capabilities by temporally regulating energy collection, utilization, and storage. To investigate the mechanisms utilized by *Prochlorococcus* that efficiently manage metabolic pathways as a function of their ever changing, but predictable energy source, we performed a set of experiments where cultures entrained in a solar cycle were sampled at various points during a simulated day. In the first of the two experiments isotopic carbon and nitrogen were tracked through the structure of glutamate and in the second the energetic status was observed by following glycogen, adenylate phosphate pools, and reductant pools.

Previous observations provide evidence that a majority of the total carbon fixed in *Prochlorococcus* cultures to occur before midday [15, 38]. This observation suggests that the photic energy captured throughout the photic cycle is partitioned to specific metabolisms. Morning sunlight is thought to supply energy demands for carbon fixation generating pools of small metabolic intermediates. After the initial high rate of carbon fixation in the morning, it has been proposed that the solar energy collected during later periods of the day is directed to anabolic metabolisms polymerizing the small metabolites fixed during the morning into essential cellular components. These two processes – morning carbon fixation and afternoon biomolecule synthesis – require different ratios of ATP and reductant. To balance this energetic demand electron flow through photosystems can be altered to increase production of ATP or NADPH (reviewed in [38]). In our experiments, we observed an increase in the polysaccharide pool and adenylate phosphate pool throughout the afternoon, while anabolic to catabolic reduction ratios (NADP[H]/NAD[H]) declined from the observed peak at noon (Fig. 4). These data may provide evidence for the segregation of linear and cyclic electron flow around PSI. Polysaccharide synthesis, which utilizes phosphorylated nucleotides for the polymerization of saccharide monomers, during the afternoon demands a larger fraction of ATP/NADPH than is required for the reduction of inorganic carbon by the Calvin cycle [38]. Our data provide evidence that this demand is met through the observed increase in adenylate pool and the ATP/ADP ratio. As anabolic reductant demand decreases, reduced electron flow to $NADP^+$ may generate an

increased electron flow around PSI and be used to produce a greater proton motive force to drive ATPase. Our data may suggest that this switch can be modulated by a simultaneous increase in the adenylate pool and decrease in the ratio of NADP[H] to NAD[H] during the afternoon.

The temporal rates of isotopically labeled carbon through glutamate appear to follow similar trends observed for previously carbon fixation rates (*i.e.* Morning (3100) > Noon (1200 and 3600) > Afternoon (1700) > Night (1900 and 2400). This flow of carbon through glutamate may be understood as evidence for loose regulation of carbon flow through metabolic pathways that can occur outside of the upregulated metabolisms as predicted by transcriptomics (e.g. oscillating expression of isocitrate dehydrogenase[15]), mirroring what has been observed in proteomic studies[14]. The observed rates of isotopically labeled nitrogen into this metabolite under the nitrogen replete conditions tested provides an additional line of evidence that nitrogen assimilation proceeds as a function of nitrogen availability and not through regulational control for most of the observed times. In the oligotrophic ocean where these cyanobacteria persist regulatory mechanisms that would bar the capacity to assimilate nitrogen as it becomes available would reduce their competitive edge. For this reason it may not be surprising to see cultures that are in a constant state with replete nitrogen pools incapable of restricting ammonium assimilation.

Shortly after dusk (1900) we observe carbon and nitrogen labeling for glutamate to be different than the patterns observed at other time points during our experiment. At this atypical time point, our data show the fractional contribution of nitrogen decreases after an initial burst during the first 30 minutes and very low carbon incorporation. The low rate of isotopic carbon incorporation into the backbone of glutamate during our dusk (1900) time point shows carbon is not fixed by phosphoenolpyruvate carboxylase – a necessary step in the *de novo* synthesis of glutamate – nor through any other mechanisms. These data provide evidence that just after sunset *Prochlorococcus* do not completely fulfill carbon demands for nitrogen assimilatory pathways and may suggest unknown regulatory mechanisms for nitrogen assimilation occur at a time in the day when *Prochlorococcus* has been observed to increase protein and transcript

abundance for GS and GOGAT [14, 15]. A few hours later (2400), incorporation of isotopically labeled inorganic carbon resumes. During our midnight time point *de novo* synthesis of glutamate appears to occur as observed by the increase in isotopically labeled glutamate (^{13}C-FC; Fig. 2), but we present evidence for inorganic carbon incorporation by means other than PepC (Fig. 3). This may be intriguing as it appears that the carbon is fixed through RuBisCO or some other carboxylation reaction. The increased in isotopic carbon in glutamate observed at midnight provides evidence that inorganic carbon can be incorporated into glutamate through means other than the anaplerotic mechanism of PepC. This unexpected results raises questions regarding why it is necessary and the pathways utilized in this process.

After the first 30 minutes of the dusk time point in our labeling experiment, labeled nitrogen was observed at very high levels in glutamate but the amount of isotopically labeled nitrogen progressively dropped as the experiment continued. The initial increase in the FC of isotopically labeled nitrogen in glutamate and subsequent drop over the next 60 mins of the dusk time point was different from other time points where the FC's were observed to increase steadily as a function of time. These observations may provide evidence for post-translational regulation just after sunset. At this time in the diel energy cycle of *Prochlorococcus* the available cellular reduction potential generated by photosynthesis and glycogen catabolism may be insufficient for the ferredoxin-dependent GOGAT enzyme. The recent loss of their photic energy supply may cause a hiccup in electron transport, diminishing reductant pools that can reduce ferredoxin, and/or insufficient glycogen catabolism rates limiting the carbon and energy supplies needed for continued nitrogen assimilation. The increased levels of ATP during the evening would not limit GS activity and as such our data cannot make claims on the regulatory mechanisms involved in this ammonium assimilating reaction. Our data may be understood to suggest that the loose control over metabolic pathways allows for opportunistic ammonium assimilation while periods of tight regulational control may be tied to the availability of carbon and energy stores.

Materials and Methods

Culturing and Sample collection

For both experiments described culturing conditions were identical. For these experiments axenic *Prochlorococcus* sp. MED 4 cultures were grown from a master culture maintained in successive batch culture for greater than 6 months at experimental conditions; nutrient replete AMP media, 22°C, 14 hours of gradually increasing and decreasing light levels designed to mimic natural levels of light over the course of the day. Duplicate cultures were grown in slowly stirred 13.25 L Pyrex carboys. At experimental time-points culture was non-invasively sampled using a peristaltic pump. All materials and containers contacting culture were acid washed.

Diel Metabolomics Methods

In order to maintain the purity of the culture we collected samples from the 10L carboys using a peristaltic pump system designed to reduce the risk of contaminating the cultures during sample collection. At each diel time point approximately 0.9L was pumped from each replicate carboy into graduated cylinders. The 210ml was quickly transferred to sterile 250ml acid washed bottles, spiked with nutrient cocktail and placed back into the incubator. From the collected parent culture 20 ml was simultaneously collected on 0.22μm MAGNA nylon filters. At each time point during the labeling experiment 40 ml was removed from the spiked culture and collected on two 0.22μm MAGNA nylon filters – 20 ml each. Filters were then collected and flash frozen in liquid nitrogen and stored at -140°C until extraction and analysis (2-4 weeks).

Nutrient spike:

Nutrient additions were added to a final concentration of 3.2mM NH_4Cl, 24mM HCO_3^- and 0.2 mM PO_4^- where either the nitrogen in NH_4Cl or the carbon in HCO_3^- was labeled (^{15}N and ^{13}C respectively) resulting in a nutrient addition five times that of ambient levels.

LC-MS/MS:

Samples flash frozen and stored -140°C were extracted as previously described. Briefly defrosted samples on filters were thawed, extraction solvent containing internal standards (1.7mM benzoic acid and 4.25mM Tris for negative and positive mode respectively) was repeatedly pipette over the filters to remove cells and metabolites from filters, and transferred to Eppendorf tubes. Extraction solvent containing metabolites was centrifuged at 16.1 rpm for 5 mins to remove particulates and supernatant was transferred to an autosampler vial. Samples were analyzed on a Finnigan TSQ Quantum Discovery Max.

Data analyzation

Data was analyzed using Thermo Scientific™ Xcalibur™ software platform. Known metabolites were manually selected and integrated by m/z and retention time for each sample. Fold changes were calculated and the data were transformed and clustered using Cluster software [47]. Heat maps were then generated from clustered data using Java Treeview [48] software.

The Mass Distributed Vector (MDV) [eq. 1] and Fractional Contribution (FC) [eq. 2] analyses are useful tools to interpret labeling in metabolomics experiments and have been described previously [42]. The MDV is a method to measure the fractional abundance of each isotopologue to the sum of all isotopologues of that metabolite. This method describes the distribution of labeled isotopologues for each metabolite. Fractional Contribution (FC) may be used to develop a better understanding the abundance of isotopic label within each metabolite over an experiment. This can be determined by calculating ratio of the relative number of labeled carbon atoms (relative labeled carbon; RLC) to the total relative number of carbon atoms in that metabolite (relative total carbon; RTC) [eq. 2].

$$[1]\ Mass\ Distributed\ Vector\ (MDV) = \frac{\mathrm{IC}}{\mathrm{TIC}} = \frac{\mathrm{IC}_{(M+i)}}{\sum_{(i=0)}^{c}(\mathrm{IC}_{(M+i)})}$$

$$[2]\ Fractional\ Contribution\ (FC) = \frac{\mathrm{RLC}}{\mathrm{RTC}} = \frac{\sum_{i=1}^{c}(\mathrm{IC}_{(M+i)} * i)}{c\sum_{(i=0)}^{c}(\mathrm{IC}_{(M+i)})}$$

The RTC per metabolite was quantified by summing integrated ion count peaks for each isotopologues ($IC_{(M+i)}$) specific to that metabolite – the same as TIC in eq. 1. The TIC is scaled to the total number of carbon atoms in the metabolite (c) to get the RTC. Next, the relative abundance of isotopically labeled carbon associated with that metabolite is determined (RLC). This was calculated as the sum of the product of isotopologues, $IC_{(M+i)}$, and the number of labeled carbon atoms in the metabolite (*i*).

Cell Energetic cycle methods

Adenylate energy charge, glycogen pool sizes, NAD[H], and NADP[H] were measured at 9 time points over the course of the day. At each time point approximately 950 ml of culture was pumped from replicate vats, to 1 L polycarbonate bottles. The cultures are subdivided into 3 technical replicates of 300 ml each. Biological replicates in technical triplicate were pelleted via centrifugation (15 minutes at 15000 g with half speed acceleration and deceleration) and resuspended in 1 ml fresh AMP. Cell concentrate was partitioned for analysis as described below.

Sample Collection and extraction

Nucleotide extraction, enzymatic conversion and firefly luciferase assay was modified from the previously described protocol of Karl and Holm-Hansen [49]. Briefly, 0.5 ml of resuspended pellet was added to 2.0ml boiling 25mM Trizma base (pH 7.40). The samples were boiled for 15 mins, allowed to cool to room temperature, flash frozen in LN_2, and stored at -80°C.

Enzymatic conversion and assay

Samples were defrosted to room temperature and 0.1 ml sample was added to each of 3-96 well plates containing 0.05 ml of enzymatic buffer (A“T”P, A“D”P, or A“M”P; see below). Extracts were sealed in 96 well plates and incubated at 30°C for 30 mins. Transfer of the sealed plates to a boiling water bath for 3 mins stopped the enzymatic conversion. Following the

enzymatic conversion and subsequent stoppage of reactions the plates were allowed to return to room temp when they were assayed for total ATP concentration using the firefly luminescence method. ATP concentration was measured using an Orion-L microplate luminometer (Berthold Detection Systems, Pforzheim, Germany). In short, 0.1ml firefly luciferase extract is injected into wells and the peak luminescence was determined over a 5 second period following an initial 2 second delay.

Adenylate Energy Charge

The enzymatic buffers- "T", "D", and "M"- were 0.75 mM sodium phosphate buffer (pH 7.4; Cold Spring Harbors protocol) where the "D" and "M" buffers both contained 0.6mM phophoenolpyruvate (PEP) and 40 u/ml pyruvate kinase. The "M" buffer was also amended with 80 u/ml myokinase. Firefly luciferase extract was made as described by manufacturers, as per the manufacturers suggestion an additional 0.26 mM luciferin was added to increase sensitivity of the assay. The extract was aged for 6 hours at room temperature in the dark prior to the assay.

Glycogen

Sample collection, extraction, and precipitation of glycogen – Glycogen extraction and measurement was performed as previously described [50]. Briefly 0.5 ml resuspended pellet was flash frozen in LN_2 and stored at -80°C until samples were extracted. Frozen culture was freeze dried, resuspended in 0.5 ml 30% KOH, and vortexed vigorously for approximately 20 mins. Following resuspension samples were placed in a boiling water bath for 4 hours with intermittent shaking and then allowed to cool to room temp until the next step.

Glycogen, which is resistant to alkali environments of the extraction protocol, was then purified and precipitated through the stepwise additions of Milli-Q water (1 ml) and absolute ethanol (2.77 ml). Glycogen was pelleted by centrifugation at 10,000 RCF for 15 mins. The pellet was washed in 1 ml ice cold 60% EtOH, supernatant aspirated, and the pellet was vacuum desiccated for quantification.

Glycogen quantification – Desiccated samples were resuspended in 0.25 ml Milli-Q water and transferred to an Eppendorf tube containing 0.25 ml 5% phenol solution. After samples were vortexed, 1 ml concentrated sulfuric acid was added hydrolyzing glycogen to glucose. Samples cooled to room temperature for approximately 15 mins prior to their measurement. Glycogen concentration was determined through measurement of absorbance at 488 nm on a Beckman Coulter DU 800 spectrophotometer. The linear regression of glucose standards at 250, 100, 75, 50, 25, and 10 mg/ml in 0.15% Benzoic provide estimates of glucose associated with the glycogen macromolecules.

Reduction Potential

Sample collection and extraction – Protocol and buffers were prepared as described by manufacturer (PROMEGA NADP/NADPH-Glo™ cat # G9081 and PROMEGA NAD/NADH-Glo™ cat # G9071 Assays) where modifications for freezing were made according to personal communications with manufacturer's researchers. As per manufacturer's suggestion; pellets were extracted, treated for either oxidized or reduced nicotinamide, and neutralized prior to freezing.

Resuspended pellet (0.1ml) was added to 0.1ml DTAB lysis buffer, divided into two tubes – "R" (reduced) and "O" (oxidized) – where the "O" tubes had been previously filled with 0.05 ml 0.4N HCl. The Eppendorf tubes are incubated for 15 mins at 60°C, then returned to room temp for 10 mins. Extracts are neutralized by transferring to "R" and "O" cryovials containing 0.1 ml Trizma/ HCl buffer and 0.05 ml Trizma buffer respectively. Cryovials are flash frozen in LN_2, and stored at -150°C.

Samples were defrosted and quantified as described by manufacturer using an Orion-L microplate luminometer. Briefly, "O" tubes used to measure NAD^+ and $NADP^+$ and "R" tubes used for the measurement of NADH and NADPH. For measurement 0.05 ml sample and 0.05 ml detection reagent specific to either the phospohorylated or unphosphorylated form was added to 96 well microplates. The plates were incubated at room temperature for 60 mins and average

luminescence over 3 seconds was quantified. Measurements for oxidized and reduced forms of each reductant form (NAD[H] and NADP[H]) were pooled to generate total reductant pools used for ratio analysis.

Cell counts

Concentration of cells in resuspended pellet was measured through flow cytometry using a Millipore Guava 5HT flow cytometer. Resuspended cell pellets were preserved by diluting 0.01 ml culture into 0.985 ml AMP and 0.005 ml 25% glutaraldehyde, inverted 10x and incubated in the dark at room temperature for 10 mins prior to flash freezing in LN_2 and storage at -80°C.

CHAPTER 3: CARBON FATE AND FLUX IN *PROCHLOROCOCCUS* UNDER NITROGEN LIMITATION

Abstract

Phytoplankton growth rates are limited by nutrient availability in the world's euphotic oligotrophic oceans. In these vast biomes, the dominant planktonic populations are characterized by small genomes and cell sizes, traits thought to provide selective advantages during nutrient-limited growth by reducing cell quotas for the limiting nutrients and by improving acquisition of scarce nutrients. However, the impacts of reductive evolution on metabolism of the oligotrophic specialists remain poorly understood. To develop a better understanding of carbon fate and flux under nutrient limitation, we grew axenic *Prochlorococcus* under nitrogen-limited and nitrogen-replete conditions and measured metabolite pools, the rate of carbon moving through these pools as well as bulk photosynthesis, photosystem health and efficiency. Cells under nitrogen limitation had reduced rates of both metabolite labeling and total carbon fixation. These N-limited cells also had elevated metabolite pool levels and released a larger proportion of total fixed carbon to the environment. Accounting for these observations, potential metabolic mechanisms that contribute to the fitness of *Prochlorococcus* in the nutrient limited oceans will be discussed. Through a greater characterization of the metabolic pathways utilized by the most abundant photosynthetic organism on Earth, we attempt to lay the structural framework necessary to not only build upon our knowledge base of photosynthesis, but to generate a deeper understanding of the implications these mechanisms have on carbon and energy flow through global biogeochemical cycles.

Introduction

As the numerically-dominant phytoplankton in the world's tropical and subtropical oligotrophic oceans [5, 6], *Prochlorococcus* spp. function as key nodes in community food webs and are suspected to drive productivity in one of Earth's largest biomes. This blue water biome is characterized by persistent nutrient limitation at the sunlit surface, with limitation for phosphorus or iron in some regions, and for others such as the North Pacific, nitrogen [51, 52]. Together with a relatively stable physical environment (*e.g.* temperature, salinity, pH, DIC), nutrient limitation is thought to provide selective pressure to maximize efficiency of resource

utilization in the oligotrophic. It has been proposed that small genomes and cell sizes may improve both thrift and competition for scarce nutrients, and consistent with this hypothesis, the numerically-dominant phototroph (*Prochlorococcus*) and heterotroph (SAR11) both have genomes that have undergone dramatic reduction during their evolution [7]. However, the impact that these genomic reductions have on the utilization of nutrient resources towards biomass production is not well understood, due to the paucity of empirical data on the metabolic pathways utilized.

Over 50 years ago Fogg et al. [53] first reported photosynthate release to the environment as exudates by both healthy and stressed phytoplankton and the levels of stress and released exudate are directly correlated (see recent review [54]). This apparent inefficiency has led to hypotheses that the loss of photosynthate may be attributed to passive diffusion of metabolites to the environment akin to 'property tax' [55]. Alternatively, the overflow metabolism model may allow loss of photosynthate to the environment as a means to alleviate the stresses involved with over-energizing photosynthetic machinery and maximize growth efficiency when nutrients become available by reducing lag phase[56]. In this model, when energy input surpasses nutrient limited energy demand, cells fix inorganic carbon into low-nutrient, high-energy metabolites as a means to dissipate surplus energy. The resulting low-nutritional value (e.g. low C:N) but highly-labile byproducts are released to the environment and are presumably utilized by heterotrophic plankton.

Our ignorance regarding both the intracellular and the community-wide effects of carbon metabolism in *Prochlorococcus* under nitrogen limitation drive our research to develop a greater understanding of the metabolic mechanisms employed. To generate a deeper understanding of photosynthesis under nitrogen limitation, axenic cultures of *Prochlorococcus* were grown under nitrogen-limited continuous chemostats and nitrogen-replete batch cultures. We measured intracellular metabolite pool sizes and their labeling rates, photosynthesis, and photosystem health and efficiency. Observations show cells under nitrogen limitation reduce photosynthetic rates and release a larger proportion of fixed carbon to the environment than nitrogen replete

cultures. We also observed the general trend of reduced labeling of metabolites while maintaining elevated metabolite pool levels in nitrogen limited cultures. These observations were compared against metabolomics data collected during a recent cruise in the geographic region (oligotrophic N. Pacific) from which the isolate used in this study – *Prochlorococcus* VOL 29 – was cultured. Data presented here describe metabolite-labeling patterns for *in vivo* *Prochlorococcus* populations and suggest their metabolisms follow similar trends to those observed in laboratory cultures.

Results and Discussion

Culture growth and response to rescue from N limitation

Cultures of N-limited *Prochlorococcus* VOL29 cells were destructively sampled 6 days after chemostat dilution rates (~0.09 day $^{-1}$) were set. At this point the cultures were stabilized (Fig. 6) at concentrations similar to those found in previously observed continuous cultures maintained for longer periods (Fig. 7). The cells maintain suppressed but active metabolisms (*e.g.* measured photosynthesis), and the addition of excess NH_4^+ to batch cultures following destructive sampling during our experiment was observed to induce log phase growth while raising the mean fluorescence*cell^{-1} to levels observed in N replete cultures within 3 days (Fig. 6). Batch cultures that did not receive NH_4^+ additions were not observed to grow and maintained culture densities for approximately 5 days prior to declining in density. N replete cells were grown in batch culture and collected during early log phase growth ($\mu \approx 0.44$) at which point cultures were near cell density of N limited chemostat cultures. Following experimental destruction of cultures, addition of NH_4^+ to 5 ml batch cultures (growth after day 0; Fig. 6) was not observed to affect the growth of N replete batch cultures. These observations suggest cells in the chemostats were metabolically active but nitrogen availability limited growth and metabolism while growth of N replete batch cultures was not limited due to nitrogen availability.

Nitrogen Deficiency Limits Primary Production and Enhances Organic Carbon Release

The effects of nitrogen limitation on the rate of photosynthetic carbon fixation was measured during two, two-hour incubations initiated at noon (12:00) and midafternoon (16:00;

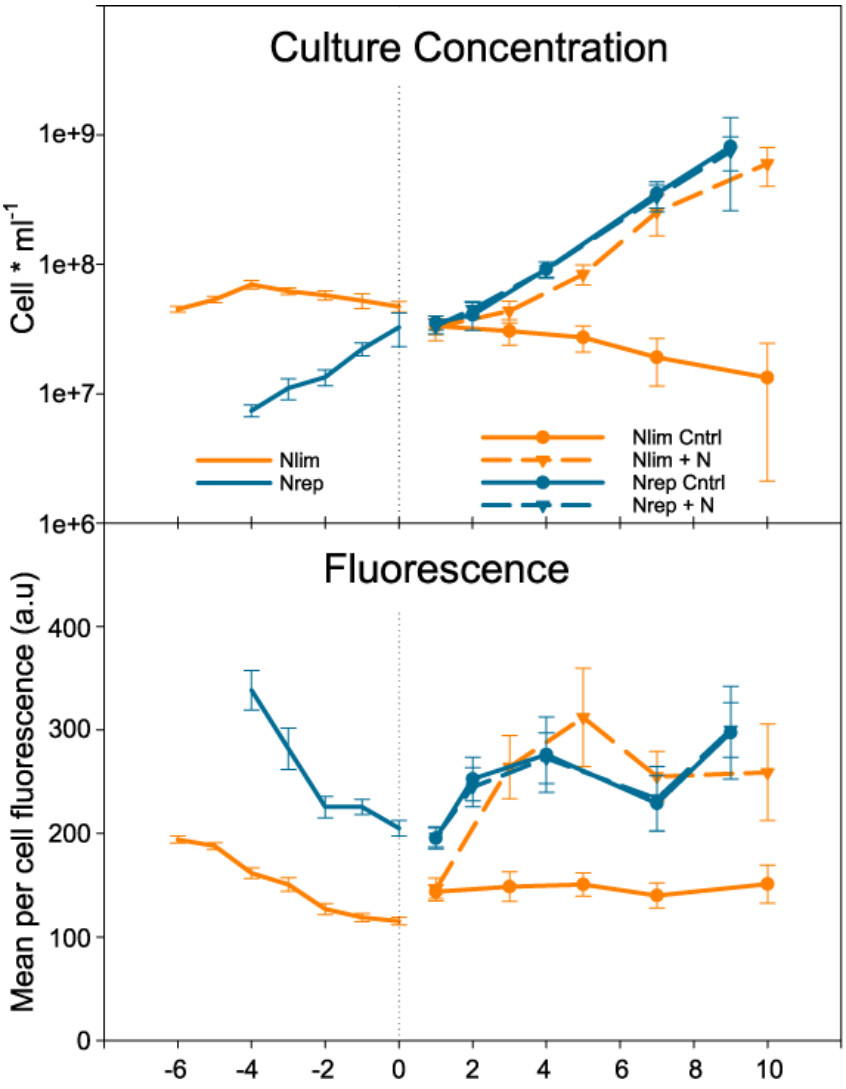


Figure 6: Culture growth analysis

Comparisons of VOL29 growth under nitrogen limited (orange) and – replete (blue) growth conditions leading up to and following the day of the experiment (day 0; dotted vertical line). After day 0, nitrogen amendment experiments (day 1 – 10) were performed in batch culture. Mean per cell fluorescence, as determine by the average fluorescence of events counted by flow cytometry, allows for the comparison of the average chlorophyll content per cell. Error bars represent standard deviation.

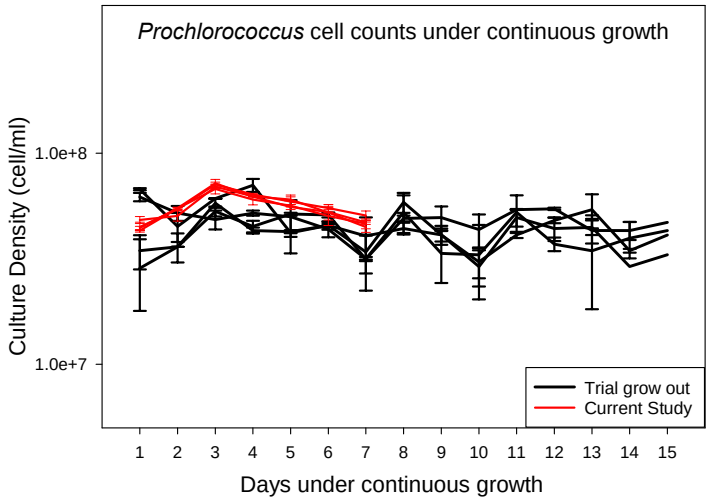


Figure 7: VOL29 growth in described current and trial grow out experiments

Under identical growth conditions to our current study (red lines) VOL29 cultures grown in N-limited chemostats were observed to stabilize around $4.5x10^7$ over a 15 day grow out experiment (black lines) suggesting that growth rate for the conditions tested are approximately balanced to the dilution rate of the chemostat (~0.09 day^{-1}).

Fig. 8) as well as measurements for both net (photo period; 13 hr) and gross (full diel; 24 hr) primary production. For each, measurements were made for total organic carbon (TOC), ≥ 0.2μm particulate organic carbon (POC), and ≤ 0.2μm dissolved organic carbon (DOC) providing rates for total (TOC), intracellular (POC), and extracellular (DOC) carbon fixation rates.

At noon, N-limited VOL29 cultures were photosynthetically active, but their activity was less than half that of the N-replete cultures at noon (Fig. 8A). This difference was also manifest in measurements of net and gross primary production (data not shown), indicating that N-limited cells, while capable of fixing inorganic carbon into biomass, are limited in this capacity by a lack of available nitrogen. Importantly, N-limited cells incorporated a smaller fraction of the fixed carbon into (particulate) biomass (Fig. 8B). This indicates that N-limitation may force the release of fixed carbon as metabolic waste due to a bottleneck at the step of nitrogen assimilation, which we further investigate below.

In N-replete conditions, photosynthetic carbon fixation by *Prochlorococcus* has been previously observed to be maximal at local noon and declines during the afternoon [15]. Consistent with these prior studies, we observed a dramatic decline in photosynthesis for the N-replete VOL29 cultures from 1200 to 1600, but the 1600 measurements for carbon fixation for N-limited cultures only marginal declined from the rates observed at noon (Fig. 8A). Under N replete conditions, photosynthesis rates are thought to slow in the evening as metabolism shifts from the carbon fixing reactions of the Calvin cycle to synthesis of macromolecules (e.g. DNA, glycogen) from the precursors generated earlier in the day [15, 16, 38]. The marginal temporal difference in carbon fixation rates of N limited cells may suggest the above proposed metabolic switch does not occur, for reasons that are not readily apparent, and thus required a deeper investigation of the physiology of *Prochlorococcus* as a function of nitrogen status.

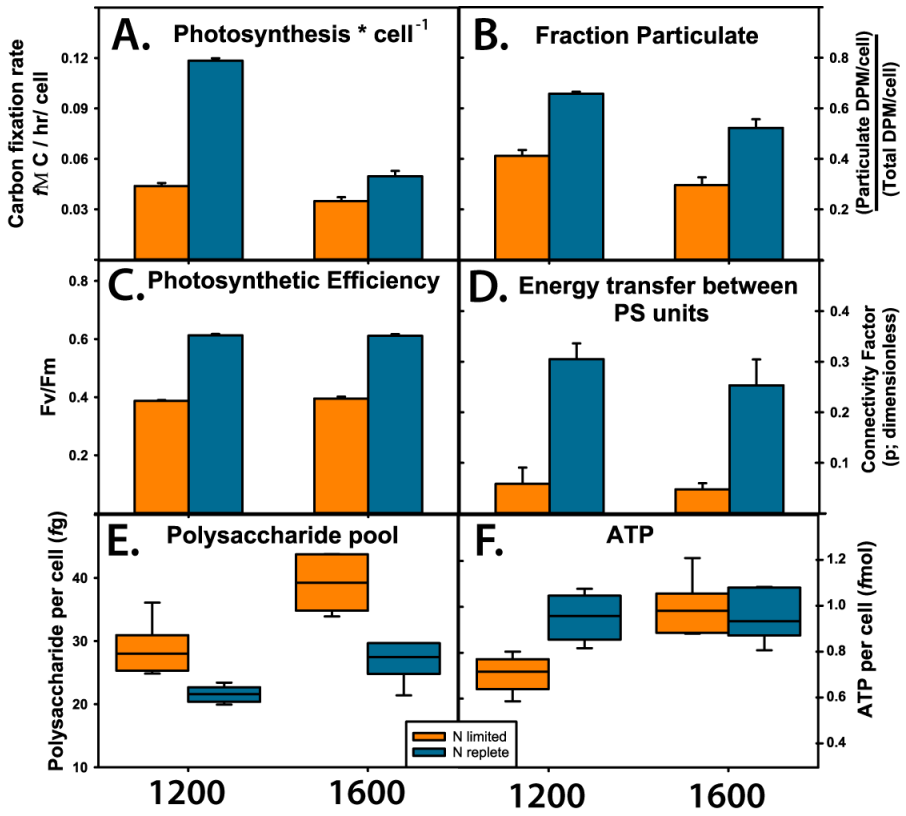


Figure 8: Photosynthesis and cellular carbon and energy stores

Comparisons of the effects of temporal (1200 and 1600; left and right respectively) and nitrogen (limiting and replete; orange and blue respectively) on carbon fixation rates (A) and the fraction of fixed carbon that is associated observed in the particulates (B) photosystem health and efficiency (Fv/Fm; C) and the connectivity/energy transfer between PSII units(p; D). Cellular carbon and energy stores were determined through measurements of total polysaccharides (E) and ATP (F) per cell.

Photosystem health and efficiency

The general health and efficiency of photosystems was measured using a Satlantic Flourescence Induction and Relaxation (FIRe) system. We observed N-limited cultures to exhibit a decrease of photosystem efficiency at both noon and late afternoon (Fig. 8C; Fv/Fm). A similar, but more dramatic drop was reported when MED4 was starved for nitrogen by transfer to nitrogen free media for several hours [33], suggesting that the slow but steady supply of nitrogen in our chemostats provided some ability to maintain photosystem health in VOL29. This drop in Fv/Fm was manifest through an increase in minimum fluorescence (F_0) while having insignificant effects on the maximum fluorescence (F_m) (Table 2). These results indicate N-limited cells possess a similar maximal light harvesting capacity (F_m) but have an increased abundance of damaged or closed photosystem reaction centers that cannot accept photic energy (F_0). Measurements for connectivity or energy transfer between PSII units (Fig. 8D; p) suggest that N-limitation causes a reduction in the ability to move electrons between open and closed reaction centers resulting in the release of excess energy as fluorescence or heat. The reduced energy flow connectivity between photosystems may lead to over excitation of the damage prone D1 and D2 proteins, while insufficient nitrogen constrains the capacity of cells to replace damaged proteins. These data may imply that N-limitation causes a reduction in the energy transfer mechanisms of photosynthesis without reducing maximum light harvesting capacity.

Overview of metabolite pools and labeling rates in nitrogen-replete and -limited cultures

Measurements of the standing pool size for small, biologically relevant molecules and the incorporation of newly fixed inorganic 13C trace ($H^{13}CO_3^-$) into them can provide insights into the carbon metabolism utilized by *Prochlorococcus* under nitrogen limitation. Although our metabolite coverage is incomplete, due to the limits of detection for the instrument and the inherently small pool sizes of some metabolites, those metabolites that were detected provided new insights into known processes and suggested previously unrecognized metabolic strategies for *Prochlorococcus*. For almost all metabolites, we observed cell normalized pools to be greater in nitrogen limited compared to nitrogen replete cells. Large metabolite pools were found in N-limited cultures at key intersections between carbon and nitrogen metabolisms such

Table 2. Photophysiology of nitrogen limited and replete cultures of VOL 29

Photophysiology of VOL29 cultures was measured using a Satlantic FIRe fluorometer system allowing for the measurement of photosynthetic parameters. Photosynthetic efficiency (Fv/Fm) of PSII where Fv is the variable fluorescence (Fv = Fm – Fo) and Fo, Fm are the minimal and maximal yields of chlorophyll-a fluorescence respectively. The connectivity factor of PSII (p) describes transfer of energy between photosynthetic units. The functional cross section of PSII is measured as σ.

		Fv/Fm (dimensionless)	Fo (relative units)	Fm (relative units)	p (dimensionless)	σ (relative units)
N-Limited	12:00	0.39 ± 0.003	774 ± 48	1263 ± 76	0.06 ± 0.03	211 ± 12
	16:00	0.40 ± 0.006	805 ± 91	1330 ± 144	0.05 ± 0.01	216 ± 7
N-Replete	12:00	0.61 ± 0.005	474 ± 8	1225 ± 17	0.31 ± 0.03	204 ± 5
	16:00	0.61 ± 0.006	497 ± 5	1277 ± 14	0.25 ± 0.05	199 ± 3

as 2-oxoglutarate (2-OG) and glutamate (Glu), as well as the Calvin cycle, glycogen biosynthesis, peptidoglycan biosynthesis, and nucleotide biosynthesis (Fig. 9A). Large metabolite pools may be understood to represent points in metabolic pathways where reaction rates producing the metabolite are greater than the rates of reactions that consume them, but the mechanisms driving the unequal reaction rates may be reaction or pathway specific.

The labeling rate of metabolite pools can depend on many factors including photosynthetic rates, the size of the metabolite pool, the pool size labeling rates of metabolic precursors, as well as the rates of reactions producing and consuming the metabolite. With a limited understanding regarding how the sum of these processes affects labeling measurements, caution must be exercised not to confuse enzymatic reaction rates with labeling rates. To better understand the flow of fixed carbon through *Prochlorococcus* metabolisms we employed two analytical methods to track isotopically labeled carbon into metabolites; Mass Distribution Vector (MDV), which allows for an observation of the spread of isotopic labeling within the carbon backbone metabolite and Fractional Composition (FC) analysis, which accounts for the fraction of labeled to total carbon atoms in each metabolite over the labeling experiment time series. As described below, the rate of newly fixed carbon moving through the measured metabolites occurs more rapidly and generates a greater abundance of multiply labeled isotopologues in N-replete compared to N-limited cells. Although these data are suspected to be strongly influenced by the smaller standing pool sizes of these metabolites in N-replete cells, they do suggest that carbon flow into metabolites from carbon fixing metabolisms cycle are repeatedly recycled before they are directed to alternative metabolisms.

N assimilatory metabolites

We observed intracellular pools of 2-oxoglutarate (2OG) to be an order of magnitude greater in N limited cells than in cells grown under N-replete conditions (Fig. 9A). Importantly, the pool size of 2OG is widely considered to be the signal for N availability in cyanobacteria [21]. Pools of this metabolite are thought to form when N is limiting because 2OG makes up the carbon backbone for N assimilatory metabolites glutamine and glutamate through the

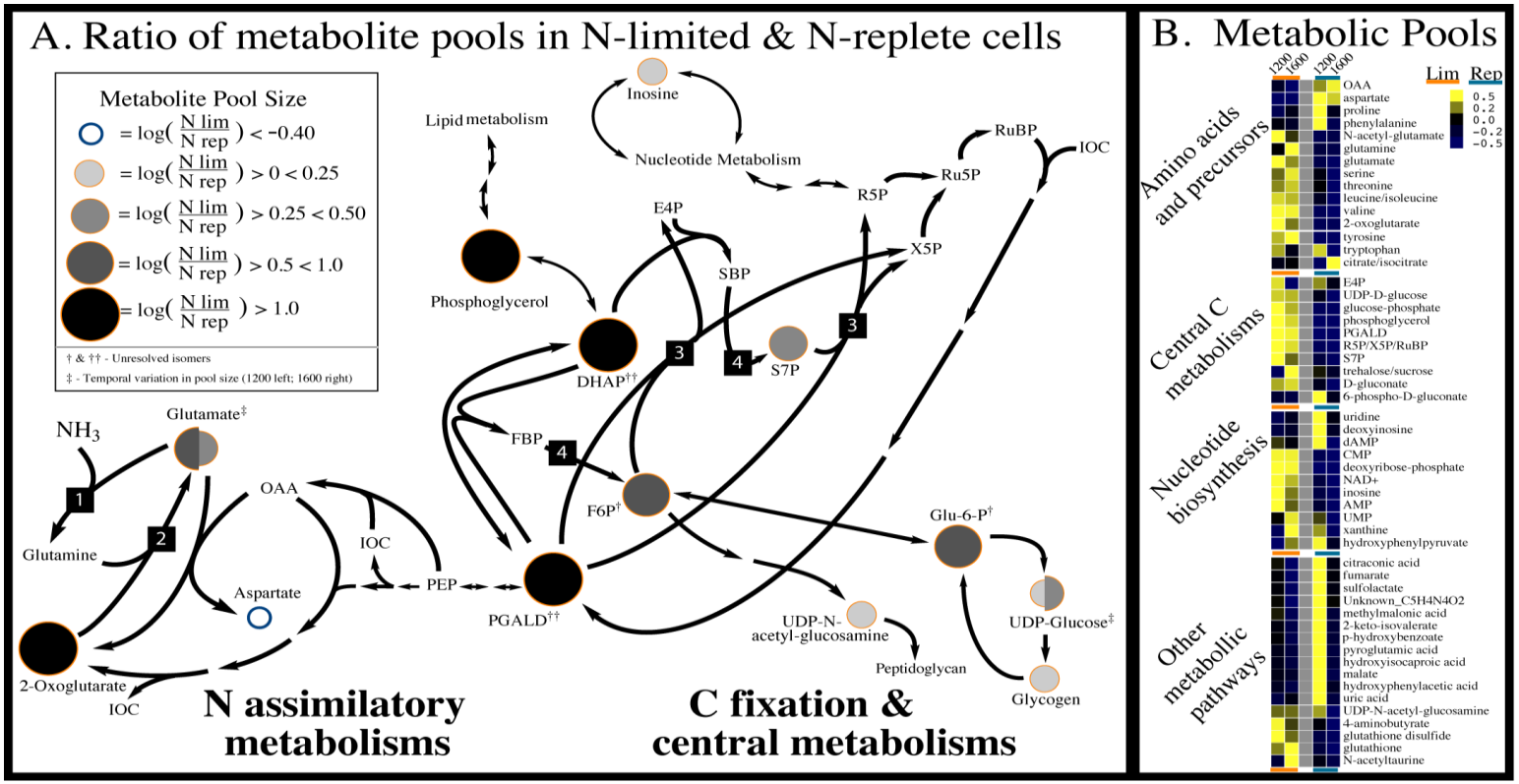


Figure 9. Metabolite Pool Analysis

Comparisons of per cell normalized metabolite pools between nitrogen limited and replete cultures of VOL29. Select metabolite pool comparisons were displayed as circle size over the metabolic map (A); specific enzymes addressed in discussion are glutamine synthetase (1), glutamine-oxoglutarate amidotransferease (2), transketolase (3), and fructose-1,6-bisphosphatase II / sedoheptulose-1,7-bisphosphatase (4). Direct comparisons of normalized metabolite pools across treatments (B), values (0.5 to -0.5) describe pool sizes within each metabolite subset scaled by range. See Table S5 for values and scaling methods. Abbreviations used: erythrose 4 phosphate (E4P), fructose 6 phosphate (F6P), fructose bisphosphate (FBP), inorganic carbon (IOC), phosphoenolpyruvate (PEP), phosphoglyceraldehyde (PGALD), oxaloacetate (OAA), ribose 5 phosphate (R5P), ribulose 5 phosphate (Ru5P), sedoheptulose 7 phosphate (S7P), sedoheptulose bisphosphate (SBP), xylulose 5 phosphate (X5P).

mechanisms of *g*lutamine *s*ynthetase (GS; Fig. 9A reaction 1) and *g*lutamine-*o*x*o*g*l*utarate *a*mido*t*ransferase (GOGAT; Fig. 9A reaction 2). Specifically, when GS activity is constrained by low availability of its substrate, NH_4^+, glutamine production is limited. Glutamine is the other substrate for the 2OG consuming reaction catalyzed by GOGAT, and its limitation therefore results in a buildup of 2OG.

If the buildup of 2OG was due to bottleneck at the GOGAT reaction, one might expect a priori that the pool size of reaction's product, glutamate, to be smaller in the N-limited cells. However, glutamate pools in N-limited cells were in fact three times higher than in N-replete cells. Glutamate was our most robustly observed metabolite; integrated ion counts (IC) for this metabolite dwarfed most features we observed and suggested that as in other microbial systems [39-41], *Prochlorococcus* maintains very large glutamate pools. The formation of larger glutamate pools in N-limited conditions may suggest that *Prochlorococcus* must balance the benefit of maintaining pools of metabolites to drive the GS reaction forward while minimalizing N cost associated with large pools of glutamate. Isotopic carbon labeling experiments show carbon moves through glutamate pools at greater rates in N replete cells than N limited cells, but we did not observe temporal differences within treatments (Fig. 10).

Pools of glutamine in N limited cells are approximately 50% and 300% larger than under replete conditions (noon and afternoon respectively). The large pools of glutamine that continue to pool during the afternoon of N limited cultures raises questions regarding the mechanisms regulating this process. Large pools of 2OG and glutamine observed under nitrogen limited conditions would be expected to proceed through GOGAT. The pooling of these metabolites suggest the regulatory mechanisms may inhibit GOGAT under the experimental conditions.

Glutamate pools serve as the metabolic precursor for arginine in an eight-step synthetic pathway that is thought to be regulated at the second step by the nitrogen sensing regulator P_{II}. Arginine is a nitrogen rich metabolite that in addition to protein synthesis is involved in nitrogen metabolisms. Although arginine is not observed in our data set we do measure the intermediate

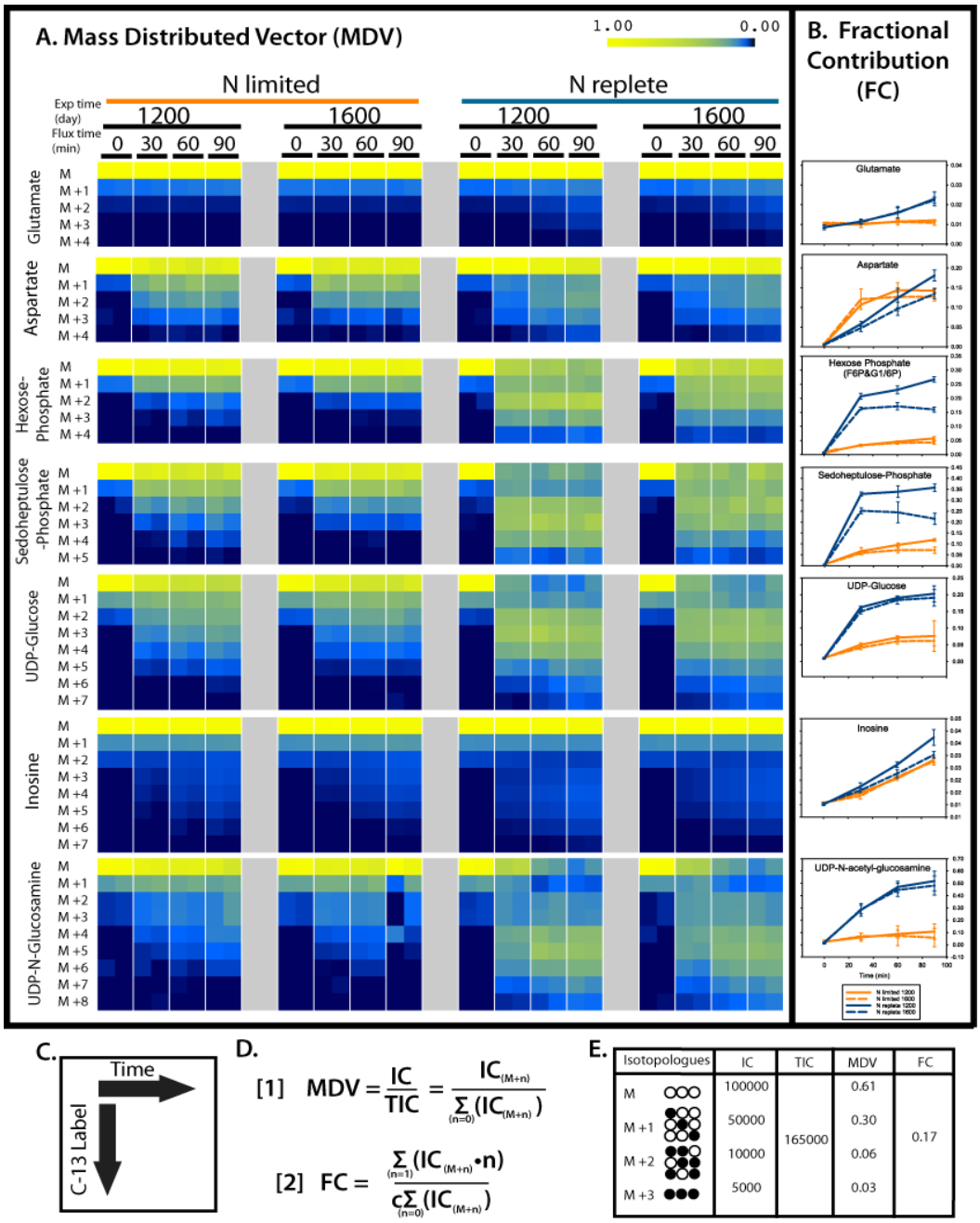


Figure 10: Metabolite Labeling by Isotopic Carbon

Isotopic carbon labeling of metabolites as measured by mass distribution vector (MDV; A) and fractional contribution (FC; B). Additional support for data comprehension is provided as diagram describing axis for MDV heat maps (C), equations used to generate MDV and FC (D), and hypothetical metabolite labeling pattern showing application of MDV and FC (E). See Table S6 for IC values.

metabolite *N*-acetyl-glutamate (NAG) that precedes the regulated second step of arginine synthesis. In our nitrogen-limited cultures the cell normalized abundance of this metabolite is two to three fold greater than what is observed in our N replete cultures (Fig. 9B). The pool of NAG in our nitrogen limited cultures may suggest the function of P_{II} in *Prochlorococcus* is similar to observations in other cyanobacterial systems where P_{II} is believed to bind intracellular 2OG pools when nitrogen is limiting. As nitrogen becomes available and 2OG pools are drawn down, free P_{II} can enhance the activity of *N*-acetyl-glutamate kinase (NAGK) initiating the pathway for conversion of NAG to nitrogen rich arginine [26, 57].

Our analyses of the metabolite aspartate provide evidence for a previously unrecognized metabolic strategy in *Prochlorococcus.* Along with this metabolite's involvement in protein synthesis, aspartate is also involved in the *de novo* production of arginine and nucleic acids (pyrimidines). These biomolecules, proteins and nucleic acids, are rich in nitrogen and as such it may not be that surprising that we observe interesting trends for both the pools and labeling rates of aspartate under the tested conditions.

Aspartate was the only metabolite observed to have larger standing pools in the N-replete than limited treatment during both time points (Fig. 9A) and the labeling of this metabolite provides evidence that alternative pathways are utilized by *Prochlorococcus* under the experimental conditions (Fig. 10). In our N limited cultures FC analyses suggest quick uptake of isotopic label into the carbon skeleton of aspartate. Following this initial uptake both the FC and MDV for isotopologues were observed to hold at steady state for the remainder of the experiment. The larger pools of aspartate observed in N replete cultures became labeled at a slower but increased in label richness throughout the time series. MDV analysis of isotopologues show continuous increase in the abundance of label within the metabolite as the experiment progresses. In contrast to what was observed in N limited cultures, N replete labeling rates during our noon experiments were greater than the afternoon experiments. It is important to remind the reader that large pools of metabolites can suppress the apparent labeling rate when compared against the labeling rate of smaller metabolite pools and as such labeling

rate cannot be used as a proxy for enzymatic rates but should be used to understand pathway utilization. The physical and chemical similarities between glutamate and aspartate allows for direct comparisons of the ion counts (IC) for these metabolites as they will reflect on the actual concentrations of these metabolites (Table S5). The IC of glutamate was observed to be 2 – 3 orders of magnitude greater than those of aspartate. These data suggest that glutamate pools dwarf those of aspartate and as such it is unlikely that aspartate would serve as a reservoir for nitrogen under replete conditions but the labeling of these pools may suggest that aspartate is rapidly turned over and serves an important role in the assimilation of nitrogen.

To understand the aspartate labeling data it is important to note that without an intact TCA cycle *Prochlorococcus* spp. *de novo* synthesis of this metabolite is performed by fixing inorganic carbon – HCO_3^- – to the three-carbon metabolite phosphoenolpyruvate (PEP) forming the product oxaloacetate (OAA). Aspartate is then generated when the amino group of glutamate is transferred to OAA. This process results in a four-carbon metabolite where three of the carbon atoms are fixed via the Calvin cycle and the other fixed by phosphoenolpyruvate carboxylase. Under N-replete conditions our MDV data provide evidence for the labeling of precursor metabolites (*i.e.* PEP) via the Calvin cycle prior to picking up another label through the action of PEP carboxylase. On the other hand, under N-limited conditions, aspartate quickly picks up label but FC reaches steady state and the MDV analyses show isotopic labeling in the isotopologue do not become enriched. This observation may suggest that doubling of the concentration of bicarbonate – 0.6mM $NaH^{13}CO_3^-$ tracer was added to culture with the same initial concentration of unlabeled $NaHCO_3^-$ – resulted in an increase rate of PepC, immediately driving forward the production of aspartate. These high rate of labeled inorganic carbon entering the large pool of aspartate provides evidence that new carbon in aspartate is sourced from photosynthate that has not been repeatedly cycled through the Calvin cycle in N limited cells whereas *Prochlorococcus* grown under N replete conditions utilize carbon sourced from isotopically enriched metabolites from the Calvin cycle to N assimilatory reactions.

In contrast to glutamate, we observe inorganic carbon labeling of aspartate to be greater at noon than during the afternoon rate in our N-replete cultures (but not in our N limited cultures). This observation may simply reflect differences in photosynthetic rates in our N replete cultures, but the lack of temporal variation in glutamate labeling suggests photosynthetic rate is not the only factor driving this observation. Taken together these data may suggest that a regulatory mechanism may direct carbon to aspartate at noon and provide evidence that under the nitrogen replete conditions carbon flow through aspartate pools supports demand for nucleotides needed in genome replication. In the afternoon genome replication is finishing up and new pyrimidines are not needed as such the flux may through this pool may decrease.

Central Carbon metabolites

All detectable Calvin cycle intermediates – PGALD (DHAP), F6P (G1/6P), S7P, & an undifferentiated pentose phosphate isomer (X5P, R5P, or Ru5P) – are more abundant in N limited cells than N replete cells. In N limited cells these metabolites may accumulate as a result of reduced photosynthetic efficiency and rates. Large pools of these metabolites we do observe may be indicative of regulated steps in the Calvin cycle. The metabolites PGALD, F6P, and S7P are all substrates for the bidirectional transketolase reaction (Fig. 9A; reaction 3). During glycogen catabolism, *Prochlorococcus* utilizes the pentose phosphate pathway in which this enzyme proceeds in the opposite direction producing PGALD, F6, and S7P. Therefore it might be understood that the large pools of these metabolites may prevent backflow during the Calvin cycle. Additionally, the generation of pools at F6P and S7P peak our curiosity because these are both products of the bisphosphatase reaction encoded for by the gene *glp*X (Fig. 9A; reaction 4). Little is known about the regulation of this enzyme in cyanobacteria, but the energy consuming reaction (loss of phosphate) and large pools of its products may suggest this enzyme is an important regulatory step.

The rate of inorganic carbon labeling for Calvin cycle metabolites S7P and F6P is affected by both treatment and temporal differences in carbon fixation pathways. The labeling observed in N replete cultures at noon saturates at a higher level than during the afternoon and

MDV analysis show this observations is manifest through the abundance of multiple labeled isotopologues at noon. The increased fraction labeled and abundance of heavy isotopologues provides evidence for multiple rounds of metabolic cycling within the Calvin cycle at noon while the photosynthetic rates are highest, but the observation that FC reaches steady state suggests some labeled metabolites are removed from the cycle before becoming completely labeled.

Polysaccharide production

The method used in this study for direct polysaccharide measurements targets cellular glycogen content but polysaccharides with similar solubility properties (*e.g.* capsule) can contaminate the measurements. While the abundance of structural polysaccharides are poorly understood they are not expected to vary greatly between noon and afternoon. On the other hand, carbon and energy stored as glycogen is synthesized from carbon fixed during morning hours when photosynthetic rates are greatest and use photosynthetic energy (ATP) collected during the afternoon to fuel the anabolism of these macromolecules. These stores are utilized by *Prochlorococcus* to power metabolic processes during periods of low photic energy resulting in the building up of reserves during the day and their subsequent depletion at night. We observe a significant increase in the pools of polysaccharides from 1200 to 1600 as cells prepare for the evening irrespective of the nutrient treatment they receive, suggesting -as predicted- the production of glycogen stores over the course of the day. Additionally, the pools of polysaccharides in the N-limited cells are 25 and 30% greater than the stores observed in N-replete cells for 1200 and 1600 time points respectively. These data provide evidence that the production of glycogen in *Prochlorococcus* is both temporally and environmentally regulated. Although we see a significantly greater pool of polysaccharides in the N-limited cells, we do not observe differences at the same scale as we see in many of the metabolites including those of glycogen's precursor metabolites. This observation may suggest that the pool of glycogen in N-replete cells nears the maximal storage capacity for these phytoplankton. The very small cell size of *Prochlorococcus* may necessitate a cap on overflow metabolism into these macromolecules as glycogen granules can form large insoluble complexes that take up significant fractions of intracellular volume. Therefore, under N-limited conditions the stores of

glycogen can increase slightly over what is physiologically needed before precursor metabolites are directed to other metabolisms or released to the environment.

We observed pools of UDP-glucose – a suspected substrate for glycogen anabolism – in N limited cells to be greater than those in replete conditions and this ratio increases from noon to the afternoon time point. Taken with the observation that glycogen pools in N limited cells are not much greater than N replete cells, these observations may suggest that carbon directed to glycogen under N limited conditions hits a bottleneck as the quota for stored carbon and energy is met resulting in elevated precursor metabolites pools. In N replete cultures we observe greater rates of new carbon labeling in UDP-glucose than in N limited cultures. The increased FC in the N replete cultures appears to be attributed to the abundance of heavy isotopologues (M+2, M+3, and M+4) in the smaller pool size of N replete cells. Due to the general lack of heavy isotopologue in hexose-phosphate at this same time (Fig. 10), this abundance of heavy UDP-glucose isotopologues suggest that label is not coming from the glucose in but from the phosphorylated pyrimidine (UDP) as discussed in the nucleotide section below.

Lipid biosynthesis

Lipids are biomolecules that are utilized for both cell structure (i.e. membranes) and energy storage. Cyanobacteria, without intact TCA cycles, are not capable of the catabolism of acetyl-CoA and therefore are not suspected to use lipids as energy storage molecules. As such, the main role of lipids in cyanobacteria is largely considered to be structural. In our N limited cultures we observed large phosphoglycerol pools whereas pools of this lipid precursor were observed near the limit of detection in N replete cultures. As the precursor metabolite for lipid biosynthesis, the low growth rate of N limited cells may reduce demand for this metabolite leading to the formation of large pools. N replete cultures in early log phase growth are rapidly dividing, generating demand for membrane lipids possibly leading to the observed draw down of this metabolite's pool.

Metabolites in Nucleotide & Peptidoglycan metabolisms

In addition to the large pools of glutamate, nitrogenous metabolites involved in purine and peptidoglycan metabolisms – inosine and UDP-n-acetylglucosamine respectively – were also observed to pool in N limited cultures. This surprising observation of nitrogenous metabolite pools in cells stressed for nitrogen suggests that N thrift does not result in a reduced pool of nitrogenous metabolites.

FC analyses of the labeling trends for inosine provide evidence that N-replete cells direct more of its fixed carbon to nucleotide production at noon than during the afternoon, but we do not observe similar temporal differences in the labeling pattern of inosine in N limited cells. As discussed above for the labeling pattern of aspartate, the *de novo* synthesis of nucleotides and their precursors must precede afternoon genome replication for dividing cells. The isotopic labeling observed in inosine of N replete cells was greater at noon than during our afternoon labeling experiment but temporal differences were not observed in the labeling of inosine for N limited cells (Fig. 10). As discussed for pyrimidine precursor aspartate (see above), our data provides evidence that cultures grown under N replete conditions were preparing to divide at night and therefore generate new stocks of nucleotides prior to the demand of afternoon genome replication.

The small pools of UDP-glucosamine and UDP-glucose observed in N replete cultures are observed to have an abundance of multiply labeled isotopologues while the precursor for both of these metabolites – hexose phosphate – picks up less isotopically labeled carbon during the experiments (comparisons of MDV's for uridine-sugars and hexose phosphate; Fig. 10). Additionally, we observe unequal temporal (*i.e.* compare 1200 and 1600) FC for hexose phosphate but this trend is not transferred to UDP-glucose or UDP-glucosamine. These observations provide evidence that the UDP component for both of these metabolites is picking up label suggesting *de novo* synthesis of this pyrimidine. One should note that in N limited cultures similar trends can be observed but the rate of labeling is suppressed in all metabolites and therefore is not as plainly observed in the color scales. Pyrimidine (uridine) biosynthesis

involves the condensation of ribose-5-phosphate, aspartate, and carbamoyl-phosphate. The synthesis for two of these metabolites; aspartate and carbamoyl phosphate, involve the direct fixation of inorganic carbon. These observations provide evidence for *de novo* uridine (UDP) biosynthesis in both N limited and replete cultures that does not appear to be temporally regulated and is utilized for production of sugar-nucleoside phosphate moieties.

ATP

Measurements of ATP provide estimates of the "at the ready" energetic capacity of the cells. The observed pools normalized to cell counts in both the N limited and N replete cells suggest ATP per cell is not greatly affected by nitrogen limitation but may be affected temporally (Fig. 8F). In our N limited culture we observed less ATP in the morning than in our afternoon measurement. This might be attributed to an increase of demand for reductant as the cell is fixing more carbon earlier in the day. If electrons flow to $NADP^+$ instead of being passed back through for cyclic electron transfer around PSI we would expect a reduced proton pumping and the resulting drop in the production of ATP. For N replete cultures where we observe no difference between our time points, electron flow is believed to occur through a more linear mechanism and may not be affected as greatly by the shift between high and low photosynthetic rates.

Field Metabolite analysis

To assess whether natural populations of *Prochlorococcus* spp. metabolisms mirror those observed in the laboratory we performed 13-C metabolomics experiments in the oligotrophic N. Pacific. Taking advantage of their unique physiology- the smallest known free living photosynthetic organisms- we enriched and select for metabolisms specific to *Prochlorococcus*. Although data from the field are less robust than those collected in the laboratory setting, we were able to detect carbon labeling of intracellular pools for both glutamate and aspartate. The labeling profile of these metabolites appears to mirror the labeling trends observed in laboratory settings when environmental conditions are considered (Fig. 11). When NH_4^+ is observed at

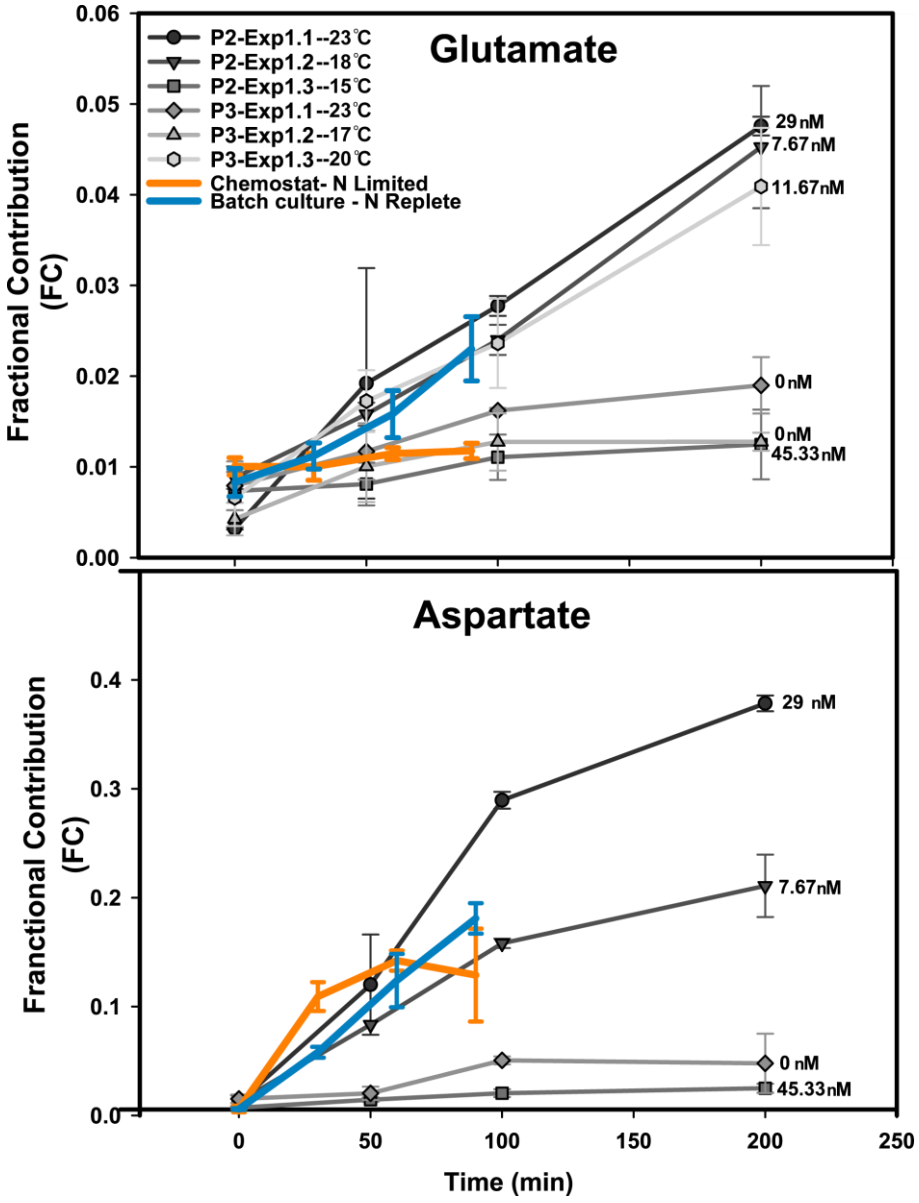


Figure 11: Glutamate and Aspartate isotopic labeling in natural populations

Over a series of two research cruises, six experiments were performed measuring the incorporation of inorganic isotopic carbon into metabolites of cells in *Prochlorococcus* enriched microcosms. Comparisons of FC analysis of cruise data (grey scale lines) and the laboratory nitrogen limited and nutrient replete (orange and blue lines respectively). Sea surface temperatures for each station are noted in the legend and measurements of ammonium concentrations are noted at the end of the line that they describe. P2-Exp1.3 was observed to have the highest ammonium concentration and lowest sea surface temperature (15°C).

detectable concentrations, carbon labeling of glutamate closely matches the labeling profiles for those of laboratory N-replete cultures. When *in vivo* NH_4^+ is below the limit of detection, labeling profiles trend with those of the laboratory N-limited chemostat cultures. The lone exception to this trend is observed during POWOW Exp1.3 when surface seawater temperatures dropped to 15°C. Although NH_4^+ was observed at high concentrations (~45 nM), isotopic carbon labeling was not observed in *Prochlorococcus* enriched cultures as pools of labeled metabolites are below the limit of detection. Isotopic labeling of the carbon backbone of aspartate was only observed during two of the six stations where this experiment was performed. Both of the stations where aspartate levels were above the limit of detection, NH_4^+ was observed. The labeling pattern observed in aspartate at these two stations matched the labeling pattern observed in N-replete cultures – *i.e.* the continuous increase of label into aspartate.

Conclusions

Throughout large regions of the ocean, *Prochlorococcus* growth is thought to be limited by nitrogen. In this study, we performed the first comparisons of carbon and nitrogen metabolism for *Prochlorococcus* under replete and nitrogen-limited conditions. Patterns of carbon utilization and other physiological properties were strikingly different in both conditions. While pools and the flow of labeled inorganic carbon into these pools (FC and MDV) were quantified, it has become clear that future investigations will be required to ascertain if such differences were due to passive effects, or if there is regulatory control (e.g. allosteric feedback inhibition, expression regulation, post-translational modification) at play for the anabolic pathways analyzed. As observed in other phytoplanktonic systems [58-60], nitrogen limitation on growth of *Prochlorococcus* reduces photosynthetic carbon fixation rates, photosynthetic efficiency, and per cell fluorescence while increasing glycogen stores. This apparent conserved physiological response to nitrogen limitation suggests shared underlying dynamics of nitrogen deficiency on photosynthetic organisms but the mechanisms remain poorly understood. Metabolic analysis allows for additional insights into the underlying mechanisms of photosynthesis under nitrogen limitation. Our data show nitrogen limitation in *Prochlorococcus* generates large stagnant metabolite pools compared to the small pools with high turnover

observed in our nitrogen replete experiments. For natural populations of *Prochlorococcus* the maintenance of metabolite pools may provide fitness advantages through a variety of mechanisms. We propose large metabolite pools may increase fitness in the nitrogen-limiting environment through increased enzymatic velocity, directional control of ambiguous reactions, and/or decreased protein demand. This might be understood to occur if metabolic pools not only result from pathway bottlenecks, but also are involved in promoting enzymatic rates through Michaelis-Menten kinetics. The maintenance metabolites pools (substrates) greater than the K_m may promote metabolic potential by increasing enzymatic reaction rates (velocity) [41]. As such, the increased enzymatic rates would reduce the need for large pools of nutrient expensive enzymatic proteins while supporting metabolic demands of the cells.

Our observations of aspartate pools and labeling under the conditions tested may suggest aspartate has an important role in nitrogen assimilation for *Prochlorococcus*. Contrary to our observations for most metabolites, we observed aspartate pools to be much larger in the nitrogen replete cultures than the limited cultures. The large pools of aspartate in N replete cultures may suggest that *Prochlorococcus* uses OAA as a nitrogen accepting carbon backbone when biologically available nitrogen is abundant. The generation of aspartate pools during N-replete conditions may provide an additional source of N carrying metabolites while repopulating the GS-GOGAT substrate pool. In addition to reducing carbon demand by replenishing the carbon backbone necessary pool for N assimilation, it is also possible that utilization of aspartate reduces the regulation mechanisms necessary to shift the carbon to metabolisms involved in N assimilation. For example, the transcription of the pyruvate dehydrogenase genes in MED4 appears regulated as a function of the time of day [15] but the enzyme produced by this gene is necessary to synthesize N assimilatory metabolites; 2-OG, GLU, and GLN. By reducing the demand for these metabolites by passing nitrogen through aspartate pools, *Prochlorococcus* can assimilate reduced nitrogen while reducing the need to induce regulatory mechanisms to shuttle recently fixed carbon to necessary pathways. In this way flux through aspartate pools to nitrogen storage metabolites such as spermidine may function as a sink for nitrogen assimilation during periods of nitrogen excess. Because pathway redirection is not necessary to assimilate the

available nutrients in *Prochlorococcus*, fleeting pools of reduced nitrogen endemic to the oligotrophic N. Pacific (eg. small and infrequent releases of nitrogen due to cell lysis and sloppy feeding) can be exploited more quickly than an opportunist that must upregulate and express nitrogen regulation mechanisms.

Although *Prochlorococcus* appear to utilize a non-canonical regulatory mechanism for nitrogen assimilation [31-33], we present data that suggests some of the functions for this canonical regulatory system are observed in VOL29. In the canonical cyanobacterial nitrogen regulation system, lack of nitrogen availability decreases GS-GOGAT activity and leads to pooling of 2OG as we observe in our nitrogen limited cultures. These pools are believed to be the intracellular signal for nitrogen limiting conditions and this metabolite can interact with the three cyanobacterial nitrogen regulators – NtcA, PipX, and P_{II} – modulating their activity [21, 26-28]. When nitrogen is abundant, high activity of GS-GOGAT draws down pools of 2OG reducing its associations of NtcA and P_{II}. The NtcA-2OG-P_{II} complex, which has been observed to play a role in the regulation of carbon fixation, disassociates when 2OG pools shrink under nitrogen replete conditions allowing for upregulation of carbon fixation. In VOL29 we observed a reduction of carbon fixation under nitrogen limitation suggesting that nitrogen limitation may result in the regulation of carbon fixation. In canonical regulation system, low abundance of 2OG results in free P_{II} that can promote the synthesis of nitrogen rich arginine by binding and promoting the key biosynthetic enzyme *N*-acetyl-glutamate-kinase (NAGK) [26, 29]. The observed large pools of *N*-acetyl-glutamate in our nitrogen limited cultures suggest that like in other cyanobacterial systems NAGK may be under control of this regulation system. The nitrogen rich arginine produced downstream in this pathway has been implicated in nitrogen storage processes. Although lack of homologous genes in *Prochlorococcus* spp. suggests these organisms do not make the common cyanobacterial nitrogen storage metabolites cyanophycin or urea, they do appear to make spermidine, a polyamine synthesized from aspartate and arginine with poorly understood function. We propose that this metabolite may possibly serve as a nitrogen storage metabolite and its synthesis is under control of P_{II}.

Under nutrient limiting and replete conditions metabolic pathway utilization and their resulting energetic demands can influence energy flow through photosynthetic membranes (Fig. 12). Under N limitation carbon flow to nitrogenous biomolecules such as proteins and nucleic acids is thought to be reduced and redirected to polysaccharides (Fig. 12 - 1), but large pools of metabolic precursors for synthesis of the nitrogenous biomolecules may raise questions regarding the regulatory steps involved. We propose that a stringent response or similar mechanism may possibly signal and regulate metabolisms during nitrogen limitation in *Prochlorococcus.* Our data show aspartate pools are low under N limited conditions and provide evidence that regulatory mechanisms may block a synthetic step in the production of arginine, suggesting lack of these amino acids to charge tRNA's may signal nitrogen limitation. Although no previous evidence for a stringent response type mechanism has been suggested in *Prochlorococcus,* a homologous gene for RelA/SpoT has been identified in the genome. Because genes are lost through genome streamlining if they are not necessary, the presence of this gene raises questions regarding its purpose and might be considered as support for this hypothesis.

General trends of large metabolic pools, low rates of carbon labeling in these pools, and low total carbon fixation rates were observed in N limited cells. Because reduction of inorganic carbon by the Calvin cycle requires the reductant (NADPH) from photosynthetic electron transfer, low rates of carbon fixation in N limited cultures reduce reductant demand (Reviewed in [38]; Fig. 12 -2). The observed low but active carbon fixation rates and large standing pools of metabolites in the nitrogen limited cultures may cause exudate release to the environment by either a directed or indirect overflow metabolism mechanisms. This release to the environment can be inferred from our particulate fraction data (Fig. 8B) where the ratio of fixed particulate organic carbon (cell associated) to the fixed total organic carbon (cellular and dissolved) provides evidence that nitrogen limited VOL29 releases more of the carbon they fix as dissolved organic carbon than nitrogen replete cells (Fig. 12 -3).

Electron and proton transport through carrier proteins provide energetic supply for metabolisms as either ATP or NADPH. Because the demand for these energy sources change as

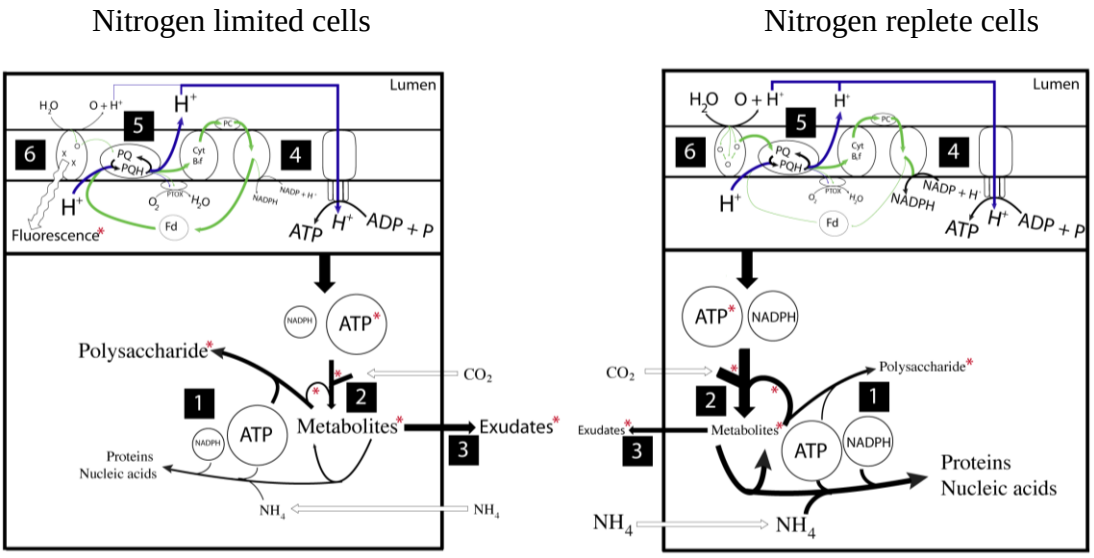


Figure 12: Model of the Interaction between Photophysiology and Metabolisms in *Prochlorococcus* sp. VOL29

Under nutrient limiting conditions (left) and nutrient replete conditions (right) metabolic pathway utilization and energetic demands influence energy flow through photosynthetic membranes; green lines represent electron flow, blue line represent proton flow, and red asterisks denote measurements made in this study. Arrow thickness and size of text are representative of the rates and pools; respectively, for the described feature but are not quantitative. The pool of cellular PSII is displayed where open circles (o) represent photosystems with open reaction centers and crosses (x) represent photosystems with closed reaction centers. See text for description of model.

a result of the current metabolic state of the cell, photosynthetic organism must modulate electron flow to fulfill the energetic demand of their metabolisms. For N limited cells, reductant demand of the Calvin cycle and high demand of phosphorylated nucleosides for the production of polysaccharide biosynthesis is thought to invoke cyclic electron flow around PSI. The high rates of carbon fixation observed in N replete conditions generate demand for reductant fulfilled through linear electron flow through the photosystems. It should be emphasized that the use of these electron flow pathways are non-exclusive and a gradient of cyclic and linear electron flow through photosystems cyanobacteria is balanced with the energetic demand of the cell [38]

Low photosynthetic rates utilize less NADPH, this results in a reduced supply of oxidized reductant ($NADP^+$) and diverts flow of electrons to ferredoxin initiating cyclic electron flow. Conversely, high reductant demand during carbon fixation requires electrons from PSI to be transferred to available reductant pools ($NADP^+$). The loss of electrons from the photosystems requires resupply through linear electron flow originating at PSII (Fig. 12 -4). Electrons from either reduced ferredoxin (cyclic flow) or PSII (linear flow) and protons are transferred to oxidized carrier proteins (PQ) (Fig. 12 -5). These now reduced carrier proteins (PQH_2) can transfer protons to the luminal side of the membrane and the electrons to Cyt B_6f. If the cytochrome cannot accept the electron from PQH_2 due to insufficient pools of downstream oxidized reductant (Fd or $NADP^+$) the electrons and protons can be dumped on the mid-term oxidase, PTOX, resulting in no net proton motive force or reductant potential.

Because electrons are supplied to the PQ pool by reduced ferredoxin during cyclic electron flow charge separation at the oxygen evolving complex of PSII the water splitting is under low demand. Through currently poorly understood processes possibly due to low energy transfer between PSII units (Fig. 8C), excess energy must be released as either fluorescence or heat (Fig. 12 -6).

Materials and Methods

Culture and incubator conditions

Axenic *Prochlorococcus sp.* VOL29 - a member of the eMED4 ecotype isolated from a cruise in the North Pacific during POWOW 1 (2012) - was grown from a master culture maintained in serially-passaged batch cultures for greater than 6 months at experimental conditions; 22°C, 14 hours of gradually increasing and decreasing light levels designed to mimic natural levels of light over the course of the day.

Prior to the experiment N-replete batch cultures were transferred from 20ml test tubes in standard AMP-A [61]to successively larger bulk culture vessels containing modified AMP-A media (augmented to 5mM TAPS) and slowly stirred with a Teflon coated magnetic stir bar. Four days prior to the experiment, culture was transferred from a single 2 L Pyrex culture flasks to four identical 2.2 L cultures at a dilution rate of 1:10, allowed to reach log phase growth, and experiment began when culture concentrations were near those of known steady state concentration of chemostat (Fig. 7).

N-limited cultures were generated through use of a chemostat. Briefly, 400 ml of late log phase N-replete batch culture was pelleted, resuspended in 100ml N-free basal medium (Turks Island Salt Mix), and divided evenly to four 2 L Pyrex bottles containing about 2 L modified N-limited AMP-A (5mM TAPs; 16μM NH_4Cl). To achieve N-limited growth, cultures were grown for 4 days prior to initiating the pump. At chemostat start (day -6, Fig. 6), the system was initially primed at a high flow rate prior to dropping flow rate to a constant rate replacing ~9% of culture volume daily. All materials and containers contacting culture were acid washed.

For both treatments, growth cultures were sampled at two time points, 12:00 and 16:00, in order to observe the role of cell cycle on overflow metabolism. At each time point two 2 L cultures were removed from the incubator to be distributed for sample collection in a flow through hood.

Photosynthetic rates and efficiency

Inorganic carbon fixation was measured using methods previously described [15] and photosynthetic efficiency was measured using a Satlantic FIRe fluorometer system [15].

Lab metabolomics sample collection

550ml of culture from the main 2 L flask was transferred to 1 L Pyrex bottles containing a Teflon coated magnetic stir bar and enough 13-C sodium bicarbonate to raise culture concentrations to 0.6mM over ambient levels (standard AMP starts at 0.6mM). Cultures were immediately brought back to the incubator and placed on the stir plate for measurements of metabolite isotopic labeling at 30, 60, and 90 minutes. While the labeling experiment was being moved to the incubator time zero measurements were collected using unaltered culture from the parent flask. All samples were collected using high vacuum filtration on 0.2 μm Isopore filters (Millipore), flash frozen in liquid nitrogen, and stored at -150 °C until extraction.

Field metabolomics sample collection

Seawater was collected from the mixed layer of the oligotrophic N. Pacific Ocean in the winter and summer of 2013 (POWOW 2 and POWOW 3) by CTD-Niskin rosette. Once the water was aboard the ship, it size fractionated through gentle 0.8μm filtration, thereby enriching phytoplankton communities for *Prochlorococcus*. Following size fractionation the "size fractionated" water pool was transferred to 250 ml polycarbonate bottles. Bottles were completely filled, ~300 ml, to eliminate air bubbles and reduce bottle effects. The bottles were placed in a surface sea temperature flow-through incubator to acclimate for 2-3 hrs. Shortly after noon, time zero samples were collected and the remaining samples were spiked with isotopically labeled inorganic carbon (IOC; 0.6mM $NaH^{13}CO_3$) to trace inorganic carbon into observed metabolites. At 50, 100, and 200 minutes, 0.6 L – two bottles, were removed from the incubator, collected via high pressure filtration on 0.2 μm MAGNA nylon filters, flash frozen, and stored in LN_2 and -150 °C deep freezer prior to sample extraction in the laboratory.

Extraction of metabolites from filters

Filters were defrosted and washed from filter in 1.3 mL of extraction solvent (40:40:20 HPLC grade methanol, acetonitrile, water with 0.1% formic acid) kept at 4 ˚C in 1.5 mL centrifuge tubes. Extraction proceeded for 20 minutes at -20 ˚C. Samples were centrifuged for 5 minutes (16.1 rcf) at 4 ˚C and supernatants were transferred to new vials. Vials containing extraction supernatants were evaporated under a stream of N_2 until all the extraction solvent had been removed. Solid residue was resuspended in 300 µL of sterile water and transferred to 300 µL autosampler vials. Samples were immediately placed in autosampler trays for mass spectrometric analysis.

UPLC-MS Analysis

Samples in the autosampler tray were kept at 4 ˚C. A 10 µL aliquot was injected through a Synergi 2.5 micron Hydro-RP 100, 100 x 2.00 mm LC column (Phenomenex) kept at 25 ˚C. The mass spectrometer was run in fullscan mode with negative ionization using a previously described method.[62] The eluent was introduced into the mass spectrometer via an electrospray ionization source coupled to a Thermo Scientific Exactive Plus orbitrap mass spectrometer through a 0.1 mm internal diameter fused silica capillary tube. The samples were run with a spray voltage was 3 kV. The nitrogen sheath gas was set to a flow rate of 10 psi with a capillary temperature of 320 ˚C. AGC target was set to 3e6. The samples were analyzed with a resolution of 140,000 and a scan window of 85 to 800 m/z for from 0 to 9 minutes and 110 to 1000 m/z from 9 to 25 minutes. Solvent A consisted of 97:3 water:methanol, 10 mM tributylamine, and 15 mM acetic acid. Solvent B was methanol. The gradient from 0 to 5 minutes is 0% B, from 5 to 13 minutes is 20% B, from 13 to 15.5 minutes is 55% B, from 15.5 to 19 minutes is 95% B, and from 19 to 25 minutes is 0% B with a flow rate of 200 µL/min.

Data Processing

Files generated by Xcalibur (RAW) were converted to the open-source mzML format[63] via the open-source ProteoWizard package[64]. MAVEN software [65, 66] (Princeton University) was used to align and automatically correct the total ion chromatograms based on the

retention times for each sample. Known metabolites were manually selected and integrated by m/z (± 5 ppm) and retention time for each sample. Fold changes were calculated and the data were transformed and clustered using Cluster software[47]. Heat maps were then generated from clustered data using Java Treeview[48] software.

ATP and glycogen pool sizes.

Biological replicates were measured in triplicate. For each of the measurements 300 ml was collected via centrifugation (15mins at 15K g with half speed acceleration and deceleration) and resuspended in 1 ml fresh AMP. The culture concentrate was partitioned for analysis as described below.

ATP

Sample Collection and extraction – Nucleotide extraction, enzymatic conversion and firefly luciferase assay was modified from the previously described protocol of Karl and Holm-Hansen [49]. Briefly, 0.5 ml of resuspended pellet was added to 2.0ml boiling 25mM Trizma base (pH 7.40). The samples were boiled for 15 mins, allowed to cool to room temperature, flash frozen in LN_2, and stored at -80°C.

Enzymatic conversion and assay – Samples were defrosted to room temperature and standards were made containing ATP at 0.1 ml sample was added 96 well plates containing 0.05 ml of 0.75 mM sodium phosphate buffer (pH 7.4). Extracts were sealed in 96 well plates and incubated at 30°C for 30 mins and transferred to a boiling water bath for 3mins. Once plates returned to room temp they were assayed for total ATP concentration using the firefly luminescence method. ATP concentration was measured using an Orion-L microplate luminometer (Berthold Detection Systems, Pforzheim, Germany). In short, 0.1ml firefly luciferase extract is injected into wells and the peak luminescence was determined over a 5 second period following an initial 2 second delay. Firefly luciferase extract was made as described by manufacturers, as per the manufacturer's suggestion an additional 0.26 mM

luciferin was added to increase sensitivity of the assay. The extract was aged for 6 hours at room temperature in the dark prior to the assay.

Glycogen

Sample collection, extraction, and precipitation of glycogen – Glycogen extraction and measurement was performed as previously described [50]. Briefly 0.5 ml resuspended pellet was flash frozen in LN_2 and stored at -80°C until samples were extracted. Frozen culture was freeze dried, resuspended in 0.5 ml 30% KOH, and vortexed vigorously for approximately 20 mins. Following resuspension samples were placed in a boiling water bath for 4 hours with intermittent shaking and then allowed to cool to room temp until the next step.

Glycogen, which is resistant to alkali environments of the extraction protocol, was then purified and precipitated through the stepwise additions of Milli-Q water (1 ml) and absolute ethanol (2.77 ml). Glycogen was pelleted by centrifugation at 10,000 RCF for 15 mins. The pellet was washed in 1 ml ice cold 60% EtOH, supernatant aspirated, and the pellet was vacuum desiccated for quantification.

Glycogen quantification – Desiccated samples were resuspended in 0.25 ml Milli-Q water and transferred to an Eppendorf tube containing 0.25 ml 5% phenol solution. After samples were vortexed, 1 ml concentrated sulfuric acid was added hydrolyzing glycogen to glucose. Samples cooled to room temperature for approximately 15 mins prior to their measurement. Glycogen concentration was determined through measurement of absorbance at 488 nm on a Beckman Coulter DU 800 spectrophotometer. The linear regression of glucose standards at 250, 100, 75, 50, 25, and 10 mg/ml in 0.15% benzoic provide estimates of glucose associated with the glycogen macromolecules.

CHAPTER 4:

METABOLOMIC ASSESSMENT OF INORGANIC CARBON ASSIMILATION BY PHYTOPLANKTON IN THE N. PACIFIC OCEAN

Abstract

In the euphotic zone of the oligotrophic North Pacific Ocean, research suggests phytoplankton growth is constrained through nutrient limitation. To investigate the effects of nutrient availability on phytoplankton metabolism, we traced inorganic carbon into metabolites of cells in whole community and *Prochlorococcus*-enriched fractions in unamended control and ammonium-amended natural seawater microcosms. The rate of carbon incorporation from stable isotope labeled carbon dioxide - supplied as ^{13}C-bicarbonate - into intracellular metabolites of our microcosms was quantified using ultra performance liquid chromatography—mass spectrometry based metabolomics. Observed rates of labeling in the key metabolites glutamine and glutamate suggest that different size classes of phytoplankton utilize different metabolic strategies for assimilating nitrogen during periods of nitrogen influx.

Introduction

The North Pacific Subtropical Gyre (NPSG), where plankton persist under nutrient limitation, has been called the largest contiguous biome on the Earth's surface. Although life in oligotrophic biomes is severely constrained by nitrogen availability [51, 52, 67, 68], the phytoplankton in these expansive ecosystems are responsible for much of the world's total primary production. Of this primary production, a significant fraction is thought to be performed by *Prochlorococcus* spp. [5] where *Prochlorococcus* can outcompete larger phytoplankton (e.g protists) [4]. The metabolic mechanisms underlying the fitness advantage for *Prochlorococcus* spp. in these low-nutrient environments are not well understood, but likely involve tradeoffs for growth in nutrient replete environments, given that conditions of high nutrient abundance (e.g. coastal runoff, upwelling, deep water mixing events), favor the growth of large phytoplankton [52, 67, 68].

Previous studies involving nutrient addition assays have shown phytoplankton growth to be limited by nitrogen in the N. Pacific [51, 67, 68]. While these assays provided evidence that nitrogen limits growth, they cannot provide information on the mechanisms by which nitrogen availability impacts the pathways that feed the carbon backbone for the assimilatory reactions

(glutamine synthetase and GOGAT). To investigate the effects of nitrogen limitation and pulses of availability on phytoplankton metabolism, we traced inorganic carbon incorporation into metabolites of cells in nitrogen amended and control microcosms containing either size-fractionated (*i.e. Prochlorococcus*-enriched) or whole communities. Because our tracer is inorganic carbon it allows us to target metabolites associated with microbes capable of fixing carbon (photoautotrophs). To observe the metabolism of *Prochlorococcus* spp. in the natural mixed community we size-fractionated half of our microcosms to remove all other phytoplankton and large heterotrophic plankton. Size fractionation was performed using gravity filtration through 0.8μm pore size filters, enriching for *Prochlorococcus* spp. (nominal size 0.6 μm). Comparisons of the whole community and *Prochlorococcus*-enriched metabolisms were made over six experiments split over a paired set of winter and summer research cruises within the same year and general body of water - the N. Pacific. The observed intracellular metabolites and rate of carbon labeling in them provide the first descriptions of the *in vivo* metabolic responses to nutrient enrichments in the oligotrophic oceans. Insights into the rates of metabolite labeling in key nitrogen assimilatory molecules such as glutamate and glutamine suggest carbon and nitrogen assimilatory metabolic pathways may proceed through different mechanisms in whole community and *Prochlorococcus* enriched microcosms.

Results

The similar patterns observed in global cellular metabolism assessed by untargeted mass spectrophotometry analysis, suggest that the *Prochlorococcus*-enriched and whole communities utilize many of the same metabolic pathways [see Figure 13 for results from a representative field station sampling (POWOW 2 cruise, experiment 1.1)]. Overall, nitrogen amendments did not appear to cause dramatic changes in the profiles of mass to charge metabolite features observed in the whole community or the *Prochlorococcus* enrichments. Several metabolic features (glutamate, glutamine) showed differences between treatments (Figure 13, center of heat map), and will be the focus of the remainder of the study.

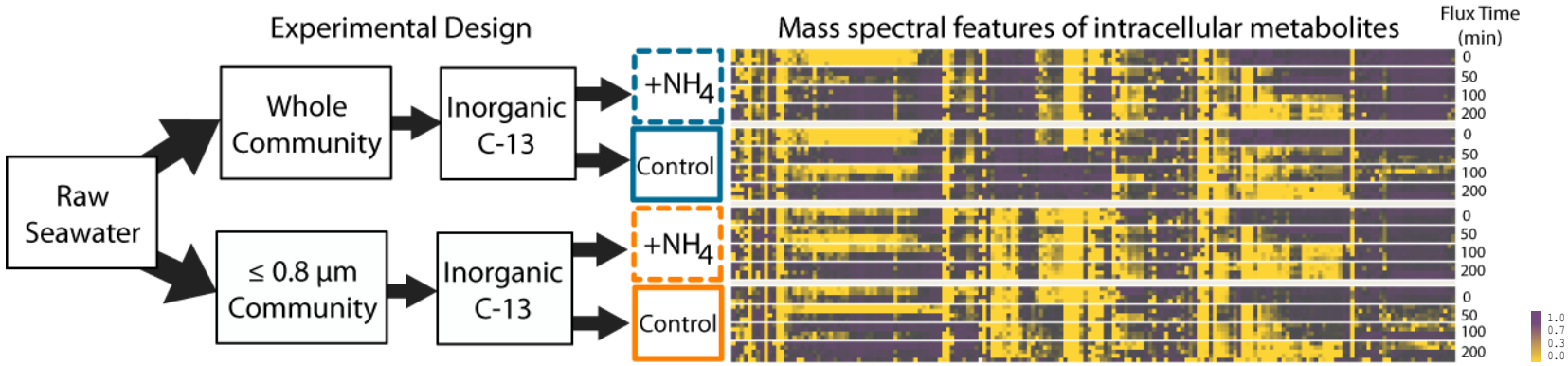


Figure 13: Experimental design and heat map of untargeted MS features from POWOW2 Exp1.1

Experimental design: Whole and size exclusion seawater were acclimated to deck incubation for 2-3 hrs. Shortly after local noon, microcosms were spiked with isotopically labeled carbon and either left at *in vivo* nutrient concentrations or provided an ammonium addition. Microcosms were sampled over 200 min labeling experiments (y-variable of segregated heat maps) to observe carbon fixation metabolisms. Heat map displays abundance unidentified mass spectral features selected from an untargeted set of observed peaks from P2 Exp1.1. Abundances were scaled by range and clustered by Kendall's τ correlation rank.

The complexity of the communities and natural environments we sampled hindered identification of the majority of the features discussed above, but pool sizes and rates of isotopically labeled inorganic carbon incorporation into the backbone of two key nitrogen assimilation metabolites - glutamate and glutamine - were established. In all six experiments, sampling 6 field stations from winter and summer and spanning 15-23 °C, metabolic pools of glutamate decreased following ammonium additions to the microcosms relative to unamended controls (Fig. 14 A,B) while pools of glutamine were observed to increase in the 5 field stations that this metabolite was detected (Fig. 15 A, B). These observations were not affected by the community composition (*i.e. Prochlorococcus*-enriched or whole communities; Figures 14 and 15; panels A,C and B,D respectively). As a result of the non-homogenous nature of the open oceans environmental and/or community composition are expected affect station to station variability, but in all cases the general trend of decreasing pools of glutamate while pools of glutamine are observed to increase albeit to varying degrees.

In addition to metabolic pool sizes we observed rate of isotopically labeled inorganic carbon incorporation into the backbones of these metabolites. Isotopic labeling of carbon in the metabolite glutamate was measured and generally we observed these rates to increase following ammonium additions. In the whole water community the rate of inorganic carbon incorporation appears to be slightly greater but differences between size fractionated and whole community are not clear (Fig. 14 C and D). The similarities between metabolisms of size fractionated and whole water samples are not continued when labeling into the carbon backbone of glutamine is considered. Glutamine becomes highly labeled for whole communities when ammonium is added (Fig. 15 C), but only the isotopically label is barely observed in the size fractionated glutamine pool (Fig. 15 D).

At the station - P2 Exp1.3 - where surface water temperature was observed to be the lowest (15°C) and ammonium concentrations were the highest (45nM; Table 3) we observed a very small response in the pool and labeling of glutamate following ammonium amendments in both size-fractionated and whole community microcosms (Fig. 15). Unfortunately, glutamine

Table 3. Experimental Station Details

Experiments and sampling occurred over two similar cruise tracks separated by approximately 6 months in the North Pacific Ocean.

Experiment	Date	Latitude	Longitude	Surface Temp (°C)	Ammonium concentration (nM)	*Prochlorococcus* counts	*Synechococcus* counts	Picoeukaryote counts
P2 Exp1.1	1/12/13	26° 41' N	-158° 0.0 W	23	29	1.77E+05	1.59E+03	7.86E+02
P2 Exp1.2	1/14/13	33° 20' N	-159° 0.2 W	18	7.7	1.19E+05	1.20E+03	1.51E+03
P2 Exp1.3	1/19/13	36° 32' N	-158° 40 W	15	45.3	5.51E+04	7.44E+03	7.34E+03
P3 Exp1.1	7/4/13	30° 43' N	-158° 0.0 W	23	0	1.61E+05	1.09E+03	8.45E+02
P3 Exp1.2	7/11/13	40° 61' N	-151° 47 W	17	0	1.01E+05	9.62E+03	1.80E+03
P3 Exp1.3	7/16/13	36° 88' N	-140° 60 W	20	11.7	1.00E+05	4.90E+03	1.77E+03

levels were below our limit of detection at this experimental station, possibly due to low concentrations of *Prochlorococcus* (Table 3). During the summer cruise, the coldest surface seawater temperatures reached for experimental stations in our cruise tracks was slightly greater than those discussed above (17°C), while *in vivo* ammonium levels were below our level of detection (P3 Exp1.2). At this station, like P2 Exp1.3 discussed above, we observed only small response in the pool size and rates of carbon incorporation into glutamate following addition of nitrogen. Interestingly, glutamine was observed at this station and although the labeling of glutamine in the *Prochlorococcus* enriched samples was very low, the response of glutamine labeling in the whole community enrichments were similar to those observed at our warmer water stations.

Discussion

The observed increase glutamine pools following ammonium addition and the concurrent drop in glutamine pools provides evidence that both the size fractionated and whole communities assimilate free ammonium through the high affinity mechanism of glutamine synthetase and glutamate-oxoglutarate amidotransferase (GS and GOGAT respectively). If, on the other hand, the low affinity enzyme glutamate dehydrogenase (GDH; 2-OG + NH_4^+ + NAD(P)H $\Leftrightarrow$ GLU + $NAD(P)^+$) was utilized for the incorporation of free ammonium, we would expect the pool of glutamate to increase or remain stable. Because we observe a decrease in the glutamate pools following addition of ammonium, an alternative hypothesis might be understood that glutamate is used at a faster rate than it can be replenished by GDH. If this uneven flow of carbon through the metabolite was occurring – faster out than in – we would expect to see recently fixed carbon move through the glutamate pool, but do not see the predicted highly enriched pools of isotopically labeled glutamate (Fig. 14 C). The above-described intracellular pools of metabolites consist of molecules from all members in our microcosm communities including the heterotrophic bacteria that are be present. As such the general metabolisms described above cannot be attributed to a specific population in our microcosm communities.

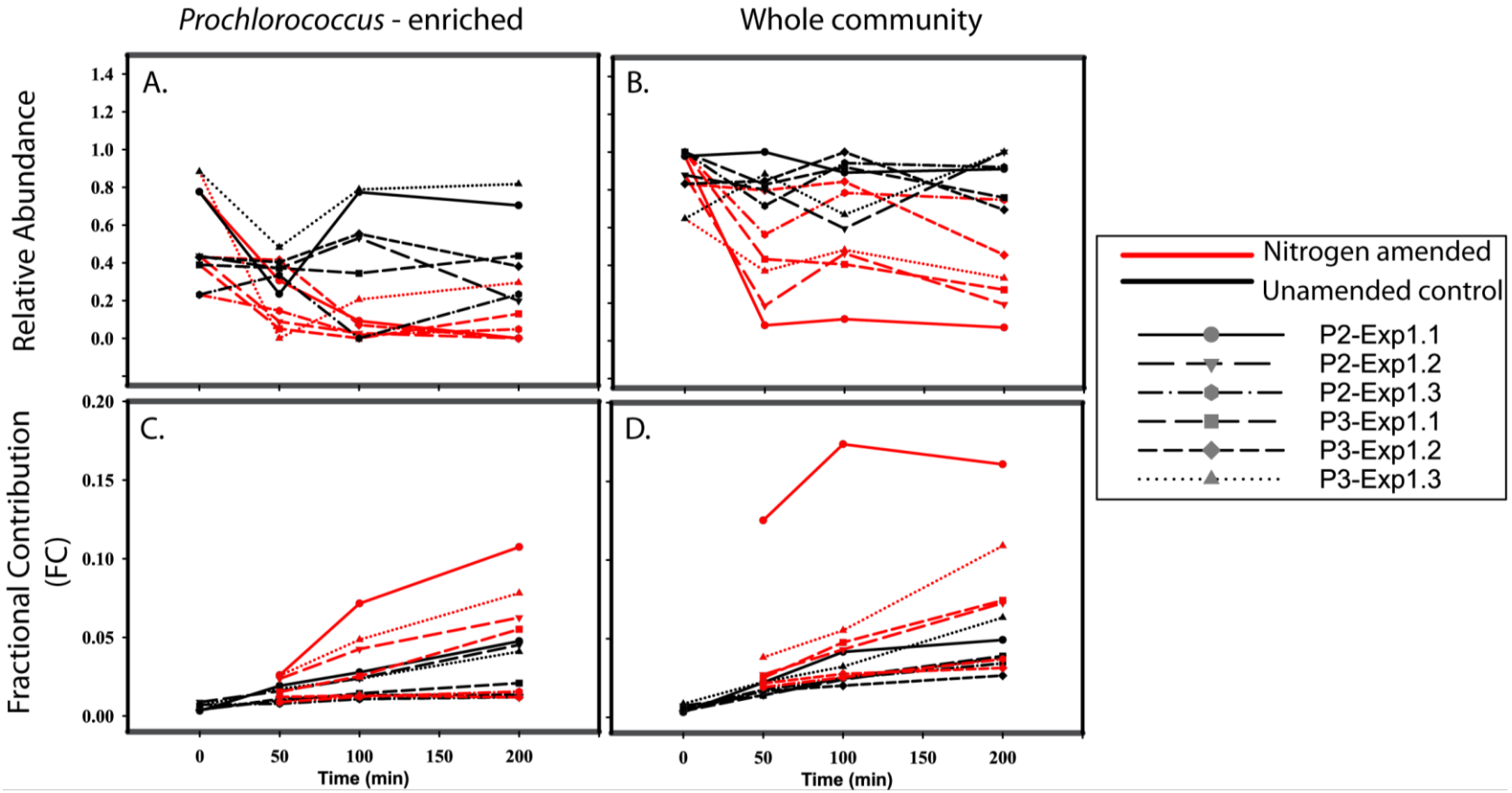


Figure 14: Intracellular Glutamate Pools and inorganic carbon incorporation

The effect of nitrogen amendment (red lines) compared to unamended controls (black lines) on intracellular glutamate in *Prochlorococcus* enriched (A,C) and whole communities (B,D) over a series of six experiments (represented by similar symbols; see legend). Pools of metabolites for glutamate (A,B) and isotopic carbon labeling of pools (C,D).

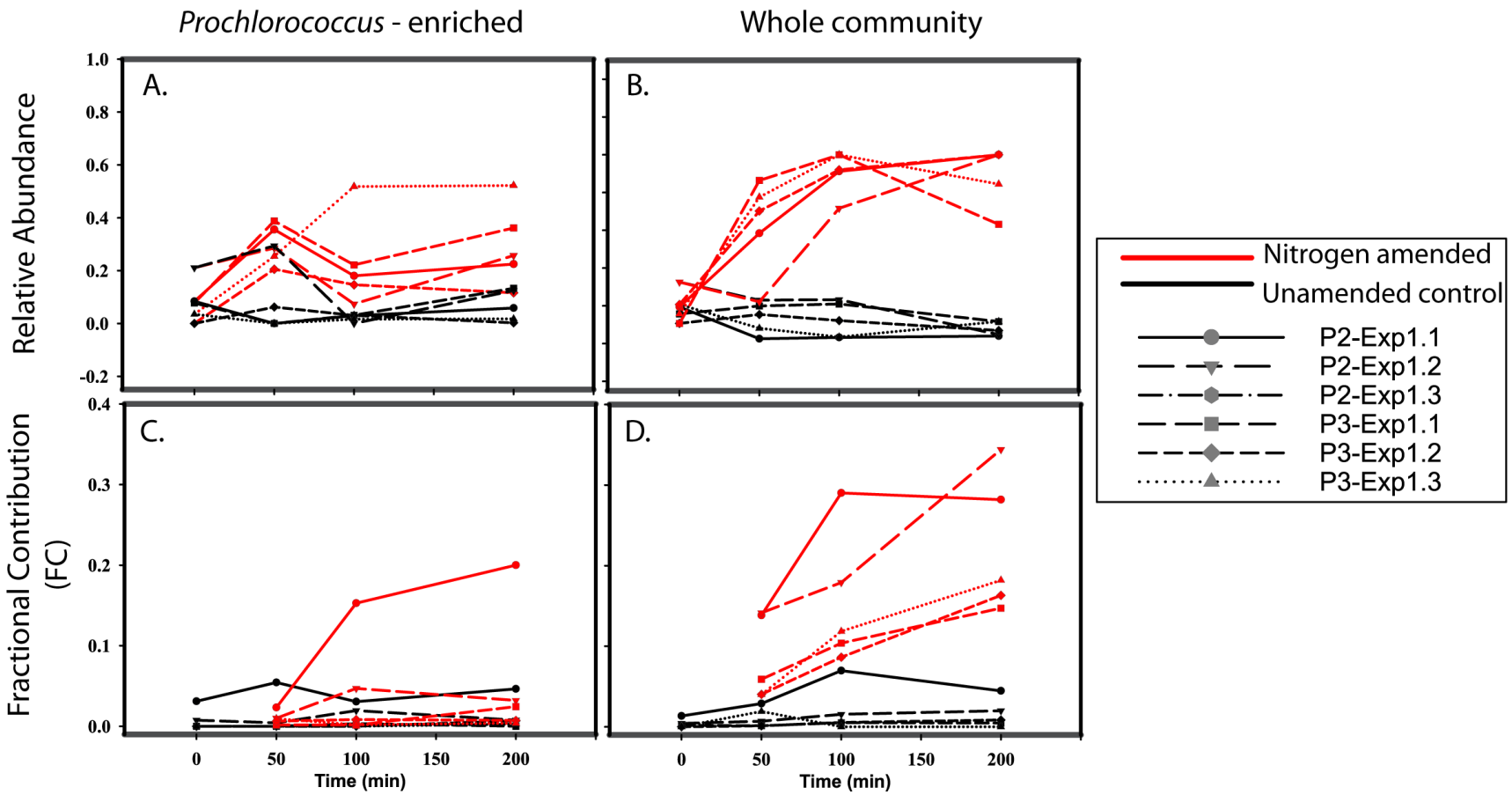


Figure 15: Intracellular Glutamine Pools and inorganic carbon incorporation

The effect of nitrogen amendment (red lines) compared to unamended controls (black lines) on intracellular glutamine in *Prochlorococcus* enriched (A,C) and whole communities (B,D) over a series of six experiments (represented by similar symbols; see legend). Pools of metabolites for glutamine (A,B) and isotopic carbon labeling of pools (C,D). Note: Glutamine was not observed at the POWOW2 Exp1.3 station

Our interpretation of the data may be unsurprising as GDH is a low affinity enzyme and as such is not suspected to play a significant role even though it consumes less energy per assimilated N atom – one reducing equivalent compared the to one reducing equivalent and one ATP used in GS. The ammonium concentrations in the euphotic oligotrophic N. Pacific is generally measured to be very low. The low abundance of this nitrogen source combined with the low affinity of the enzyme reduces its usefulness for nitrogen assimilation in these environments. In addition to the poor efficiency of using a low affinity enzyme in low substrate environments, the mere presence of active GDH may play a counterproductive role as GDH has been described as a bidirectional enzyme. When the *in vivo* concentrations of free ammonium are considered along with our observations of large intracellular glutamate pools, the bidirectional enzyme GDH would favor a reaction where free ammonium is released from glutamate generating 2-OG and one reducing equivalent. It is interesting to note that the gene for glutamate dehydrogenase (*gdhA*) has been identified in four genomes of *Prochlorococcus*. While the underlying reasons for this divergence are not known, it predicts both evolutionary and physiological factors may be driving the metabolic strategies. A previous study seeking to understand the regulatory and physiological role of GDH in *Prochlorococcus* MIT9313 provides evidence that the function of this enzyme is catabolic in nature, catalyzing the deaminating reaction proposed above [25].

Differences in the incorporation rate of newly synthesized organic carbon incorporation into glutamate and glutamine suggest that *Prochlorococcus* utilizes a mechanism for ammonium assimilation that is distinct from that observed in the whole phytoplankton community. It may be hypothesized that compartmentalization or spatial segregation of enzymes and metabolite pools enriches the metabolite pool with labeled metabolic precursors of the end product. Through the spatial segregation of recently synthesized and labeled metabolites in larger phytoplankton, metabolites may label at rates higher than those of other actively produced metabolites through co-localization or metabolic channeling. In this scenario, if a metabolite is randomly selected from its pool, the probability that it is labeled the fraction of the labeled metabolites in the total pool. This hypothesis is supported when one considers that in higher

plants GS and GOGAT are localized in the stromal fraction of chloroplasts. Cyanobacteria, void of chloroplasts, do not have stroma and the pH of thylakoid lumen during photosynthetic hours is suspected to very low (pH 4). As such cyanobacteria, specifically *Prochlorococcus*, cannot compartmentalize their metabolic functions leading to labeling rates of metabolites that mirror the labeling rates of the pool of their precursor metabolites.

Alternatively, our data support the hypothesis that *Prochlorococcus* utilize alternative metabolic processes than larger phytoplankton. Larger phytoplankton, such as bloom forming diatoms, may activate enzymatic pathways to increase carbon flow to nitrogen assimilatory processes. Specifically, we would expect the high rates of carbon fixation observed as isotopic labeling in the carbon skeleton if large phytoplankton in the "whole" water samples utilize newly synthesized carbon to form the backbone of metabolites for nitrogen assimilation. Small phytoplankton primarily utilize preexisting pools of metabolites for the carbon backbone of nitrogen uptake metabolites would incorporate less isotopically labeled carbon (Fig. 15). These conclusions are supported by laboratory studies where axenic cultures of *Prochlorococcus* PCC 9511 were not observed to respond to changes nitrogen or light by altering GS abundance or activity [69].

As a result of the non-homogenous nature of the open oceans, it may not be surprising that inter-station variability in our data suggest the physical environment and community structure affects metabolisms of the organisms. At the two stations samples with the lowest sea surface temperature (P2 Exp1.3 and P3 Exp1.2), we observed minimal response to nitrogen amendment in the pool sizes and rates of isotopic labeling of glutamate for both size fractionated and whole community samples. Although glutamine was below the signal detection for P2 Exp1.3, we observed the labeling of this metabolite in P3 Exp1.2 to follow similar trends as the warmer water stations. These data may provide evidence that water temperature affects ability of the community to both incorporate ammonium through the GS-GOGAT mechanism (as observed through the minimal response to the glutamate pool), but further investigation of

environmental and community composition data will be required to gain a clearer understanding of these effects on metabolism.

Conclusion

Under the assumed N limiting conditions found in the oligotrophic NPSG we tracked incorporation of inorganic carbon into the carbon skeletons of key N assimilation metabolites following nitrogen supplementation. Over a series of six field experiments, we observed a drop in glutamate pools and concurrent rise in glutamine pools in both size fractionated and whole seawater samples. This observation may be considered as evidence for the widespread use of the GS-GOGAT ammonium assimilation mechanism over GDH. Key differences in the labeling patterns of glutamine were observed between *Prochlorococcus*-enriched and whole community microcosms. These data provide evidence that although all plankton appear to utilize the GS-GOGAT mechanism for ammonium assimilation the mechanisms utilized to generate the carbon skeleton needed for this process may vary for large and small phytoplankton. We show large phytoplankton respond to nitrogen availability by directing recently fixed carbon into N assimilatory pathways (Fig. 16). The lower rates of labeling observed in the carbon skeletons of these metabolites in *Prochlorococcus* enriched microcosms but observed evidence for GS-GOGAT activity may suggest these minimalists incorporate free N through the utilization of previously synthesized metabolites. We hypothesize that the 'r' type lifestyles of bloom forming diatoms are better suited to respond to significant increases in limiting resources by altering carbon flow to assimilate great pools of nutrients when they become available. Alternatively, the 'K' lifestyle championed by *Prochlorococcus* spp. are adapted to quickly scavenge small pools of briefly available nutrients, but once the immediate needs of nutrients are fulfilled tight temporal regulation on transcription limits further benefit from the available nutrient pool. This model for carbon utilization during nitrogen pulses may provide a mechanism to describe the previous observations in the NPSG that show additions of reduced inorganic nitrogen to seawater can select for rapidly growing phytoplankton, of which a majority is observe to be eukaryotic [67, 68].

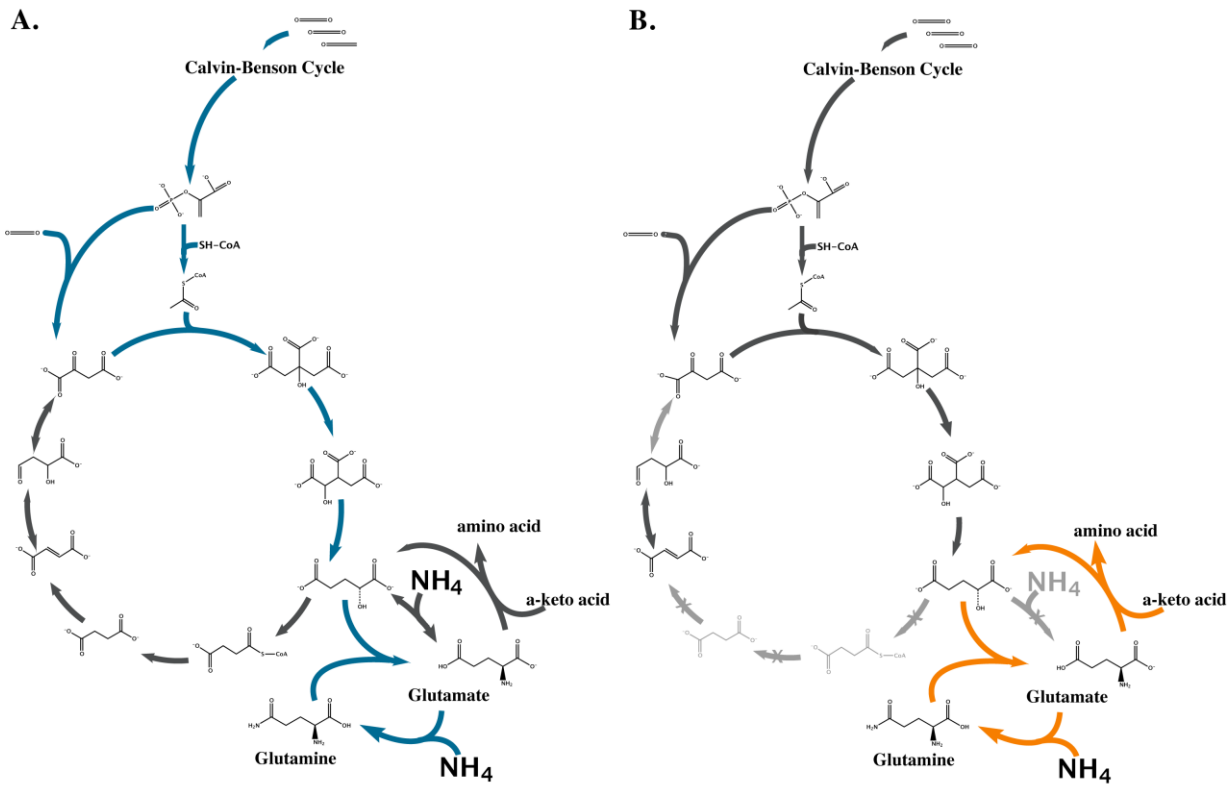


Figure 16: Nitrogen assimilation mechanism model in *Prochlorococcus* and whole community microcosms

Metabolic model predicting rates in nutrient "boom" scenarios for both large and small phytoplankton. Predicted metabolite pathways used by large (A) and small phytoplankton (B) to incorporate biologically available nitrogen. Colored arrows represent pathways utilized in metabolic strategies as predicted by metabolic labeling patterns. Grey pathways in the small phytoplankton model represent genes absent in *Prochlorococcus* spp. annotations.

Materials and Methods

To discern the effects of nutrient limitation on the metabolisms of plankton in oligotrophic environments, we compared intracellular metabolic profiles of cells grown in nitrogen-augmented microcosms to those of unamended controls in both *Prochlorococcus*-enriched and whole seawater samples. During the winter and summer of 2013 we collected seawater at research stations in the North Pacific Ocean (Table 3). Seawater was collected from the mixed layer CTD-Niskin rosette. Once the water was aboard the ship, half was size fractionated using gentle 0.8μm filtration (gravity filtration during POWOW2 and low positive pressure POWOW3) to selectively remove large plankton from the community resulting in microcosms enriched for *Prochlorococcus* spp. Following size fractionation the "whole" and "size fractionated" water pools were transferred to 250 ml polycarbonate bottles. Bottles were completely filled, ~300 ml, and placed in a surface sea temperature flow through incubator to acclimate for 2-3 hours prior to beginning the experiment. Shortly after approximately noon, time zero samples were collected as described below for both "whole" and "size fractionated" treatments. The remaining samples were spiked with isotopically labeled inorganic carbon (IOC; 0.6mM $NaH^{13}CO_3$) allowing us to trace recently fixed inorganic carbon into observed metabolites. Following IOC additions, bottles were subdivided into control – presumed N-limited – and nitrogen supplemented (2.5 μM NH_4Cl spiked) treatments. At 50, 100, and 200 minutes, 0.6 L – two bottles, were removed from the incubator, collected via high pressure filtration on a 0.2 μm 47mm MAGNA nylon filter, flash frozen, and stored in LN_2 and -150 °C until samples could be analyzed. To control for dark or non-photosynthetic carbon fixation, samples were collected after 200 mins for each of the variables from microcosms which had been kept dark by wrapping the bottles multiple times with black electrical tape.

The rate of inorganic ^{13}C incorporation into intracellular metabolites of our microcosms was quantified using high resolution accurate-mass data collected on an Exactive Plus Orbitrap mass spectrometer.

For each of the here within described experiments metabolite features were identified using the MAVEN software platform [65]. Briefly, mass spectral chromatograms for each experiment were aligned prior to running an untargeted peak detection analysis. The identified peaks were then culled manually by identifying features that had substantially smaller or insignificant peaks in the negative control chromatograms (i.e. extraction solvent only) and displayed visible, but untested, trends peak intensity between samples. Unidentified metabolic features discussed in figure 13 were scaled by range and clustered by Kendall's τ correlation rank using Cluster and Javatreeview software platforms [48]**.** Relative abundances of discussed key metabolites were identified based on known m/z ratios and retention times of the mass spectral features.

To determine metabolite labeling, we used the ratio of the relative number of labeled carbon atoms associated with a metabolite to the total relative number of carbon molecules observed. This method has been described previously as the Fractional Composition (FC) [42].

Although there are means of nonphotosynthetic (anaplerotic) carbon fixation, the collective effect it has on observed rates inorganic carbon incorporation is suspected to be dwarfed by photosynthetically based mechanisms. Indeed, samples incubated in the absence of light (nitrogen limited and – replete) were observed to contain only slightly more isotopically labeled carbon associated with glutamate than time zero and between 5 fold and order of magnitude less isotopic carbon than samples incubated in light. In the case of glutamine no isotopic carbon was observed in any of the metabolic pools for samples kept in the dark (data not shown).

CHAPTER 5: LIFE AT THE LIMITS: OBSERVATIONS ON THE PHYSIOLOGICAL MECHANISMS CHAMPIONED BY *PROCHLOROCCOCCUS* SPP.

Abstract

Over the past few decades the scientific community has continually expanded the known limits where life is understood to not only exist, but proliferate. It seems everywhere we look new strange and wonderful life forms thrive in environments we once thought inhabitable. One of these strange and wonderful lifeforms was first described little more than a quarter century ago. It is an incredibly small but overwhelmingly abundant phytoplankton, *Prochlorococcus*. In an attempt to interpret regulation on the mechanisms utilized by these abundant phytoplankton to drive their ecological success in the resource depleted open oceans has led to observations that suggest that the continuous low and slow growth rate of *Prochlorococcus* appears to be mirrored by their metabolic rates. We show key metabolic factors are influenced by both temporal variation in light and nitrogen conditions. These data suggest that natural selection favored a slow metabolic rate that poises the cell to rapidly acquire limited resources such as nitrogen through the utilization of built up carbon and energy stores.

Balancing Carbon and Nitrogen Metabolisms in *Prochlorococcus*

The preferred nitrogen source for cyanobacteria, ammonium, is integrated into metabolism at the intersection of carbon and nitrogen metabolism by the GS-GOGAT cycle. This process requires 2-OG, generated by isocitrate dehydrogenase in the TCA cycle, to form the carbon skeletons of glutamate and glutamine. The 2-OG can originate from either the carbon fixing processes of the Calvin cycle or glycogen catabolism through the pentose phosphate pathway, pathways that are active during the day and night, respectively. As there are additional cellular demands for these carbon and energy sources it raises questions as to the capacity for inorganic nitrogen assimilation in *Prochlorococcus* over the course of a diel.

Unlike most cyanobacteria *Prochlorococcus* lack a complete TCA cycle, and instead have oxidative and reductive branches [22]. The carbon that reaches the endpoint of the oxidative branch of the TCA cycle is believed to be fated to ammonium assimilation. Cyanobacteria balance the flow of carbon with nitrogen availability with several key regulators, however in *Prochlorococcus* they do not appear to perform as described in other cyanobacterial

systems [31, 32]. In cyanobacteria, N- stress causes increased pools of 2-OG, promoting the interaction of 2-OG with the regulatory protein P_{II} (see Ch. 1 for review) and our data provide the first known evidence for generation of this metabolic pool under nutrient limitation in *Prochlorococcus* suggesting similar regulatory systems may be used. Transcription of genes involved in carbon acquisition and fixation suggest MED4 represses carbon fixation during N-stress [33], but without measurements of the rates for carbon fixation during N-limited growth our ability to generate effective models for growth and carbon fixation of *in vivo* populations has been limited.

Under the nitrogen limited environments selection for efficiency and thrift is suspected to provide growth advantages, but the ability to store nitrogen during enrichment periods may provide additional capacity to survive periods when this nutrient is not available. In cyanobacteria cyanophycin and phycobillisomes are produced during periods of nitrogen surplus and degraded when nitrogen is limited [60, 70-72]. *Prochlorococcus* is a prochlorophyte that lacks phycobillisomes, and strain MED4 does not encode the genes for cyanophycin synthesis. MED4 does appear to possess a degenerate phycoerythrin (PE) system with [73-75] as well as genes for the synthesis of the polyamine spermidine from the metabolic precursors of arginine and aspartate. Both of these systems, degenerate PE and spermidine, currently have unknown functions in *Prochlorococcus* and it is possible that one or both of these systems may be involved in a previously unrecognized nitrogen storage system.

Nitrogen Metabolism and Energetic Potential over a Diel

Previous experiments exploring the both transcript and protein abundance over a diel cycle provide seemingly contradictory evidence for regulatory mechanisms where amplitude of transcript abundance was correlated to the time of day but proteins abundance did not appear to correlate with previous transcript data [14, 15]. Disconnects between the regulation mechanisms of mRNA and protein production appear to runs antithesis to central biological dogma that transcription directs translation. As such we utilized the recently emerging technique of metabolomics in attempt to resolve the differences in these regulatory patterns. Unfortunately, low metabolic coverage limited our observations to the characterization of a single well-resolved

metabolite, glutamate. Interestingly, like the transcript abundance, our data appears to suggest that some components of metabolisms appear to be tightly correlated to temporal factors driven by available energetic potential. These observations include temporally mediated adenylate phosphate pools, glycogen, and anabolic to catabolic reductant ratios. On the other hand, our analyses of inorganic isotopically labeled carbon in glutamate, the central nitrogen and carbon hub, may suggest that loose temporal regulation of post translational mechanisms may allow metabolites to form beyond the transcriptional restrictions mirroring what was observed in the patterns of protein abundance.

Interestingly these glutamate data show nitrogen incorporation can occur at all time points over the course of the day and with the exception of one time point the rates of isotopically labeled nitrogen are all approximately equivalent. This observation raises questions regarding the mechanism of carbon and energy application for the acquisition and assimilation of nitrogen. The sources for these stores vary as a function of the time of day (*i.e.* solar energy and inorganic carbon during the day versus glycogen catabolism at night), but the metabolic rates that rely on these sources of carbon and energy do not appear to be affected. Our results suggest that shortly after dusk post-translational regulation restricts nitrogen assimilation into the cell. These data may provide evidence that the switch from sunlight driven metabolisms to the utilization of glycogen stores generates a short period where metabolic capacities may be negatively impacted where energetic potential (adenylate phosphate / reductant potential) and/or the metabolic pool size of carbon substrates may affect *de facto* regulation.

Metabolic Effects of Nitrogen Limitation on Prochlorococcus

That *Prochlorococcus* spp. can dominate the nitrogen-limited NPSG with its non-canonical regulation of nitrogen assimilation genes implies that *Prochlorococcus* may utilize previously unknown mechanisms to gain fitness advantages. Comparisons of the metabolic state and coordination of *Prochlorococcus* grown under both nitrogen limited and nitrogen replete environments described in Chapter 3 allow for previously unknown observations on mechanisms for their success. The observations made here are the first known to report the metabolic states

for both nitrogen limited and nitrogen replete non-diazotrophic marine cyanobacteria. Similar to the phosphate limited chemostat utilized by Krumhardt et al. [76], our nitrogen limited chemostat allowed cultures to acclimate to the nutrient-limiting conditions and simulate the physiological state of natural populations in the NPSG.

Comparisons of axenic *Prochlorococcus* VOL29 cultures grown under both nitrogen replete and limiting conditions show that, carbon fixation rates and the flow of fixed carbon through metabolite pools are higher when nitrogen is in excess, while both the pools of glycogen and a majority of the observed metabolites are lower than when nitrogen is limiting. Although most metabolites are observed to pool in nitrogen limiting conditions, one metabolite appeared to buck this trend. Aspartate pooled in our nitrogen replete culture and the isotopic labeling this metabolite suggests carbon fixed by RuBisCO in the Calvin cycle is directed to the synthesis of aspartate when nitrogen is abundant. Under nitrogen limiting conditions, small pools that become partially labeled quickly (<30 mins) reach steady state labeling suggest that the low levels of most of the isotopic carbon flowing into this metabolite is from PepC while the remaining carbon skeleton (phosphoenolpyruvate) is generated from pre-existing pools of precursor metabolites. These observations suggest aspartate may perform a previously undescribed role in nitrogen assimilation. It is interesting to note that *Prochlorococcus* spp. do not have genes for the synthesis of common cyanobacterial nitrogen storage metabolites - urea or cyanophycin - but do encode genes homologous for spermidine biosynthesis. The presence of these genes may suggest the possibility that *Prochlorococcus* spp. can utilize aspartate for the generation of this polyamine as a nitrogen storage molecule when reduced inorganic nitrogen is abundant. Spermidine was not measured in this study, but should be quantified in future investigations of nitrogen limitation in *Prochlorococcus*.

In the nitrogen-limited NPSG *Prochlorococcus* numerically dominates over larger and more genomically-complex phytoplankton. To determine whether the observations we measured in the laboratory are indicative of the mechanisms utilized by *in vivo* populations of *Prochlorococcus* we tracked inorganic carbon fixation by following isotopic carbon through

nitrogen assimilatory metabolites and compared them against the metabolisms of the whole phytoplankton community. Additionally, we asked how the metabolisms for the observed communities might respond to influx of ammonium. Our data provide evidence that *Prochlorococcus* uses preexisting (unlabeled) carbon pools to generate the carbon skeletons necessary for nitrogen assimilation while carbon labeling of the metabolites involved in nitrogen assimilation of cells in whole phytoplankton microcosms appear to utilize recently fixed carbon (isotopically labeled carbon) to assimilate the influx of newly available nitrogen.

Application of a Metabolic Flywheel

Oscillations between nutritional and/or energetic resource 'feast and famine' are experienced by organisms at all levels of life. The mechanisms that balancing these resources through management of the essential metabolic building blocks during the peaks and troughs of resource availability can drive life strategies. These strategies appear to split between two general camps; either store resources acquired during periods of feasting to carry metabolisms through the subsequent periods of fasting or to find a way to survive on the limited resources available during the famine. Observations of many commonly studied organisms utilize the first of these two methods; e.g. diatoms boom and bust as wind or anthropogenic sources prime the environment for growth while *E. coli* feast when you feast and fast when you fast. Unlike organisms that avoid famine by building stores to carry them through while they persist at low metabolic activity, *Prochlorococcus* thrives during periods of low nutrient availability when others are lying in wait for something better. By reducing their nutritional demands through a variety of mechanisms [8, 9, 69], *Prochlorococcus* can sustain life in the oligotrophic waters of the tropical and subtropical oceans providing a driving force for global biogeochemical cycles.

In the oligotrophic oceans substantial inputs of nutrients are rare and generally are regionally specific (equatorial upwelling) or seasonal (deep mixing events). During nutrient enrichment events such as those mentioned above, large phytoplankton such as diatoms and *Synechococcus* spp. dominate the water column [52, 67]. Outside these enrichment events, the

tropical and subtropical oligotrophic oceans have very little nutritional variation as measurable using current techniques. *Prochlorococcus* spp. survive through the efficient utilization of the limited supplies of nutrients, but also can assimilate nutrients that become available. In these environments cell death of neighboring planktonic cells can release nutrients as short and disperse bursts with low concentrate but life-sustaining nutritional availability. One mechanism of cell death in these biomes, predation by phage, is suspected lyse a significant but highly variable fraction of the total planktonic community on a daily basis (reviewed in [77]). The resulting small localized release of nutrients to these environments are competed for by the whole community but both the cellular proximity to the source and the ability to assimilate these short-lived resource pools may provide a competitive advantage.

In the photic zones of the open oceans *Prochlorococcus* must balance surplus of solar energy with the lack of available resources. To protect photosynthetic machinery while maintaining metabolic potential cells data discussed in chapter 4 provides evidence for low metabolic rates and overflow metabolism as a mechanisms that may help balance the energetic and nutritional resources, but questions remain regarding the efficiency of this mechanism. We propose the low metabolic rates of organisms under nutrient limitation as well as their constant collection and utilization of energy might drive a metabolic mechanism analogous to the flywheel, a simple device used to store mechanical energy. Using this system an energy source such as electrical current drives a motor that accelerates a rotation around a drive shaft of a wheel. The spinning of the wheel stores the energy until it is applied back to the drive shaft causing the motor to generate electrical current back through the system. This system has been employed to supply an even source of energy when supply is unstable but it can also work in reverse where stable energy can be added to the system and build up over time. When demand for energy is high the flywheel can release its stored energy as instantaneous rates that are exceed those of the continuously applied source.

In our model, predictable daily solar energy is applied to the generation of large pools of metabolites that act as stores of carbon and energy. These stores might be considered as the

wheel where the speed it rotates around the drive shaft might be understood as rate of reactions. Energy spun through the wheel of carbon fixation pathways can be applied in short powerful bursts for nutrient collection and utilization. In the resource poor environments when small unpredictable pools of nutrients become available instantaneous power supply may generate a competitive advantage over organisms that lie and wait for nutrient pools to become available. Like friction releasing energy as heat in a flywheel, the continuous build up and maintenance of these pools when nutrients are scarce may result in the pooling of carbon and energy rich metabolites that exceed the physical storage capacity of cell. This may result in energy and carbon must be released through the process of overflow metabolism.

The sum of the energy that can be stored in a flywheel is dependent on the inertia of the wheel in motion. Because inertia is a function of both the angular velocity and mass of the wheel, the mass of a flywheel is a central determinant of the energetic storage capacity for a system. This might be better understood by considering two flywheels of different mass spinning at the same velocity, the flywheel with lower mass will contain less energy and as such have a reduced capacity to release energy when compared to a flywheel of with a greater mass. For *Prochlorococcus* we consider the mass of the flywheel to be analogous to the size of the metabolite pool while the energy input is solar derived. Because solar energy intensity is equally applied to all members of a community (assuming limited cell shading under the low cell densities of the oligotrophic oceans), organisms with a metabolic flywheel of greater mass (*i.e.* larger metabolite pool) will have an increased source of instantaneous energy that can be applied under nutrient limiting conditions and during periods when available energy is scarce (*i.e.* night). This flow is much like the release of energy from a flywheel where it provides short bursts of carbon and energy to supply the metabolic demands of nitrogen assimilation, but once the pools of carbon and energy are depleted the system must refill the metabolic pools to recharge its metabolic flywheel.

Under nutrient replete conditions when *Prochlorococcus* is outcompeted by larger and more metabolically diverse organisms our model suggests that the constant draw on the energy

stored in *Prochlorococcus*'s metabolic flywheel reduces their capacity for resource acquisition. In our experiments when *Prochlorococcus* was grown under nitrogen replete conditions we observed low levels of metabolic pools. The small size of these pools and tight temporally regulated transcription may diminish ability to compete for large nutrient pulses while larger phytoplankton can 'wake up' from their slowed metabolic state and upregulate the pathways needed for nutrient assimilation. Our observations of the labeling patterns and pools of glutamate, glutamine, and aspartate provides key insights into the metabolic flywheel in *Prochlorococcus*. In our laboratory experiments where we compared metabolisms of nitrogen limited and nitrogen replete cultures, aspartate pools and labeling rates suggest that this metabolite may act as a sink for assimilated nitrogen when it can be scavenged. Subsequent observations of *in vivo* populations discussed in Chapter 4 compare metabolisms of *Prochlorococcus* against those of whole community phytoplankton. Our reported carbon incorporation into glutamate and glutamine suggest that larger phytoplankton generate pools of highly labeled metabolites while the low isotopic labeling of carbon in *Prochlorococcus* enriched cultures but generation of the necessary pools suggest previously fixed pools of carbon are utilized to form the carbon backbone of nitrogen assimilatory metabolites suggesting large pools of intracellular metabolites are used to assimilate nitrogen as it becomes available.

Future Directions

The data presented for my dissertation describe general metabolic topographies of *Prochlorococcus* as a function of the environmental conditions in which they persist. Although strong metabolic connections and mechanisms are difficult to establish with confidence, we draw a number inferences from these gathered data that can be applied to generate a new set of questions and hopefully open up new avenues of study to further our collective understanding of the mechanisms employed by one of the most successful organisms on Earth. Of particular interest are the regulatory mechanisms used by *Prochlorococcus* spp. to efficiently choreograph metabolism over the diel cycle under nutrient limiting conditions and the metabolic mechanisms they might employ to gain fitness advantages over competitors.

In eutrophic zones of the open oceans such as upwelling regions *Prochlorococcus* is outcompeted by diatoms and larger cyanobacteria. This may raise the question: if *Prochlorococcus* is more abundant in the oligotrophic open oceans where low nutrient levels persist what are the factors contributing to their loss of fitness when nutrients are constitutively abundant? The nutrient replete conditions that we commonly grow *Prochlorococcus* in the laboratory can reach concentrations 3 to 4 orders of magnitude greater than they are observed at sea. The inability to outcompete the larger phytoplankton in the nutrient replete environment, but can benefit greatly from the nutrient rich waters, raises questions regarding the mechanisms that drive ecological success in nitrogen limited environments, but lead to their general inability to compete in resource rich environments. This observation is furthered through the common observation of *in vivo* nutrient enrichment experiments where cell counts of *Prochlorococcus* drop while increases are observed in the cell abundances of larger phytoplankton[67, 68]. The drop in *Prochlorococcus* populations may be caused by chemical warfare or predation during these nutrient rich pulses, which could be tested by simply removing the large phytoplankton from the nitrogen enriched communities and testing whether the *Prochlorococcus* growth is still inhibited. Alternatively, the loss of competitive advantage under these conditions suggest efficiencies gained in nutrient poor environments are not as effective when the nutrient pools rise. We ask whether de-energization of the metabolic flywheel may be negatively impacting their ability to compete or if another mechanism may be reducing fitness in these environments?

Experiments designed to test the metabolic strategies used by both pure cultures of *Prochlorococcus* and competitive co-cultures with larger phytoplankton during simulated feasts and famine of nutrients may provide insights into the interactions of the test subjects. This might be achieved by comparing growth of test cultures grown under nitrogen limitation following nitrogen enrichment. In addition to the phytoplankton that *Prochlorococcus* must compete with for the sparse nutrients, heterotrophic plankton and ammonium oxidizing archaea also rely on available ammonium to survive, but the competition kinetics and mechanisms for this shared resource is poorly understood.

For *Prochlorococcus* the disconnect between balance of energy acquisition, utilization, and storage in our observed diel incorporation patterns of nitrogen assimilation suggest they may take advantage of loose metabolic regulation and large pools of metabolites to benefit from the fleeting nutrient pool that become availability in the open oceans. To allow for this 'loose' regulatory control necessities energetic balance and carbon stores which may not be always available. Our diel experiments shows that shortly after dusk *Prochlorococcus* metabolism is at a transitional state for energy utilization (*i.e.* switch from glycogen synthesis to degradation) while carbon and nitrogen incorporation into glutamate suggests tight regulatory control at this time that was not observed at other points during the diel cycle. As the only time point observed during the diel where we observed no inorganic carbon incorporation and nonlinear ammonium assimilation, the transition to complete darkness at night but before catabolism of glycogen provides a key regulatory point in *Prochlorococcus* that may be exploited to gain deeper understanding of the mechanisms of regulation. Further investigations into his currently uncharted field of study will provide information regarding the rate limiting mechanisms the regulatory mechanisms. Specific fields that can be addressed will approach whether it is energetic potential, lack of carbon skeletons, or metabolic focus on cell division.

One tool that may be employed to approach the goals stated above is the glutamine synthetase (GS) inhibitor methionine sulfoximine (MSX). My preliminary data with this inhibitor showed pooling up of glutamate when GS was inhibited, decreased pools of glutamate when cultures were starved of photic energy by transferring to opaque culture vessels, and increased labeling of aspartate following MSX treatment. These data may suggest GOGAT is powered by photosynthetically derived NADPH and blocking glutamine synthetase results in the pooling of glutamate and label through aspartate. Further experiments can be designed to explore the regulation of GS-GOGAT at dusk when temporal regulation was observed to be the greatest for carbon and nitrogen metabolisms. Additional insight can come from use of metabolic inhibitors such as proton motive force uncouplers (eg. CCCP) or enzymatic inactivators of isocitrate dehydrogenase that block the assembly of *de novo* 2-OG.

REFERENCES

1. Falkowski, P., et al., *The Global Carbon Cycle: A Test of Our Knowledge of Earth as a System.* Science, 2000. **290**(5490): p. 291-296.
2. Falkowski, P.G., *The role of phytoplankton photosynthesis in global biogeochemical cycles.* Photosynth Res, 1994. **39**(3): p. 235-58.
3. Goericke, R. and N.A. Welschmeyer, *The marine prochlorophyte Prochlorococcus contributes significantly to phytoplankton biomass and primary production in the Sargasso Sea.* Deep Sea Research Part I: Oceanographic Research Papers, 1993. **40**(11–12): p. 2283-2294.
4. Zubkov, M.V., *Faster growth of the major prokaryotic versus eukaryotic CO2 fixers in the oligotrophic ocean.* Nat Commun, 2014. **5**.
5. Flombaum, P., et al., *Present and future global distributions of the marine Cyanobacteria Prochlorococcus and Synechococcus.* Proceedings of the National Academy of Sciences, 2013. **110**(24): p. 9824-9829.
6. Partensky, F., W.R. Hess, and D. Vaulot, *Prochlorococcus, a Marine Photosynthetic Prokaryote of Global Significance.* Microbiology and Molecular Biology Reviews, 1999. **63**(1): p. 106-127.
7. Giovannoni, S.J., J. Cameron Thrash, and B. Temperton, *Implications of streamlining theory for microbial ecology.* ISME J, 2014. **8**(8): p. 1553-1565.
8. Morris, J.J., R.E. Lenski, and E.R. Zinser, *The Black Queen Hypothesis: Evolution of Dependencies through Adaptive Gene Loss.* mBio, 2012. **3**(2).
9. Bragg, J.G., *How Prochlorococcus bacteria use nitrogen sparingly in their proteins.* Molecular Ecology, 2011. **20**(1): p. 27-28.
10. Van Mooy, B.A.S., et al., *Sulfolipids dramatically decrease phosphorus demand by picocyanobacteria in oligotrophic marine environments.* Proceedings of the National Academy of Sciences, 2006. **103**(23): p. 8607-8612.
11. Kettler, G.C., et al., *Patterns and implications of gene gain and loss in the evolution of Prochlorococcus.* PLoS Genet, 2007. **3**(12): p. e231.
12. Raven, J.A., et al., *Interactions of photosynthesis with genome size and function.* Philosophical Transactions of the Royal Society B: Biological Sciences, 2013. **368**(1622): p. 20120264.
13. Coleman, M.L., et al., *Genomic Islands and the Ecology and Evolution of Prochlorococcus.* Science, 2006. **311**(5768): p. 1768-1770.
14. Waldbauer, J.R., et al., *Transcriptome and Proteome Dynamics of a Light-Dark Synchronized Bacterial Cell Cycle.* Plos One, 2012. **7**(8): p. e43432.
15. Zinser, E.R., et al., *Choreography of the Transcriptome, Photophysiology, and Cell Cycle of a Minimal Photoautotroph, Prochlorococcus.* Plos One, 2009. **4**(4).
16. Bruyant, F., et al., *Diel variations in the photosynthetic parameters of Prochlorococcus strain PCC 9511: Combined effects of light and cell cycle.* Limnology and Oceanography, 2005. **50**(3): p. 850-863.
17. Holtzendorff, J., et al., *Genome streamlining results in loss of robustness of the circadian clock in the marine cyanobacterium Prochlorococcus marinus PCC 9511.* J Biol Rhythms, 2008. **23**(3): p. 187-99.

18. Binder, B.J. and M.D. DuRand, *Diel cycles in surface waters of the equatorial Pacific.* Deep Sea Research Part II: Topical Studies in Oceanography, 2002. **49**(13–14): p. 2601-2617.
19. Claustre, H., et al., *Diel variations in Prochlorococcus optical properties.* Limnology and Oceanography, 2002. **47**(6): p. 1637-1647.
20. Stanier, R.Y. and G. Cohen-Bazire, *Phototrophic prokaryotes: the cyanobacteria.* Annu Rev Microbiol, 1977. **31**: p. 225-74.
21. Muro-Pastor, M.I., J.C. Reyes, and F.J. Florencio, *Ammonium assimilation in cyanobacteria.* Photosynth Res, 2005. **83**(2): p. 135-50.
22. Zhang, S.Y. and D.A. Bryant, *The Tricarboxylic Acid Cycle in Cyanobacteria.* Science, 2011. **334**(6062): p. 1551-1553.
23. Martiny, A.C., S. Kathuria, and P.M. Berube, *Widespread metabolic potential for nitrite and nitrate assimilation among Prochlorococcus ecotypes.* Proceedings of the National Academy of Sciences, 2009. **106**(26): p. 10787-10792.
24. Berube, P.M., et al., *Physiology and evolution of nitrate acquisition in Prochlorococcus.* Isme j, 2015. **9**(5): p. 1195-207.
25. Rangel, O.A., et al., *Physiological role and regulation of glutamate dehydrogenase in Prochlorococcus sp. strain MIT9313.* Environmental Microbiology Reports, 2009. **1**(1): p. 56-64.
26. Espinosa, J., et al., *PipX, the coactivator of NtcA, is a global regulator in cyanobacteria.* Proc Natl Acad Sci U S A, 2014. **111**(23): p. E2423-30.
27. Muro-Pastor, M.I., J.C. Reyes, and F.J. Florencio, *Cyanobacteria Perceive Nitrogen Status by Sensing Intracellular 2-Oxoglutarate Levels.* Journal of Biological Chemistry, 2001. **276**(41): p. 38320-38328.
28. Herrero, A. and F.G. Flores, *The Cyanobacteria: Molecular Biology, Genomics, and Evolution*. 2008: Caister Academic Press.
29. Forchhammer, K., *Global carbon/nitrogen control by PII signal transduction in cyanobacteria: from signals to targets.* FEMS Microbiol Rev, 2004. **28**(3): p. 319-33.
30. Zhang, Y. and J.D. Zhao, *PII, the key regulator of nitrogen metabolism in the cyanobacteria.* Science in China Series C-Life Sciences, 2008. **51**(12): p. 1056-1065.
31. Palinska, K.A., et al., *The signal transducer P-II and bicarbonate acquisition in Prochlorococcus marinus PCC 9511, a marine cyanobacterium naturally deficient in nitrate and nitrite assimilation.* Microbiology-Sgm, 2002. **148**: p. 2405-2412.
32. Lindell, D., et al., *Nitrogen stress response of Prochlorococcus strain PCC 9511 (Oxyphotobacteria) involves contrasting regulation of ntca and amt1*. Journal of Phycology, 2002. **38**(6): p. 1113-1124.
33. Tolonen, A.C., et al., *Global gene expression of Prochlorococcus ecotypes in response to changes in nitrogen availability.* Molecular Systems Biology, 2006. **2**(1): p. n/a-n/a.
34. El Alaoui, S., et al., *Glutamine synthetase from the marine cyanobacteria Prochlorococcus spp.: characterization, phylogeny and response to nutrient limitation.* Environmental Microbiology, 2003. **5**(5): p. 412-423.
35. Giovannoni, S.J., et al., *Genome Streamlining in a Cosmopolitan Oceanic Bacterium.* Science, 2005. **309**(5738): p. 1242-1245.

36. Axmann, I.M., et al., *Biochemical evidence for a timing mechanism in prochlorococcus.* J Bacteriol, 2009. **191**(17): p. 5342-7.
37. Mullineaux, C.W. and R. Stanewsky, *The Rolex and the Hourglass: a Simplified Circadian Clock in Prochlorococcus?* Journal of Bacteriology, 2009. **191**(17): p. 5333-5335.
38. Behrenfeld, M.J., K.H. Halsey, and A.J. Milligan, *Evolved physiological responses of phytoplankton to their integrated growth environment.* Philosophical Transactions of the Royal Society of London B: Biological Sciences, 2008. **363**(1504): p. 2687-2703.
39. Ankrah, N.Y.D., et al., *Phage infection of an environmentally relevant marine bacterium alters host metabolism and lysate composition.* ISME J, 2014. **8**(5): p. 1089-1100.
40. Dempo, Y., et al., *Molar-Based Targeted Metabolic Profiling of Cyanobacterial Strains with Potential for Biological Production.* Metabolites, 2014. **4**(2): p. 499.
41. Bennett, B.D., et al., *Absolute metabolite concentrations and implied enzyme active site occupancy in Escherichia coli.* Nature Chemical Biology, 2009. **5**(8): p. 593-599.
42. Buescher, J.M., et al., *A roadmap for interpreting 13C metabolite labeling patterns from cells.* Current Opinion in Biotechnology, 2015. **34**: p. 189-201.
43. Beck, C., et al., *The diversity of cyanobacterial metabolism: genome analysis of multiple phototrophic microorganisms.* BMC Genomics, 2012. **13**: p. 56.
44. Wyman, M. and C. Thom, *Temporal Orchestration of Glycogen Synthase (GlgA) Gene Expression and Glycogen Accumulation in the Oceanic Picoplanktonic Cyanobacterium Synechococcus sp. Strain WH8103.* Applied and Environmental Microbiology, 2012. **78**(13): p. 4744-4747.
45. Atkinson, D.E. and G.M. Walton, *Adenosine Triphosphate Conservation in Metabolic Regulation: RAT LIVER CITRATE CLEAVAGE ENZYME.* Journal of Biological Chemistry, 1967. **242**(13): p. 3239-3241.
46. Dai, R., et al., *Relationship of energy charge and toxin content of Microcystis aeruginosa in nitrogen-limited or phosphorous-limited cultures.* Toxicon, 2008. **51**(4): p. 649-58.
47. de Hoon, M.J.L., et al., *Open source clustering software.* Bioinformatics, 2004. **20**(9): p. 1453-1454.
48. Saldanha, A.J., *Java Treeview—extensible visualization of microarray data.* Bioinformatics, 2004. **20**(17): p. 3246-3248.
49. Karl, D.M. and O. Holm-Hansen, *Methodology and measurement of adenylate energy charge ratios in environmental samples.* Marine biology, 1978. **48**(2): p. 185-197.
50. Gerhardt, P., *Methods for general and molecular bacteriology*. 1994: American Society for Microbiology.
51. Van Mooy, B.A. and A.H. Devol, *Assessing nutrient limitation of Prochlorococcus in the North Pacific subtropical gyre by using an RNA capture method.* Limnology and Oceanography, 2008. **53**(1): p. 78.
52. Saito, M.A., et al., *Multiple nutrient stresses at intersecting Pacific Ocean biomes detected by protein biomarkers.* Science, 2014. **345**(6201): p. 1173-1177.
53. Fogg, G.E., C. Nalewajko, and W.D. Watt, *Extracellular Products of Phytoplankton Photosynthesis*. Vol. 162. 1965. 517-534.

54. Thornton, D.C.O., *Dissolved organic matter (DOM) release by phytoplankton in the contemporary and future ocean.* European Journal of Phycology, 2014. **49**(1): p. 20-46.
55. Bjørrisen, P.K., *Phytoplankton exudation of organic matter: Why do healthy cells do it?1.* Limnology and Oceanography, 1988. **33**(1): p. 151-154.
56. Wood, A.M., and L. M. Van Valen, *Paradox lost? On the release of energy-rich compounds by phytoplankton.* Marine Microbial Food Webs, 1990(4): p. 103-116.
57. Maheswaran, M., et al., *PII-regulated arginine synthesis controls accumulation of cyanophycin in Synechocystis sp. strain PCC 6803.* J Bacteriol, 2006. **188**(7): p. 2730-4.
58. Joseph, A., et al., *Rre37 stimulates accumulation of 2-oxoglutarate and glycogen under nitrogen starvation in Synechocystis sp. PCC 6803.* FEBS Letters, 2014. **588**(3): p. 466-471.
59. Hasunuma, T., et al., *Dynamic metabolic profiling of cyanobacterial glycogen biosynthesis under conditions of nitrate depletion.* Journal of Experimental Botany, 2013. **64**(10): p. 2943-2954.
60. Turpin, D.H., *EFFECTS OF INORGANIC N AVAILABILITY ON ALGAL PHOTOSYNTHESIS AND CARBON METABOLISM.* Journal of Phycology, 1991. **27**(1): p. 14-20.
61. Moore, L.R., et al., *Culturing the marine cyanobacterium Prochlorococcus.* Limnology and Oceanography: Methods, 2007. **5**(10): p. 353-362.
62. Lu, W., et al., *Metabolomic Analysis via Reversed-Phase Ion-Pairing Liquid Chromatography Coupled to a Stand Alone Orbitrap Mass Spectrometer.* Analytical Chemistry, 2010. **82**(8): p. 3212-3221.
63. Martens, L., et al., *mzML—a Community Standard for Mass Spectrometry Data.* Molecular & Cellular Proteomics, 2011. **10**(1).
64. Chambers, M.C., et al., *A cross-platform toolkit for mass spectrometry and proteomics.* Nat Biotech, 2012. **30**(10): p. 918-920.
65. Clasquin, M.F., E. Melamud, and J.D. Rabinowitz, *LC-MS Data Processing with MAVEN: A Metabolomic Analysis and Visualization Engine*, in *Current Protocols in Bioinformatics*. 2002, John Wiley & Sons, Inc.
66. Melamud, E., L. Vastag, and J.D. Rabinowitz, *Metabolomic Analysis and Visualization Engine for LC−MS Data.* Analytical Chemistry, 2010. **82**(23): p. 9818-9826.
67. McAndrew, P.M., et al., *Metabolic response of oligotrophic plankton communities to deep water nutrient enrichment.* Marine Ecology Progress Series, 2007. **332**: p. 63-75.
68. S, D., et al., *Microbial response to enhanced phosphorus cycling in the North Pacific Subtropical Gyre.* Marine Ecology Progress Series, 2014. **504**: p. 43-58.
69. Garcia-Fernandez, J.M., N.T. de Marsac, and J. Diez, *Streamlined Regulation and Gene Loss as Adaptive Mechanisms in Prochlorococcus for Optimized Nitrogen Utilization in Oligotrophic Environments.* Microbiology and Molecular Biology Reviews, 2004. **68**(4): p. 630-638.
70. Li, H., et al., *Pattern of cyanophycin accumulation in nitrogen-fixing and non-nitrogen-fixing cyanobacteria.* Archives of Microbiology, 2001. **176**(1-2): p. 9-18.

71. Merritt, M.V., et al., *Variations in the amino acid composition of cyanophycin in the cyanobacterium Synechocystis sp. PCC 6308 as a function of growth conditions.* Arch Microbiol, 1994. **162**(3): p. 158-66.
72. Richaud, C., et al., *Nitrogen or Sulfur Starvation Differentially Affects Phycobilisome Degradation and Expression of the nblA Gene in Synechocystis Strain PCC 6803.* Journal of Bacteriology, 2001. **183**(10): p. 2989-2994.
73. Wiethaus, J., et al., *Phycobiliproteins in Prochlorococcus marinus: Biosynthesis of pigments and their assembly into proteins.* European Journal of Cell Biology, 2010. **89**(12): p. 1005-1010.
74. Wiethaus, J., et al., *Phycobiliproteins in Prochlorococcus marinus: biosynthesis of pigments and their assembly into proteins.* Eur J Cell Biol, 2010. **89**(12): p. 1005-10.
75. Hess, W., et al., *Phycoerythrins of the oxyphotobacterium Prochlorococcus marinus are associated to the thylakoid membrane and are encoded by a single large gene cluster.* Plant Molecular Biology, 1999. **40**(3): p. 507-521.
76. Krumhardt, K.M., et al., *Effects of phosphorus starvation versus limitation on the marine cyanobacterium Prochlorococcus MED4 I: uptake physiology.* Environ Microbiol, 2013. **15**(7): p. 2114-28.
77. Suttle, C.A., *Viruses in the sea.* Nature, 2005. **437**(7057): p. 356-361.

APPENDIX

Table S4. Diel glutamate isotopologue ion counts

Raw isotopologue abundance (integrated ion counts) for ^{13}C labeled glutamate during diel time points. Isotopologue are described as observed by the first and third quadrupole of the LC-MS/MS. The first number describes the number of heavy isotopes observed in the parent m/*z* and the second is the number of heavy isotopes observed in the product m/*z*. See Table 1 for descriptions.

Glutamate ion counts											
Experiment Time	Labeling Time (mins)	Isotopologue									
		Unlabeled	1-0	1-1	2-1	2-2	3-2	3-3	4-3	4-4	5-4
1200 (noon)	0	240505	349	7715	0	42	0	0	0	0	0
	30	312764	1998	15794	0	3031	20	105	329	0	19
	60	372028	985	18576	128	6552	230	320	930	0	338
	90	363992	3006	22456	149	7745	1543	54	1308	251	853
1700 (afternoon)	0	511478	3775	21310	0	0	0	0	0	0	0
	30	601377	6528	31493	0	3121	179	0	23	0	160
	60	568223	4470	31816	705	6133	883	45	792	23	107
	90	538483	5634	29452	2299	5946	1667	125	783	568	106
1900 (dusk/evening)	0	494609	1971	23175	0	170	0	0	0	0	0
	30	387783	2962	14281	20	82	0	0	0	0	0
	60	266081	3200	12240	62	181	18	0	0	0	0
	90	337256	8256	11977	43	59	12	0	0	0	0
2400 (midnight)	0	444767	2934	19213	0	129	0	0	0	0	0
	30	567654	9698	22588	35	227	0	0	0	0	0
	60	589907	17722	25424	218	525	0	0	0	0	0
	90	538617	20670	25363	775	462	0	0	0	0	0

Table S4. Continued

Experiment Time	Labeling Time (mins)	Unlabeled	1-0	1-1	2-1	2-2	3-2	3-3	4-3	4-4	5-4
3100 (morning)	0	227989	358	7216	0	34	9	0	0	0	0
	30	229257	861	10787	59	1034	478	0	0	49	0
	60	214750	903	11531	731	2247	535	256	1027	66	399
	90	178261	1332	6695	317	2603	1473	475	1514	98	501
3600 (noon)	0	504048	4129	18563	25	133	0	0	0	0	0
	30	451398	3967	24433	288	4379	260	27	369	0	63
	60	368516	1755	19244	172	6484	252	29	553	0	429
	90	364355	1719	20534	225	9361	1048	552	1593	0	1035

Table S5. Nitrogen Limited and Nitrogen Replete metabolite pool data

Metabolite abundance measured as the ion counts normalized to cell*ml^{-1} for both nitrogen (N) limited and replete cultures. The ratio of metabolites under experimental variables were compared within time points and log transformed for data mapping (Fig. 9A). Normalized metabolite ion counts scaled to range ($\tilde{x}_{ik} = \frac{x_{ik} - \bar{x}_k}{x_{k,max} - x_{k,min}}$), across treatment and time points allows for comparisons of pool sizes for each metabolite (Fig 9B).

	Ion Count (IC) per cell				Ratio Nlim:Nrep		Normalized IC Scaled to Range			
	N limited		N replete		Log_{10}(N limited/ N replete)		N limited		N replete	
Observed Metabolite	1200	1600	1200	1600	12:00	16:00	1200	1600	1200	1600
2-keto-isovalerate	1.1632	0.9729	1.6681	1.0304	-0.157	-0.025	-0.07	-0.34	0.66	-0.26
4-aminobutyrate	0.0289	0.0237	0.0212	0.0139	0.135	0.232	0.47	0.12	-0.05	-0.53
6-phospho-D-gluconate	0.0563	0.0547	0.0758	0.0584	-0.129	-0.028	-0.24	-0.31	0.69	-0.14
a-ketoglutarate	0.2941	0.1915	0.0143	0.0101	1.313	1.277	0.59	0.23	-0.40	-0.41
AMP	0.0464	0.0377	0.0276	0.0221	0.227	0.232	0.53	0.18	-0.24	-0.47
aspartate	0.0559	0.0557	0.1782	0.1595	-0.503	-0.457	-0.46	-0.46	0.54	0.39
Citraconic acid	0.7729	0.6106	0.9368	0.7356	-0.084	-0.081	0.03	-0.47	0.53	-0.09
citrate/isocitrate	0.1721	0.1762	0.1562	0.2040	0.042	-0.064	-0.10	-0.02	-0.44	0.56
CMP	0.0617	0.0612	0.0211	0.0135	0.466	0.657	0.46	0.45	-0.38	-0.54
dAMP	0.0030	0.0027	0.0035	0.0021	-0.073	0.127	0.10	-0.05	0.47	-0.53
deoxyinosine	0.0002	0.0008	0.0052	0.0009	-1.377	-0.041	-0.31	-0.19	0.69	-0.18
deoxyribose-phosphate	0.0553	0.0534	0.0034	0.0023	1.211	1.365	0.50	0.47	-0.48	-0.50
erythrose-4-phosphate	0.0013	0.0007	0.0013	0.0010	0.032	-0.143	0.42	-0.58	0.27	-0.11
fumarate	0.0058	0.0047	0.0073	0.0058	-0.097	-0.090	-0.03	-0.46	0.54	-0.04
gluconate	0.0130	0.0137	0.0091	0.0054	0.153	0.407	0.32	0.41	-0.14	-0.59
glucose-1-phosphate	0.3579	0.3026	0.1001	0.0913	0.553	0.520	0.54	0.34	-0.42	-0.46

Table S5. Continued

	Ion Count (IC) per cell				Ratio Nlim:Nrep		Normalized IC Scaled to Range			
	N limited		N replete		Log_{10}(N limited/ N replete)		N limited		N replete	
Observed Metabolite	1200	1600	1200	1600	12:00	16:00	1200	1600	1200	1600
glutamate	15.8031	12.9118	6.3871	5.1174	0.393	0.402	0.54	0.27	-0.34	-0.46
glutamine	0.0033	0.0057	0.0023	0.0020	0.167	0.448	0.00	0.65	-0.29	-0.35
glutathione	0.1675	0.2056	0.0963	0.0699	0.241	0.469	0.24	0.52	-0.28	-0.48
glutathione disulfide	0.1891	0.1420	0.0735	0.0584	0.410	0.386	0.56	0.20	-0.32	-0.44
glyceraldehdye-3-phosphate	0.0464	0.0437	0.0005	0.0003	1.986	2.158	0.51	0.46	-0.48	-0.49
Hydroxyisocaproic acid	0.1970	0.1751	0.2923	0.1781	-0.171	-0.008	-0.12	-0.30	0.70	-0.28
Hydroxyphenylacetic acid	0.0148	0.0124	0.0254	0.0146	-0.236	-0.070	-0.15	-0.34	0.66	-0.17
hydroxyphenylpyruvate	0.0335	0.0948	0.1122	0.0623	-0.525	0.182	-0.54	0.24	0.46	-0.17
inosine	3.0475	2.5960	1.8181	1.6180	0.224	0.205	0.54	0.23	-0.32	-0.46
leucine/isoleucine	0.0021	0.0020	0.0012	0.0005	0.239	0.575	0.41	0.35	-0.16	-0.59
malate	0.0121	0.0116	0.0157	0.0109	-0.113	0.028	-0.10	-0.20	0.65	-0.35
Methylmalonic acid	0.4201	0.3384	0.5253	0.3603	-0.097	-0.027	0.05	-0.39	0.61	-0.27
N-acetyl-glutamate	0.0348	0.0241	0.0144	0.0150	0.384	0.205	0.62	0.10	-0.38	-0.35
N-Acetyltaurine	0.0004	0.0018	0.0007	0.0003	-0.222	0.831	-0.25	0.67	-0.09	-0.33
NAD+	0.0012	0.0011	0.0005	0.0002	0.414	0.642	0.47	0.35	-0.30	-0.53
oxaloacetate	0.0029	0.0020	0.0039	0.0044	-0.139	-0.341	-0.18	-0.54	0.27	0.46
phenylalanine	0.0039	0.0034	0.0069	0.0026	-0.245	0.119	-0.06	-0.19	0.63	-0.37
p-hydroxybenzoate	0.0212	0.0167	0.0299	0.0181	-0.150	-0.034	-0.02	-0.36	0.64	-0.26
proline	0.0013	0.0017	0.0027	0.0017	-0.301	0.006	-0.38	-0.11	0.62	-0.13
Pyroglutamic acid	0.0313	0.0219	0.0772	0.0212	-0.392	0.014	-0.12	-0.29	0.70	-0.30

Table S5. Continued

	Ion Count (IC) per cell				Ratio Nlim:Nrep		Normalized IC Scaled to Range			
	N limited		N replete		Log_{10}(N limited/ N replete)		N limited		N replete	
Observed Metabolite	1200	1600	1200	1600	12:00	16:00	1200	1600	1200	1600
ribose-phosphate	0.0478	0.0442	0.0085	0.0053	0.748	0.919	0.50	0.42	-0.42	-0.50
sedoheptulose-1/7-phosphate	0.0920	0.0694	0.0387	0.0289	0.376	0.381	0.55	0.19	-0.29	-0.45
serine	0.0027	0.0033	0.0021	0.0009	0.120	0.571	0.20	0.44	-0.08	-0.56
sn-glycerol-3-phosphate	0.1742	0.1539	0.0163	0.0148	1.029	1.018	0.53	0.40	-0.46	-0.47
Sulfolactate	0.0264	0.0232	0.0312	0.0262	-0.072	-0.051	-0.04	-0.44	0.56	-0.08
threonine	0.0023	0.0026	0.0018	0.0007	0.107	0.590	0.26	0.38	-0.01	-0.62
trehalose/sucrose	0.0055	0.0124	0.0086	0.0070	-0.199	0.248	-0.42	0.58	0.04	-0.20
tryptophan	0.0013	0.0008	0.0014	0.0002	-0.030	0.547	0.31	-0.10	0.39	-0.61
tyrosine	0.1003	0.1231	0.0095	0.0051	1.022	1.382	0.35	0.54	-0.42	-0.46
UDP-D-glucose	0.1931	0.1884	0.1363	0.0809	0.151	0.367	0.39	0.34	-0.12	-0.61
UDP-N-acetyl-glucosamine	0.0689	0.0690	0.0719	0.0438	-0.019	0.197	0.19	0.20	0.30	-0.70
UMP	0.0124	0.0190	0.0142	0.0038	-0.059	0.697	0.00	0.44	0.12	-0.56
Unknown_C5H4N4O2	0.0544	0.0387	0.0689	0.0543	-0.102	-0.147	0.01	-0.51	0.49	0.01
Uric acid	0.0012	0.0039	0.0130	0.0014	-1.038	0.430	-0.31	-0.09	0.69	-0.29
uridine	0.0013	0.0018	0.0032	0.0019	-0.386	-0.036	-0.38	-0.16	0.62	-0.08
valine	0.0038	0.0038	0.0008	0.0004	0.661	0.959	0.47	0.46	-0.40	-0.53
xanthine	0.0000	0.0006	0.0004	0.0000	-1.019	1.400	-0.41	0.56	0.29	-0.44

Table S6. Nitrogen Limited and Nitrogen Replete metabolite ^{13}C labeling

Raw isotopologue abundance (integrated ion counts) for ^{13}C labeled metabolites in nitrogen limited and replete cultures at both noon (1200) and afternoon (1600) time points. Isotopologue are described in their unlabeled and labeled forms where 'metabolite + *n*' is the number of isotopic carbons in that isotopologue. Abbreviations: glutamate (Glu), hexose phosphate (HexP), aspartate (Asp), sedoheptulose 1/7 phosphate (S7P), UDP-glucose (UDP-Glc), UDP-n-acetyl-glucosamine (UDP-GlcN)

	Nitrogen Limited															
metabolite isotopologue	1200								1600							
	0		30		60		90		0		30		60		90	
Glu	5.5E+8	9.1E+8	5.6E+8	6.0E+8	7.6E+8	6.8E+8	7.7E+8	9.3E+8	7.6E+8	5.0E+8	3.9E+8	4.1E+8	6.3E+8	5.4E+8	4.3E+8	4.0E+8
Glu +1	2.3E+7	4.4E+7	2.4E+7	3.0E+7	3.8E+7	3.8E+7	4.1E+7	5.3E+7	3.8E+7	2.4E+7	1.9E+7	2.0E+7	3.3E+7	2.9E+7	1.9E+7	2.1E+7
Glu +2	1.9E+6	3.6E+6	1.7E+6	2.0E+6	2.6E+6	2.2E+6	2.6E+6	3.2E+6	3.0E+6	1.8E+6	1.2E+6	1.4E+6	2.1E+6	1.9E+6	1.4E+6	1.3E+6
Glu +3	1.9E+4	7.9E+4	5.3E+4	1.5E+5	2.1E+5	3.4E+5	2.9E+5	5.7E+5	9.2E+4	1.8E+4	1.1E+5	6.6E+4	3.2E+5	2.6E+5	2.5E+5	2.4E+5
Glu +4	1.0E+3	3.1E+4	6.5E+3	2.4E+4	3.7E+4	4.6E+4	3.6E+4	8.8E+4	2.0E+4	1.9E+3	1.3E+4	5.1E+3	3.4E+4	2.2E+4	2.9E+4	4.0E+4
HexP	1.4E+7	1.9E+7	8.4E+6	8.2E+6	9.5E+6	9.7E+6	7.1E+6	9.3E+6	1.9E+7	1.1E+7	8.2E+6	6.2E+6	5.4E+6	6.0E+6	5.7E+6	4.1E+6
HexP+1	5.9E+5	8.8E+5	1.7E+6	1.6E+6	2.4E+6	2.4E+6	2.1E+6	2.4E+6	8.9E+5	4.4E+5	1.8E+6	1.3E+6	1.4E+6	1.5E+6	1.6E+6	1.0E+6
HexP+2	1.1E+3	1.1E+4	1.8E+5	1.1E+5	4.5E+5	3.3E+5	5.6E+5	4.6E+5	6.3E+3	3.0E+3	1.2E+5	7.2E+4	1.5E+5	1.8E+5	1.5E+5	1.2E+5
HexP+3	3.8E+3	1.6E+3	2.1E+4	6.6E+3	1.0E+5	4.0E+4	1.4E+5	1.0E+5	1.7E+3	0.0E+0	5.4E+3	6.2E+3	1.5E+4	1.3E+4	2.0E+4	1.4E+4
HexP+4	1.1E+3	0.0E+0	2.3E+3	0.0E+0	7.6E+3	4.1E+3	9.3E+3	5.2E+3	5.1E+2	0.0E+0	0.0E+0	4.7E+2	7.2E+2	1.4E+3	8.9E+2	0.0E+0
Asp	1.6E+6	3.6E+6	9.6E+5	1.3E+6	1.2E+6	1.1E+6	1.1E+6	2.0E+6	3.6E+6	1.9E+6	8.1E+5	1.1E+6	1.3E+6	1.1E+6	4.4E+5	6.8E+5
Asp+1	2.4E+4	6.3E+4	2.1E+5	4.5E+5	3.3E+5	4.6E+5	3.2E+5	5.3E+5	8.9E+4	3.2E+4	3.4E+5	3.3E+5	4.4E+5	4.0E+5	1.8E+5	2.3E+5
Asp+2	1.6E+3	3.9E+3	8.8E+4	2.0E+5	1.9E+5	2.5E+5	2.1E+5	2.8E+5	1.3E+3	6.4E+2	1.4E+5	1.6E+5	2.2E+5	2.1E+5	7.5E+4	1.1E+5
Asp+3	3.7E+3	4.1E+3	2.6E+4	6.0E+4	7.1E+4	7.7E+4	7.8E+4	6.5E+4	1.7E+4	3.6E+3	1.6E+4	3.2E+4	4.9E+4	5.4E+4	6.1E+3	2.7E+4
Asp+4	1.1E+3	7.3E+2	1.8E+3	4.7E+3	5.4E+3	4.2E+3	4.9E+3	4.0E+3	5.2E+2	4.1E+2	2.3E+3	1.4E+3	3.0E+3	4.1E+3	0.0E+0	2.4E+3

Table S6 Continued

metabolite isotopologue	Nitrogen Limited															
	1200								1600							
	0		30		60		90		0		30		60		90	
S7P	3.7E+6	4.7E+6	1.8E+6	1.6E+6	2.1E+6	2.1E+6	1.4E+6	2.3E+6	4.3E+6	2.5E+6	1.7E+6	1.3E+6	1.2E+6	1.3E+6	1.1E+6	9.3E+5
S7P+1	1.2E+5	1.9E+5	7.2E+5	5.6E+5	1.0E+6	9.8E+5	7.6E+5	9.4E+5	2.1E+5	9.0E+4	6.1E+5	4.2E+5	5.3E+5	5.5E+5	5.4E+5	3.3E+5
S7P+2	4.4E+3	2.3E+4	3.0E+5	1.8E+5	5.3E+5	3.8E+5	4.6E+5	4.6E+5	2.0E+4	7.9E+3	1.8E+5	1.1E+5	2.0E+5	1.8E+5	1.8E+5	1.4E+5
S7P+3	0.0E+0	3.8E+3	6.9E+4	2.4E+4	2.0E+5	1.2E+5	2.2E+5	1.9E+5	0.0E+0	6.1E+2	3.5E+4	2.4E+4	4.4E+4	4.4E+4	3.0E+4	3.2E+4
S7P+4	0.0E+0	0.0E+0	5.1E+3	5.7E+3	4.3E+4	1.1E+4	5.0E+4	4.5E+4	0.0E+0	0.0E+0	3.3E+3	1.7E+3	3.4E+3	5.2E+3	8.9E+2	1.8E+3
S7P+5	0.0E+0	0.0E+0	1.6E+3	0.0E+0	7.0E+3	0.0E+0	7.1E+3	2.8E+3	0.0E+0	0.0E+0	0.0E+0	0.0E+0	0.0E+0	0.0E+0	1.1E+3	0.0E+0
UDP-Glc	7.0E+6	1.1E+7	4.3E+6	5.9E+6	4.5E+6	4.9E+6	4.0E+6	4.8E+6	9.9E+6	8.4E+6	4.6E+6	5.3E+6	3.7E+6	4.7E+6	2.0E+6	6.7E+6
UDP-Glc+1	9.7E+5	1.6E+6	1.3E+6	1.9E+6	1.7E+6	2.0E+6	1.9E+6	2.3E+6	1.5E+6	1.3E+6	1.4E+6	1.6E+6	1.4E+6	1.9E+6	8.1E+5	2.1E+6
UDP-Glc+2	9.6E+4	2.3E+5	7.8E+5	1.1E+6	1.4E+6	1.4E+6	1.7E+6	1.9E+6	2.1E+5	2.0E+5	7.2E+5	8.0E+5	9.8E+5	1.3E+6	6.0E+5	1.2E+6
UDP-Glc+3	3.2E+3	0.0E+0	5.2E+5	6.1E+5	9.9E+5	9.4E+5	1.3E+6	1.3E+6	1.7E+3	0.0E+0	3.9E+5	3.9E+5	5.8E+5	7.8E+5	3.3E+5	7.2E+5
UDP-Glc+4	0.0E+0	1.5E+3	2.8E+5	2.1E+5	5.6E+5	4.0E+5	7.9E+5	6.9E+5	0.0E+0	1.8E+3	1.4E+5	1.5E+5	2.5E+5	3.3E+5	1.6E+5	3.5E+5
UDP-Glc+5	0.0E+0	5.2E+3	5.5E+4	5.0E+4	1.5E+5	9.6E+4	2.6E+5	2.5E+5	0.0E+0	0.0E+0	2.4E+4	2.3E+4	7.4E+4	9.3E+4	1.9E+4	6.1E+4
UDP-Glc+6	0.0E+0	1.9E+3	8.2E+3	1.9E+3	9.2E+3	4.9E+3	3.4E+4	3.4E+4	1.2E+3	0.0E+0	5.5E+3	0.0E+0	8.3E+3	1.3E+4	2.0E+3	8.0E+3
UDP-Glc+7	0.0E+0	0.0E+0	1.4E+3	1.7E+3	0.0E+0	5.8E+3	7.7E+3	5.4E+3	0.0E+0	0.0E+0	0.0E+0	0.0E+0	0.0E+0	1.2E+3	8.8E+3	0.0E+0
Inosine	9.4E+7	1.9E+8	9.2E+7	9.6E+7	1.1E+8	1.1E+8	1.2E+8	1.4E+8	1.5E+8	1.1E+8	6.5E+7	6.8E+7	8.1E+7	7.5E+7	6.4E+7	5.5E+7
Inosine+1	8.5E+6	1.7E+7	9.5E+6	9.9E+6	1.2E+7	1.2E+7	1.4E+7	1.6E+7	1.3E+7	9.8E+6	6.7E+6	7.0E+6	9.1E+6	8.6E+6	8.0E+6	6.7E+6
Inosine+2	1.2E+6	2.4E+6	9.6E+5	1.0E+6	1.5E+6	1.4E+6	2.4E+6	2.6E+6	2.0E+6	1.4E+6	6.5E+5	7.0E+5	1.2E+6	1.2E+6	1.5E+6	1.3E+6
Inosine+3	5.6E+4	1.6E+5	5.4E+5	4.1E+5	1.3E+6	1.1E+6	2.3E+6	2.3E+6	1.1E+5	9.3E+4	2.9E+5	2.9E+5	9.6E+5	9.4E+5	1.2E+6	1.0E+6
Inosine+4	0.0E+0	4.3E+3	4.0E+5	2.5E+5	1.1E+6	7.9E+5	1.9E+6	1.8E+6	2.0E+3	0.0E+0	1.9E+5	1.9E+5	6.7E+5	6.5E+5	8.7E+5	6.9E+5
Inosine+5	0.0E+0	0.0E+0	2.3E+5	1.2E+5	6.6E+5	4.4E+5	1.2E+6	9.9E+5	1.5E+3	0.0E+0	6.5E+4	7.6E+4	3.6E+5	3.5E+5	4.8E+5	3.6E+5
Inosine+6	2.3E+3	2.7E+3	9.4E+4	2.9E+4	3.2E+5	1.4E+5	5.2E+5	3.8E+5	3.0E+3	4.5E+3	1.8E+4	1.8E+4	1.2E+5	1.2E+5	1.6E+5	1.3E+5
Inosine+7	0.0E+0	0.0E+0	3.5E+3	8.8E+3	7.3E+4	2.1E+4	1.4E+5	9.2E+4	1.8E+3	0.0E+0	2.4E+3	1.1E+3	1.4E+4	2.3E+4	2.6E+4	1.9E+4

Table S6 Continued

metabolite isotopologue	Nitrogen Limited															
	1200								1600							
	0		30		60		90		0		30		60		90	
UDP-GlcN	2.2E+6	4.1E+6	1.0E+6	2.4E+6	1.3E+6	1.5E+6	1.2E+6	1.0E+6	4.0E+6	2.7E+6	1.4E+6	1.5E+6	1.1E+6	1.4E+6	1.4E+5	1.2E+7
UDP-GlcN+1	2.6E+5	6.4E+5	2.2E+5	5.9E+5	2.6E+5	3.4E+5	2.3E+5	2.7E+5	6.1E+5	4.1E+5	3.6E+5	3.6E+5	2.3E+5	4.4E+5	4.5E+3	2.3E+6
UDP-GlcN+2	1.5E+4	3.9E+4	6.0E+4	1.7E+5	1.1E+5	1.1E+5	1.1E+5	2.1E+5	5.8E+4	2.7E+4	1.3E+5	1.2E+5	1.1E+5	1.7E+5	0.0E+0	6.1E+5
UDP-GlcN+3	1.5E+4	3.9E+4	6.0E+4	1.8E+5	1.1E+5	1.1E+5	1.1E+5	2.1E+5	6.0E+4	2.7E+4	1.3E+5	1.2E+5	1.1E+5	1.7E+5	0.0E+0	6.1E+5
UDP-GlcN+4	0.0E+0	0.0E+0	3.1E+4	5.3E+4	6.4E+4	6.1E+4	1.1E+5	1.1E+5	0.0E+0	0.0E+0	3.7E+4	4.6E+4	4.3E+4	7.0E+4	9.5E+3	1.3E+5
UDP-GlcN+5	0.0E+0	3.9E+3	6.4E+3	2.3E+4	3.6E+4	3.4E+4	6.4E+4	5.6E+4	0.0E+0	0.0E+0	1.1E+4	1.4E+4	2.6E+4	4.9E+4	0.0E+0	4.6E+4
UDP-GlcN+6	8.5E+3	1.6E+3	6.6E+3	0.0E+0	1.1E+4	6.0E+3	2.0E+4	2.1E+4	0.0E+0	0.0E+0	3.3E+3	0.0E+0	8.5E+3	1.3E+4	0.0E+0	1.7E+4
UDP-GlcN+7	0.0E+0	0.0E+0	1.4E+3	2.2E+3	3.6E+3	0.0E+0	1.6E+3	0.0E+0	0.0E+0	0.0E+0	0.0E+0	4.9E+3	0.0E+0	1.1E+3	0.0E+0	1.6E+3
UDP-GlcN+8	0.0E+0	0.0E+0	0.0E+0	6.7E+3	2.1E+3	0.0E+0	1.5E+3	0.0E+0	0.0E+0	1.4E+3	0.0E+0	1.6E+3	0.0E+0	0.0E+0	0.0E+0	0.0E+0

metabolite isotopologue	Nitrogen Replete															
	1200								1600							
	0		30		60		90		0		30		60		90	
Glu	2.2E+8	2.3E+8	1.9E+8	2.2E+8	1.9E+8	1.9E+8	2.1E+8	2.5E+8	2.8E+8	1.8E+8	2.2E+8	2.1E+8	2.3E+8	2.0E+8	2.4E+8	2.5E+8
Glu +1	8.6E+6	8.7E+6	8.2E+6	1.1E+7	1.1E+7	1.0E+7	1.4E+7	1.6E+7	1.1E+7	6.7E+6	9.3E+6	1.1E+7	1.4E+7	1.2E+7	1.5E+7	1.8E+7
Glu +2	5.6E+5	6.1E+5	7.0E+5	7.8E+5	1.5E+6	1.6E+6	3.2E+6	3.7E+6	7.3E+5	5.9E+5	7.4E+5	7.6E+5	1.6E+6	1.7E+6	2.8E+6	4.2E+6
Glu +3	1.5E+4	2.9E+4	2.6E+5	2.9E+5	6.3E+5	6.8E+5	1.5E+6	1.7E+6	3.1E+4	8.8E+3	2.4E+5	3.1E+5	7.2E+5	7.1E+5	1.2E+6	1.8E+6
Glu +4	3.9E+4	3.6E+4	7.3E+4	1.1E+5	2.5E+5	2.4E+5	5.3E+5	6.0E+5	3.1E+4	1.1E+3	6.6E+4	1.0E+5	2.5E+5	2.2E+5	3.6E+5	5.5E+5
HexP	3.3E+6	3.6E+6	6.9E+5	7.0E+5	5.0E+5	5.5E+5	4.2E+5	5.6E+5	4.3E+6	3.8E+6	1.2E+6	1.2E+6	1.0E+6	9.2E+5	1.1E+6	1.3E+6
HexP+1	1.1E+5	8.8E+4	3.7E+5	4.0E+5	3.6E+5	3.5E+5	4.0E+5	4.0E+5	1.2E+5	1.3E+5	6.4E+5	7.3E+5	6.4E+5	6.3E+5	6.9E+5	8.4E+5
HexP+2	4.3E+3	1.9E+4	5.3E+5	5.8E+5	5.7E+5	6.3E+5	6.7E+5	8.5E+5	1.2E+4	1.7E+3	5.5E+5	6.5E+5	5.8E+5	5.6E+5	5.2E+5	6.7E+5
HexP+3	0.0E+0	1.2E+3	2.3E+5	2.8E+5	2.7E+5	2.3E+5	3.7E+5	3.9E+5	1.7E+3	4.6E+2	2.1E+5	2.7E+5	2.2E+5	2.2E+5	1.9E+5	2.5E+5
HexP+4	1.5E+3	0.0E+0	3.5E+4	3.9E+4	3.3E+4	3.6E+4	8.3E+4	6.4E+4	0.0E+0	0.0E+0	2.4E+4	4.2E+4	3.0E+4	2.6E+4	1.7E+4	3.1E+4

Table S6 Continued

metabolite isotopologue	Nitrogen Replete															
	1200								1600							
	0		30		60		90		0		30		60		90	
Asp	5.8E+6	6.6E+6	3.2E+6	4.3E+6	2.5E+6	3.0E+6	2.8E+6	3.1E+6	8.4E+6	5.8E+6	4.8E+6	5.8E+6	4.6E+6	4.3E+6	3.9E+6	5.6E+6
Asp+1	1.1E+5	1.3E+5	2.6E+5	2.9E+5	3.3E+5	3.7E+5	5.2E+5	6.1E+5	1.5E+5	1.0E+5	3.1E+5	3.6E+5	4.8E+5	4.4E+5	6.3E+5	8.3E+5
Asp+2	7.1E+2	1.6E+3	1.7E+5	2.1E+5	3.3E+5	3.9E+5	6.3E+5	7.0E+5	5.2E+3	3.6E+3	2.0E+5	2.6E+5	4.3E+5	4.4E+5	6.1E+5	8.5E+5
Asp+3	3.3E+3	1.3E+4	9.4E+4	1.2E+5	2.2E+5	2.1E+5	3.9E+5	3.9E+5	1.1E+4	2.3E+3	8.6E+4	1.1E+5	2.0E+5	2.1E+5	3.3E+5	4.3E+5
Asp+4	5.2E+2	6.0E+2	4.1E+3	1.2E+4	1.4E+4	2.6E+4	6.5E+4	6.9E+4	7.1E+2	0.0E+0	9.6E+3	7.3E+3	2.6E+4	2.8E+4	3.8E+4	6.6E+4
S7P	1.1E+6	1.5E+6	1.2E+5	1.0E+5	4.3E+4	7.3E+4	8.3E+4	7.9E+4	1.3E+6	1.2E+6	2.3E+5	2.1E+5	1.8E+5	1.1E+5	2.4E+5	2.1E+5
S7P+1	3.1E+4	2.6E+4	9.5E+4	9.7E+4	3.3E+4	4.0E+4	5.0E+4	5.4E+4	2.3E+4	2.1E+4	1.7E+5	1.7E+5	1.3E+5	1.1E+5	1.7E+5	1.5E+5
S7P+2	3.8E+3	8.9E+3	1.8E+5	1.8E+5	9.1E+4	1.0E+5	1.3E+5	1.5E+5	4.1E+3	0.0E+0	1.9E+5	2.1E+5	1.6E+5	1.5E+5	1.6E+5	2.3E+5
S7P+3	2.1E+3	0.0E+0	1.9E+5	1.9E+5	1.2E+5	1.2E+5	1.4E+5	2.1E+5	0.0E+0	0.0E+0	1.5E+5	1.8E+5	1.7E+5	1.2E+5	1.1E+5	1.6E+5
S7P+4	0.0E+0	0.0E+0	1.3E+5	1.1E+5	7.7E+4	8.1E+4	1.1E+5	1.4E+5	0.0E+0	5.5E+2	7.9E+4	1.0E+5	5.8E+4	5.1E+4	3.4E+4	5.8E+4
S7P+5	0.0E+0	0.0E+0	3.4E+4	3.6E+4	9.2E+3	7.0E+3	3.7E+4	3.1E+4	0.0E+0	0.0E+0	1.2E+4	2.5E+4	1.7E+4	7.2E+3	5.2E+3	1.2E+4
UDP-Glc	3.7E+6	5.8E+6	5.0E+5	5.0E+5	1.4E+5	1.8E+5	1.3E+5	3.3E+5	3.7E+6	3.5E+6	6.5E+5	5.9E+5	3.0E+5	2.8E+5	1.7E+5	4.7E+5
UDP-Glc+1	5.1E+5	7.8E+5	4.1E+5	4.2E+5	2.3E+5	2.8E+5	2.8E+5	2.8E+5	5.3E+5	4.2E+5	5.0E+5	4.5E+5	3.8E+5	2.9E+5	2.2E+5	4.0E+5
UDP-Glc+2	4.1E+4	4.8E+4	7.9E+5	8.2E+5	6.9E+5	6.5E+5	6.6E+5	7.2E+5	4.9E+4	3.7E+4	7.0E+5	6.7E+5	6.3E+5	7.1E+5	5.2E+5	7.0E+5
UDP-Glc+3	1.5E+3	0.0E+0	8.9E+5	9.5E+5	8.9E+5	7.7E+5	8.0E+5	8.7E+5	2.3E+3	1.8E+3	7.3E+5	6.9E+5	7.4E+5	7.7E+5	5.5E+5	8.1E+5
UDP-Glc+4	0.0E+0	0.0E+0	5.5E+5	6.2E+5	5.6E+5	5.5E+5	6.2E+5	7.3E+5	0.0E+0	0.0E+0	5.0E+5	4.6E+5	5.2E+5	6.0E+5	3.8E+5	5.5E+5
UDP-Glc+5	0.0E+0	0.0E+0	2.6E+5	2.2E+5	1.5E+5	2.7E+5	3.1E+5	3.2E+5	0.0E+0	0.0E+0	2.2E+5	1.9E+5	2.4E+5	2.9E+5	2.2E+5	3.1E+5
UDP-Glc+6	1.2E+3	0.0E+0	3.1E+4	3.6E+4	4.3E+4	1.0E+5	1.4E+5	1.9E+5	2.4E+3	0.0E+0	5.5E+4	5.3E+4	9.5E+4	1.1E+5	1.2E+5	1.9E+5
UDP-Glc+7	0.0E+0	0.0E+0	6.8E+3	4.6E+3	1.9E+4	3.0E+4	8.1E+4	6.7E+4	0.0E+0	0.0E+0	1.2E+4	1.3E+4	4.2E+4	5.8E+4	6.3E+4	8.7E+4

Table S6 Continued

metabolite isotopologue	1200								1600							
	0		30		60		90		0		30		60		90	
Inosine	6.7E+7	5.9E+7	5.3E+7	6.1E+7	4.6E+7	4.8E+7	6.0E+7	6.2E+7	8.8E+7	5.7E+7	7.1E+7	7.6E+7	6.7E+7	7.3E+7	7.0E+7	9.2E+7
Inosine+1	5.8E+6	5.1E+6	4.9E+6	5.5E+6	4.1E+6	4.4E+6	5.6E+6	5.7E+6	7.7E+6	5.2E+6	6.4E+6	7.0E+6	6.2E+6	6.6E+6	6.5E+6	8.8E+6
Inosine+2	8.3E+5	6.9E+5	5.4E+5	5.9E+5	4.3E+5	4.6E+5	6.4E+5	6.7E+5	1.1E+6	7.1E+5	7.4E+5	7.7E+5	6.4E+5	7.3E+5	7.9E+5	1.1E+6
Inosine+3	3.9E+4	2.8E+4	3.0E+5	3.6E+5	5.0E+5	5.5E+5	1.2E+6	1.2E+6	5.2E+4	3.3E+4	3.4E+5	4.5E+5	7.3E+5	8.9E+5	1.1E+6	1.7E+6
Inosine+4	3.1E+3	3.6E+3	3.8E+5	4.1E+5	6.4E+5	7.2E+5	1.5E+6	1.5E+6	6.1E+3	0.0E+0	3.3E+5	4.3E+5	7.5E+5	9.4E+5	1.2E+6	1.7E+6
Inosine+5	0.0E+0	0.0E+0	2.6E+5	3.1E+5	4.7E+5	5.5E+5	1.2E+6	1.2E+6	0.0E+0	0.0E+0	2.7E+5	2.9E+5	5.1E+5	6.4E+5	8.5E+5	1.3E+6
Inosine+6	4.2E+3	3.9E+3	1.2E+5	1.6E+5	2.5E+5	2.8E+5	6.2E+5	6.3E+5	3.7E+3	0.0E+0	1.0E+5	1.2E+5	2.4E+5	2.8E+5	3.9E+5	5.6E+5
Inosine+7	2.1E+3	1.1E+3	3.1E+4	3.1E+4	5.2E+4	8.5E+4	1.7E+5	1.9E+5	2.6E+3	0.0E+0	1.4E+4	1.8E+4	4.3E+4	6.7E+4	9.9E+4	1.3E+5
UDP-GlcN	1.9E+6	3.1E+6	6.3E+5	7.1E+5	1.5E+5	1.3E+5	7.3E+4	1.4E+5	1.8E+6	2.1E+6	5.4E+5	6.1E+5	2.0E+5	2.1E+5	5.1E+4	2.0E+5
UDP-GlcN+1	2.3E+5	4.3E+5	1.7E+5	1.4E+5	1.2E+4	4.1E+4	3.6E+4	2.6E+4	2.0E+5	2.4E+5	1.5E+5	2.2E+5	7.8E+4	6.2E+4	2.3E+4	6.9E+4
UDP-GlcN+2	1.5E+4	3.7E+4	1.5E+5	1.2E+5	8.5E+4	1.2E+5	9.9E+4	9.8E+4	4.1E+3	1.1E+4	1.6E+5	2.1E+5	1.6E+5	2.0E+5	8.7E+4	1.6E+5
UDP-GlcN+3	1.8E+4	3.7E+4	1.5E+5	1.2E+5	9.7E+4	1.2E+5	9.9E+4	1.1E+5	4.1E+3	1.1E+4	1.6E+5	2.1E+5	1.6E+5	2.1E+5	8.7E+4	1.6E+5
UDP-GlcN+4	0.0E+0	2.6E+3	2.4E+5	2.6E+5	2.2E+5	1.8E+5	2.9E+5	3.0E+5	7.4E+3	1.5E+3	2.0E+5	2.6E+5	2.5E+5	2.9E+5	1.5E+5	3.2E+5
UDP-GlcN+5	0.0E+0	0.0E+0	2.1E+5	2.1E+5	2.7E+5	2.6E+5	3.2E+5	3.2E+5	2.4E+3	1.5E+3	2.0E+5	2.2E+5	2.7E+5	3.4E+5	1.7E+5	3.8E+5
UDP-GlcN+6	0.0E+0	0.0E+0	1.5E+5	1.5E+5	1.5E+5	1.6E+5	2.3E+5	2.4E+5	0.0E+0	0.0E+0	1.1E+5	1.1E+5	1.9E+5	2.7E+5	1.3E+5	3.1E+5
UDP-GlcN+7	2.3E+3	0.0E+0	5.4E+4	4.4E+4	6.0E+4	7.6E+4	1.3E+5	1.0E+5	0.0E+0	0.0E+0	4.5E+4	4.3E+4	8.7E+4	1.5E+5	5.9E+4	1.9E+5
UDP-GlcN+8	0.0E+0	5.0E+3	7.9E+3	1.1E+4	1.0E+4	3.2E+4	5.8E+4	5.4E+4	1.4E+3	4.8E+3	9.3E+3	1.8E+4	3.0E+4	6.3E+4	3.7E+4	1.1E+5

VITA

Martin J. Szul was born in 1985 in Oak Lawn, Illinois, son of Leonard and Margaret Szul. Growing up in Oak Lawn, he became enamored with the natural world. Throughout his childhood his curiosities were inspired by the National Geographic, the Discovery Channel, and library books about animals while his father – a mechanic – patiently taught him how to solve problems and the processes of cause and effect in the garage. He attended Marist Catholic High School and Moraine Valley Community College prior to transferring to the University of Tennessee, Knoxville for the fall semester of 2005. During his undergraduate career Martin was interested in pursuing medically related fields and found an undergraduate research opportunity to bolster his application. Under the mentorship of his undergraduate research advisor, Erik Zinser, Martin quickly realized an underlying passion to understand the biological world could be fulfilled through academic research. Martin graduated UTK with a bachelor's degree in Honor's Microbiology (2007) and continued academic pursuits under the mentorship of his undergraduate advisor Erik Zinser for his graduate career.

Martin met, fell in love, and married (2014) a fellow Chicago suburb native – Brenna DeLeo – while studying at the University of Tennessee. Outside of research and science, he enjoys spending time with friends and family, sports/athletics, and fermenting about anything he can – grains, fruit, milk, tea, vegetables – and then drinking/eating the byproducts.